2008

Bent Bones: The Pathological Assessment Of Two Fetal Skeletons From The Dakhleh Oasis, Egypt

Darcy Cope
University of Central Florida

BENT BONES: THE PATHOLOGICAL ASSESSMENT OF TWO FETAL SKELETONS FROM THE DAKHLEH OASIS, EGYPT

by

DARCY J. COPE
B.A. University of Central Florida, 2006

A thesis submitted in partial fulfillment of the requirements
for the degree of Master of Art
in the Department of Anthropology
in the College of Sciences
at the University of Central Florida
Orlando, Florida

Fall Term 2008

ABSTRACT

The present study evaluates two fetal individuals (B532 and B625) from the Kellis 2 cemetery (Roman period circa A.D. 50 – A.D. 450), Dakhleh Oasis, Egypt, that display skeletal anomalies that may explain their death. Both individuals exhibit bowing of the long bones in addition to other skeletal deformities unique to each individual. To assess these pathologies a differential diagnosis based on the congenital occurrence of long bone bowing is developed. Long bone bowing is selected because it is the more prevalent abnormality in the paleopathological literature and the other abnormalities are not as easily identifiable in the literature. For the purposes of this study, the differential diagnosis is defined as a process of comparing the characteristics of known diseases with those shared by an archaeological specimen, in the anticipation of diagnosing the possible condition. It is expected that the differential diagnosis will assist in providing a thorough assessment of each skeleton and yield a possible diagnosis for the condition(s).

Macroscopic and radiographic analyses are used to document and examine the bone abnormalities for each individual and compare the results with the developed differential diagnosis. Results suggest that the bent long bones of B532 were caused by osteogenesis imperfecta whereas the cause of the bent long bones of B625 is not clear. Further analyses of B625, including the pathologic abnormalities of its skull, suggest that the neural tube defect iniencephaly with associated encephalocele was the likely cause of the observed skeletal abnormalities.

The abnormalities of the long bones complicate estimations of the age-at-death of these two individuals, thus the pars basilaris bone was used to assess age estimation. A

population sample of 37 Kellis 2 fetal individuals allowed for the development of linear regression formulae of the pars basilaris measurements for long bone length estimates and a comparison of which would provide the most accurate age estimate. Finally, the diagnoses of the fetal specimens are considered in relation to the cultural aspects and disease pattern of the Kellis 2 cemetery

Dedicated to my family

for their endless love and support

that has guided me throughout my life.

ACKNOWLEDGMENTS

Writing this thesis has been an amazing journey that may have never reach its completion without the support and guidance of many people. First, I would like to thank my family and friends. For the past two years, and most recently, they have constantly heard the word "thesis" of which I am quite sure they are tired of hearing! They recognized the difficulty of completing such a task and provided their understanding, love, friendship, patience, and guidance throughout the entirety of this process. In particular, I would like to thank the following – Mamá, Papá, Duvan Cope, Delbert Cope, Dayana Cope, Chrissy Case, Christina Arcuri, Aimee Wilcox, Amanda Groff, and Lucas Johnson. Additionally, a special thanks to the UCF Anthropology faculty and staff and my fellow MA students. My deepest thanks go to Jennifer Stevens, a friend without any words to describe what an incredible person she is and how special she is in my life. This would not have been possible without her. A very heartfelt thank you to my thesis committee members for their guidance and patience: Tosha Dupras, Matthew McIntyre and Matthew Tocheri. I would also like to extend my appreciation to the Dakhleh Oasis Project for providing the opportunity for this thesis project and Sandra Wheeler and Lana Williams for contributing their assistance to my thesis.

TABLE OF CONTENTS

LIST OF FIGURES

LIST OF TABLES

CHAPTER 1: INTRODUCTION

A serious and still ongoing dilemma in anthropological studies is the exclusion of subadults[1] when reconstructing the life ways of past populations (Lewis 2007; Buikstra and Cook 1980). An emergence of subadult studies in the 1990s eventually led to new avenues of research that now include papers, books, theses, and conferences on the topic of children in archaeology and anthropology (Halcrow and Tayles 2008). For instance, in the book *Bioarchaeology of Children: Perspectives from Biological and Forensic Anthropology*, Lewis (2007) writes on topics such as the culture of child birth, child rearing practices and burial practices, dietary studies relating to child weaning and malnutrition, pathological and traumatic conditions suffered by children, and aging and sex standards for subadult skeletons.

Subadult skeletons are often underrepresented in the archaeological record and this is due to several factors (Ortner 2003; Lewis 2007; Pinhasi and Mays 2008). Cultural customs can dictate the internment of an individual and can sometimes prohibit the burial of an infant or fetus at a communal cemetery (Bowen 2003; Ortner 2003; Pinhasi and Mays 2008). Diseased individuals, particularly those that exhibit obvious abnormalities, such as leprosy, have been found separate from communal cemeteries or with different burial practices (Roberts et al. 2002). Taphonomic processes can destroy a subadult skeleton at a faster rate than that of the adult skeleton due to the more immature porous composition of bone and smaller bone elements, increasing the susceptibility to

[1] The term subadult pertains to individuals younger than 18 years of age. For aging terminology used throughout this thesis refer to Appendix A.

moisture and acidic properties (Robinson et al. 2003; Lewis 2007). Preservation may be disturbed even further for bones presenting with a pathological disease, particularly those that are degenerative to bone composition, such as osteomalacia or Paget's disease (Pinhasi and Mays 2008). Methodological factors in recovering these subadults have also been attributed to their underrepresented numbers in the archaeological record. A lack of an individual's expertise in subadult remains can result in deficiencies of identifying certain bony elements and as a consequence their exclusion from analysis (Scheuer and Black 2000; Lewis 2007). In regards to overall pathological cases, including adults, representations are very low. In a typical archaeological burial, Ortner (2003) notes that only approximately 15% of individuals will demonstrate diagnostic features of a disease affliction.

With all these factors hindering the recovery of a fetal skeleton, it becomes evident that any archaeological recovery of fetal remains can lead to important findings about past human societies and culture. The intention of the present study is to analyze two fetal skeletons (B532 and B625) from Romano-Christian Period Egypt that both present with unidentified pathological conditions that may explain their death. Both individuals are well preserved allowing for an extensive comparative pathological assessment. The cemetery site of Kellis 2, from which the fetal skeletons were excavated, presents a unique case in which many of the limitations discussed above are eliminated. Cultural, environmental and methodological factors of Kellis 2 are conducive in obtaining a high number of subadults, including those with observed pathological conditions. The dry and arid environment of Egypt combined with Christian burial practices have provided for optimal conditions for the preservation of subadult remains

(Molto 2002; Tocheri et al. 2005). This has resulted in a large fetal collection from the Kellis 2 cemetery (Fig. 1.1) that constitutes part of the comparative aspects of the present study (e.g., for obtaining age-at-death estimates).

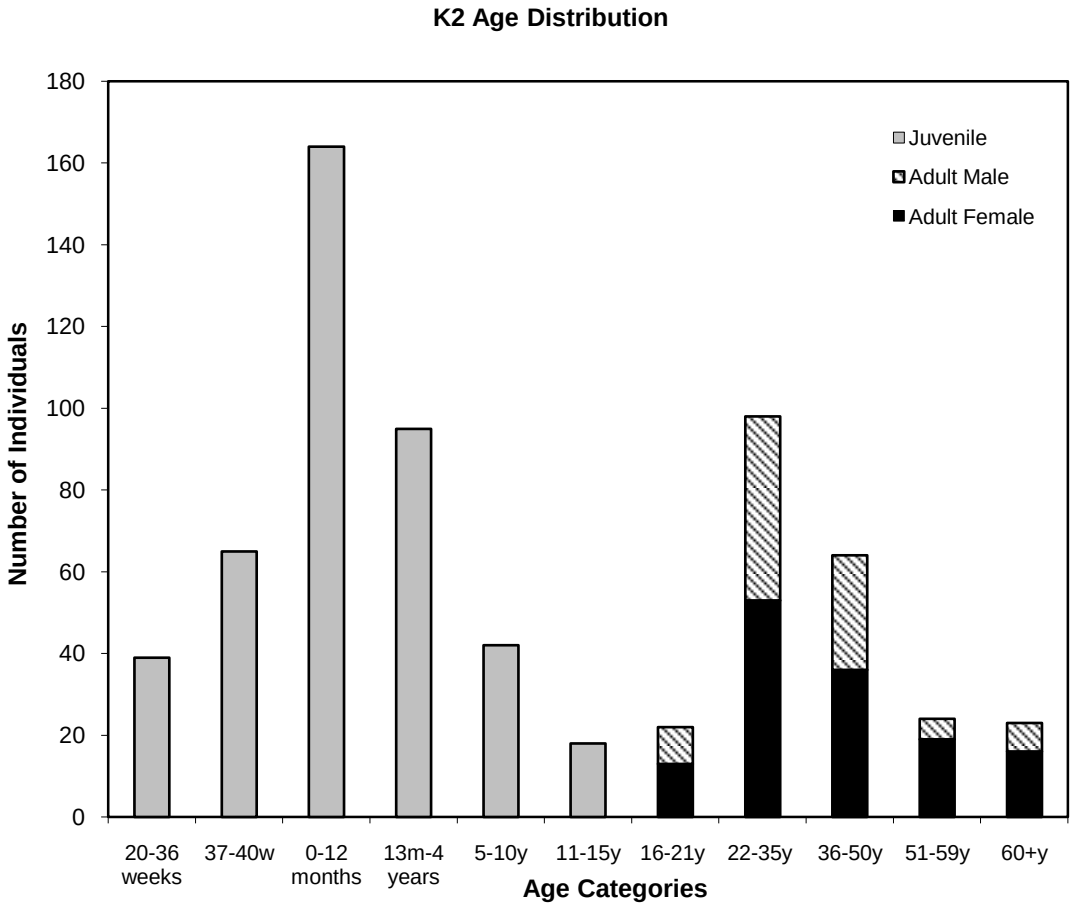

Figure 1-1 Age distribution and number of individuals excavated from the Kellis 2 cemetery site. Note the number of fetal and perinate specimens (Unpublished data, Wheeler).

Both fetal specimens present with a bowing defect of the long bones and one (B625) presents with severe malformation of the cranial bones. These abnormalities are congenital, which means they are present at birth. Congenital skeletal malformations

include pathologies such as dysplasias and neural tube defects (Ortner 2003). Skeletal dysplasias are a heterogeneous genetic group of disorders that involve disturbances in the development of the skeleton or cartilage. Early interruption in normal skeletal development can result in varying abnormalities such as disturbances in linear growth, bowing of the long bones, or hypoplasia (incomplete growth) of the bones (Rimoin et al. 2007). Instances of neural tube defects involve developmental irregularities in the closure of the neural tube, which comprises the brain, spinal cord and meninges (membrane coverings), and can lead to protrusions of these tissues through the skull or spine, also creating abnormalities of the skeleton (Padmanabhan 2006). Both skeletal dysplasias and neural tube defects have been described in the archaeological literature, but fetal individuals associated with these pathologies in particular are underrepresented in the archaeological record.

The best approach in reaching a possible diagnosis of the skeletal pathology afflicting both fetal specimens is to develop a differential diagnosis of their symptoms. The process of developing a differential diagnosis involves comparing the characteristics of known diseases with those shared by an archaeological specimen, in the anticipation of diagnosing the possible condition. The most notable pathological characteristic on both individuals is the long bone bowing, which is most severe in B532. Various congenital conditions identified in the archaeological record and in clinical cases refer to symptoms of bowing of the long bones (Ortner 2003; Spranger et al. 2002) and these will be key for developing the differential diagnosis used in this study.

Thus, this thesis develops a differential diagnosis using clinical and pathological data in an effort to derive at a disease diagnosis of two archaeological fetal individuals,

further substantiates alternative age at death estimates for these two fetuses, and interprets the cultural significance of their respective burial locations. The second chapter presents the development of a differential diagnosis of long bone bowing by reviewing the clinical and paleopathological literature for syndromes relating to congenital long bone bowing. This facilitated a differentiation of the pathologies by listing variations of the long bone bowing and other accompanied skeletal abnormalities.

In the third chapter, the age at death of the fetal specimens is estimated and their abnormalities are assessed. It was important to derive an age of death of the individuals, to determine their age cohort within the Kellis 2 cemetery and establish their total development before death, as this can indicate the viability of the fetal individual and suggest pathogeneses that are representative of their abnormalities. Traditional methods of estimating gestational age rely on linear regression relationships of gestational age with long bone length (Scheuer et al. 1980; Ubelaker 1987; Scheuer & Black 2000; Sherwood et al. 2000; Lewis and Flavel 2007). Long bone length measurements were not possible for B532, so other methods involving measurements of the pars basilaris and prediction of long bone length were substituted for age estimation. This method has shown promise in estimating age in a range of populations (Redfield 1970; Scheuer and MacLaughlin-Black 1994; Tocheri and Molto 2002). But rather than using linear regressions to calculate an exact age estimate from the predicted long bone lengths, age estimation was assessed from a Roman-British fetal population with posterior probabilities of age (Gowland and Chamberlain 2002). This methodology utilizes Bayesian estimation methods and assumes realistic prior probabilities of fetal mortality to

develop age distributions of the target population and eliminates biases enacted by linear regression formulae developed from reference samples.

In the last chapter, the fetal specimens are related back to the Kellis 2 cemetery in how cultural factors have determined their placement within the cemetery and if their pathological conditions are indicative of other disease patterns of the Kellis population. Possible explanations are offered of these disease patterns and how further studies of Kellis 2 could reveal reasons for the occurrence of the pathologies of B532 and B625 and other individuals presenting with similar pathologies.

CHAPTER 2: DIFFERENTIAL DIAGNOSIS OF BOWED OR ANGULATED LONG BONES

2.1 Introduction

Undoubtedly one of most valuable sources for paleopathology is that of the skeleton. With careful preservation and observation of skeletal remains, diagnostic features on the bone surface can aid in identifying diseases that once afflicted an individual (Ortner 2003). Identification of disease is vital in developing interpretations of a population's health and identifying disease patterns. But skeletal remains can also bring limitations, as not all afflictions will produce skeletal deformities, or the individual may not have lived long enough for a disease to create abnormal manifestations on the skeleton (Mays 1998; Roberts and Manchester 2005). This limitation is often observed for cases of infectious diseases, in which specific factors, such as age of onset, immune response and previous health of the individual, can dictate the expression of an infectious disease (Ortner 2003; Pinhasi and Mays 2008). This can lead to an underrepresentation of infectious cases in a skeletal sample that would have affected a community (Ortner 2003).

Skeletal dysplasias and their congenital occurrence are in most cases a result of a genetic defect (Sandler 2006). The presence of skeletal malformations of a genetic disease and optimal preservation allows for a better representation of a genetic disease in a population (Ortner 2003). This does not necessarily signify the number of cases is larger, as their occurrence in the archaeological record is often rare and limited in the

type of genetic defects (Ortner 2003; Pinhasi and Mays 2008). Limitations of skeletal dysplasias are present in the similar skeletal abnormalities that may occur for a variety of syndromes. Conditions relating to skeletal dysplasias can display an overlap of skeletal abnormalities (Ortner 2003), creating ambiguity when generating a list of diagnostic possibilities for syndrome diagnosis and a challenging task of distinguishing between disorders.

For clinical cases, long bone bowing or angulation is one type of symptom that is often found in association with a range of other abnormalities (Hall and Spranger 1980). The same has been observed in the archaeological record, with cases of osteogenesis imperfecta (Wells 1965; Gray 1969; Ortner 2003), achondroplasia (Bleyer 1940; Snow 1943; Brothwell 1967; Hoffman 1976; Frayer et al. 1988), and infantile cortical hyperostosis (Rogers and Waldron 1988). The focus of this research is on the formation of a differential diagnosis on the congenital deformity of long bone bowing, resulting in death of the individual, using descriptions from both the clinical and paleopathological literature. As long bone bowing is a symptomatic feature that is associated with a number of diseases, there is a possibility for uncertainty and misdiagnosis. The objective of this research is to provide a guideline for diagnosing specimens that show long bone bowing, and to identify other accompanying diagnostic features that will aid in identifying the afflicting disease.

2.2 Forming a Differential Diagnosis in Paleopathology

The differential diagnosis is a common approach used by the medical community that has been used by paleopathologists to describe diseases in the skeleton (Ortner 2003). In the clinical sphere the process of a differential diagnosis is described as "the methods by which we consider the possible causes of a patient's clinical findings before making final diagnoses" (Richardson et al 2000: 164). Similarly in paleopathology, a differential diagnosis must ask the question, "What are all the possible causes of a pathological condition and which one is most likely the cause?" (Ortner 2003:4). The premise of a differential diagnosis for clinical and paleopathological cases is the same, that of observing the symptoms of an individual afflicted with a pathology and deriving a list of possible disorders. But their differences exist in the finality of what the differential diagnosis will provide. In a clinical setting, the purpose of a differential diagnosis is to provide for an absolute diagnosis of the disorder so that the correct treatments can be selected. In paleopathology, the differential diagnosis does not always aim for an exact diagnosis, a result that is considered acceptable as paleopathologists are limited to skeletal remains and the researcher is often left with multiple possible causes of the pathology (Pinhasi and Mays 2008).

Before developing a paleopathological differential diagnosis, a few key points should be considered. First, as mentioned earlier, a limiting factor of paleopathology is the assessment of only the skeletal remains. This is unlike clinical cases that can include soft tissues, cells, blood, or organs, as well as a family history of a disease (Ortner 2003). With this limitation there are also limits as to the type of techniques used to study a

skeleton. Traditionally, skeletal remains are studied by macroscopic observances on the bony surface, with supplemental help from radiographic evidence from the clinical literature or the skeleton itself. Other methods, such as microscopic or histological analysis and DNA analysis, are used less often, due to a lack of equipment, considerable cost or badly preserved skeletal remains (Ortner 2003; Pinhasi and Mays 2008). The information provided by medical cases is not always effective. The descriptive assessment of a disease represented on a dry bone specimen can be dissimilar to that described in the clinical literature. Clinical cases involving skeletal abnormalities are dominated by radiographic analysis, but in some situations radiographs are not inclusive of the entire skeleton, or radiographic representations do not account for the subtle features on the bone surface (Ortner 1991). This can result in a deficiency of the descriptive data provided by clinical cases. Recognizing these limitations is important to developing a differential diagnosis, as they can determine what type of information is available and what lines of inquiry can be further pursued (Pinhasi and Mays 2008).

When developing a differential diagnosis it is common practice in the medical field to choose disorders that have a higher probability of occurring. Richardson and colleagues (2000) advocates the use of "pretest probabilities" in helping to choose which disorders should be further investigated. The method mainly consists of favoring those disorders that been diagnosed more often for use in a differential diagnosis. This was similarly used in the present study and will be discussed later. Byers and Roberts (2003) have recently outlined how using Baye's theorem of posterior probabilities of disease prevalence can aid in calculating the probability of an unknown disease in an archaeological context. The development of posterior probabilities of diseases is

available from health statistics of a living population, statistics collected from industrialized populations in the 1800s or 1900s, as well as data from human skeletal collections, such as the Terry and Hamann-Todd Collections. Problems of this methodology arise from the inconsistencies in the representation of disease prevalence of ancient populations versus that of modern population or skeletal collections. Additionally, there is also the question if a correct diagnosis was reached, especially in data relating to the 1800s and from skeletal collections. The applicability of the method in paleopathology is evident, but its usage is not possible for the scope of the present study but attention should be given as it does provide a new methodology for disease diagnosis.

The differential diagnosis for this present study was formed by selecting pathologies from the clinical literature that identify congenital campomelic defect of the long bones and result in a stillborn birth or death after only living a few days. Any disorders that were mentioned as being similar to the chosen disorder and also recognized long bone bowing as a symptom were also included in this differential diagnosis. According to a differential diagnosis by Alanay and colleagues (2007), more than 40 distinct disorders are associated with bowed or angulated femurs alone. Those disorders most commonly occurring are campomelic dysplasia, thanatrophoric dysplasia, and osteogenesis imperfecta, and each of these are included in the present differential diagnosis. A review of the clinical literature resulted in a compilation of the following pathologies: campomelic dysplasia, osteogenesis imperfecta, hypophosphatasia, achondrogenesis, thanatophoric dysplasia, infantile cortical hyperostosis, and Stüve-Wiedemann syndrome. The incorporation of paleopathological literature can facilitate

the differential diagnosis by providing a comprehensive description of skeletal abnormalities, at least for those diseases that are represented in the archaeological record. Archaeological representations were available for osteogenesis imperfecta and infantile cortical hyperostosis. Descriptions of the bowing of the long bones and associated skeletal abnormalities are explored for each disorder. Following these descriptions is a table that lists both skeletal and soft tissue abnormalities, as well as archaeological findings. As the main focus of this study is of skeletal abnormalities, specifically bowing of the long bones, soft tissue malformations are not mentioned in-depth, but their inclusion is nonetheless important in cases involving soft tissue survival or soft tissue malformation affecting the integrity of the skeleton. A detailed summary table of the skeletal abnormalities of each disorder is presented at the end of the differential diagnosis.

2.3 Campomelia or "Bent Limb" as Described in the Clinical Literature

Congenital bowing or angulation of long bones is termed campomelia, camp referring to "bent" and melia to "limb" (Romero et al.1988) and results from defective skeletal growth that occurs during prenatal development (Figure 2-1). Bowing abnormalities of the long bones did not receive proper attention until 1947, when Caffey reported on 3 infants that showed symmetrical bowing of the femora and humeral shafts and asymmetrical bowing of the radii, tibiae, and ulnae. The bowing was accompanied by thickening of the tubular bones and dimple manifestations on the skin of the arms and legs. Caffey (1947) attributed the development of campomelia to a mechanical stress on

the fetal body in response to a defective position within the uterus. In accordance with Caffey (1947), Angle (1954) also detailed a case involving bilateral femoral angulation, also assigning mechanical principles as the cause of the bowing. In both studies, Caffey (1947) and Angle (1954), observations were made from living patients and radiographs, without noting any other significant abnormalities of the skeleton.

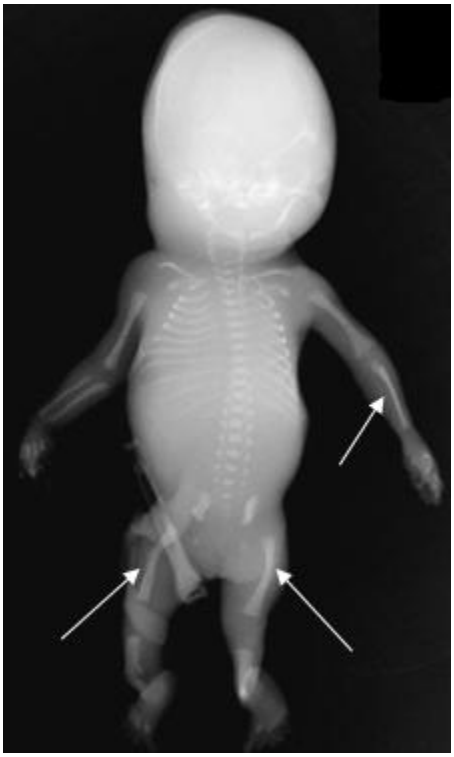

Figure 2-1: Campomelia of a newborn. Bowing is best evidenced on the femora with minor bowing of the upper extremities (adapted from Alanay et al. 2007: 1163).

Later studies distinguished skeletal abnormities that accompanied a bowing defect of the long bones. In a case study by Bain and Barrett (1959), analysis of long bone bowing involved a stillborn child whose body was macerated and the bones were consequently examined. Findings revealed severe anterior bowing of lower leg bones and humeri. The study also revealed additional abnormalities, which included an

abnormally shaped pelvis with splaying of the ischia, spina bifida, underdevelopment of the scapulae, and cleft palate. Rather than mechanical forces as causation of the bowing, Bain and Barrett (1959) concluded that the etiology of the bowing was due to an abnormal development of the cartilaginous model, with deficiencies in vascular and cellular support of the perichondrium, an irregular tissue surrounding the cartilage of developing bone. These same findings were resonated by Lee and colleagues (1972).

A specific syndrome of congenital bowing of the bones was not delineated until 1971, when Maroteaux and colleagues described "campomelic dysplasia", malformations consisting of long bone bowing, micrognathia, hypoplastic fibulae and scapulae, and other abnormalities (Maroteaux et al. 1971). Following this distinction, a number of cases reported on the campomelic dysplasia syndrome (Lee et al 1972; Storer and Grossman 1974), while a growing number of other cases reported on variants or subdivisions of the disorder (Stüve and Wiedemann 1971; Rogers et al., 1975; Hovmöller et al., 1977) resulting in confusion of the term campomelia, with some experts treating the term as a distinct syndrome, rather than a symptom (Hall and Spranger 1980; Alanay et al. 2007). This eventually led experts to delineate classifications and form differential diagnoses of those conditions presenting with congenital bowing of the long bones.

2.4 Campomelic Dysplasia

Campomelic dysplasia is described as a rare genetic disorder that is commonly fatal in infancy (Mansour et al.1995). Genetic transmission is autosomal dominant, meaning only one abnormal gene is needed from a parent for inheritance of the disease. Clinical

cases have reported on ultrasound detection as early as 16th to 18th week gestation, with a more definite diagnosis at around 24 weeks gestation (Winter et al. 1985; Promsonthi and Wattanasirichaigoon 2006). Cases have also reported on individuals living with the disorder up to the adulthood (Mansour et al. 2002). These individuals are often beset with respiratory infections and skeletal deformities, most notably shortened long bones with bowing, macrocephaly, a depressed nasal bridge, dislocations (especially at the hip), scoliosis, and kyphoscoliosis (Mansour et al. 2002). Sex reversal of the genitals is also symptomatic of campomelic dysplasia, with a higher prevalence among males that have a male karyotype but are born with female or ambiguous genitalia (Houston et al.1983). A study conducted by Mansour and colleagues (1995) identified eleven of 15 cases (73%) with a male karytoype XY that had female or ambiguous genitalia.

The SOX9 gene, mapped to chromosome 17q, is responsible for campomelic dysplasia and as the cause of sex reversal (Kwok et al. 1995; Olney et al. 1999; McDowall et al. 1999). Deformities in bone development are due to the dependence of the SOX9 gene as a regulator for type II and type IX collagen. Abnormalities in regulating these collagen types affect chondrogenesis (development of cartilage) and eventual bone development, as cartilage serves as a precursor to bone.

At birth, individuals with campomelic dysplasia are likely to die from respiratory implications associated with defective tracheobronchial cartilage (Mansour et al.1995; Spranger et al. 2002). During the fetal period, radiological features of the disorder are apparent. Mansour and colleagues (1995) found a high prevalence of hypoplastic scapulae (underdevelopment and abnormally high position of the scapula), a lack of mineralization of the thoracic pedicles, narrow iliac bones and underdevelopment of the

pubic bones, bowing of all the long bones, and a small chest with only 11 pairs of ribs in development with a thin morphology (Figure. 2-2). Of the lower extremities, the femora showed a typical length and density, but the tibiae demonstrated more severe bowing and associated hypoplastic (underdeveloped) fibulae. Those cases showing radiographic evidence of scoliosis or kyphosis were somewhat rare, but clinical features of surviving patients showed an increase in this deformity in the form of kyphoscoliosis, curvature of the spine in both the coronal and sagittal plane. The most prevalent clinical features included bowed tibiae (Mansour et al. 1995). Similar findings are reported by Cheema et al. (2003), in particular angular anterolateral bowing of the limbs, with more severe bowing of the femora and tibiae as compared with the upper extremities (Figure 2-3). A summary of characteristics associated with campomelic dysplasia are found in Table 1.

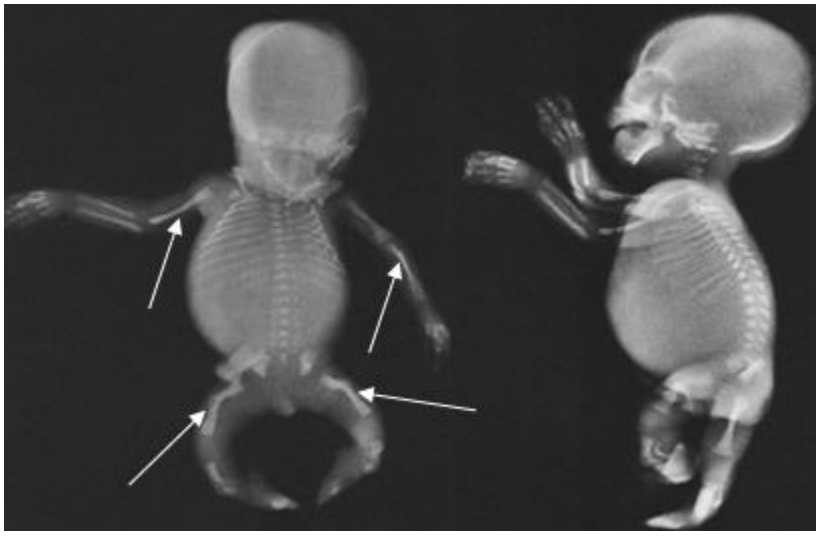

Figure 2-2: Stillborn diagnosed with campomelic dysplasia. Femora and tibiae are severely bent and shortened, and there is minor bowing of the arm bones. Accompanied abnormalities include a bell-shaped ribcage, 11 pair of ribs, narrow iliac bone, absent ossification of pubis and ischium (adapted from Spranger et al. 2002: 43).

Figure 2-3: Five-month old girl diagnosed with campomelic dysplasia. Bowing is most noticeable on the femora and tibia (adapted from Cheema et al 2003: 878).

Table 2-1: Skeletal and soft tissue abnormalities of campomelic dysplasia.

Skeletal abnormalities		Soft tissue abnormalities
Limbs: Anterolateral bowing of the femora and tibiae Shortening of leg bones Hypoplastic fibulae **Skull**: Microcephaly (small head) Depressed nasal bridge **Thorax**: 11 pairs of ribs Thin ribs	**Spine**: Scoliosis Kyphosis Kyphoscoliosis Lack of mineralization of thoracic pedicles **Pelvis**: Narrow Underdevelopment of pubic bones	Sex reversal of the genitals Low set ears Skin dimples Defective tracheobronchial cartilage Small facial features

2.5 Osteogenesis Imperfecta

Osteogenesis imperfecta (OI) is commonly termed the "brittle bone disease" in reference to the characteristic bone fragility that can result in a high number of fractures, which can occur intrauterine and after birth (Glorieux and Rauch 2006; Rauch and Glorieux 2004). Soft tissue deformities associated with OI are blue sclera, skin hyperlaxity, and hearing loss (Glorieux and Rauch 2006; Plotkin et al. 2003; Kuurila et al 2000). Osteogenesis imperfecta is a genetic disorder with most affected individuals having a mutation on either of the two genes for type 1 collagen, COL1A1 or COL1A2 (Ries 2000; Rauch and Glorieux 2004; Glorieux and Rauch 2006; Aerts et al. 2006). Mutations in other genes are also possible and can produce similar clinical features (Plotkin et al. 2003). In a collagen type 1 mutation, a glycine residue in COL1A1 or COL1A2, which is important in the collagen type 1 molecule structure, is modified, causing abnormalities in collagen production which is a highly important organic product of bone (Rauch and Glorieux 2004). A disturbance in normal collagen formation, which results in an insufficient amount of cancellous and cortical bone, is responsible for the characteristic brittleness of bones and causes the individual to have a higher risk for fractures (Ward et al. 2002). These deficiencies create a thinning of the bone due to slow periosteal bone formation from bone forming cells (osteoblasts). Despite the increase in osteoblastic activity, bone resorption by the osteoclasts (bone destroying cells) work at a heightened rate that does not allow osteoblastic cells to keep up (Sarathchandra et al. 2000; Rauch and Glorieux 2004).

Depending on the severity and clinical features, an individual diagnosed with OI is typically placed within a type category. Sillence (1979) created the classical classification system that is still used to this day, which arranges the disorder according to the severity: Type I, Type II, Type III, and Type IV. Continued research on the disorder recognized three additional type categories, Type V, Type VI, and Type VII (Glorieux et al. 2000; Glorieux et al. 2002; Ward et al. 2002). Many individuals with Type II OI are stillborn due to the severe skeletal deformity, particularly rib fractures (Rauch and Gloriexux 2004; Glorieux and Rauch 2006). Individuals with Type III OI usually die following birth or within the first few years of life (Spranger et al. 2002). Type II and Type III are the only types of OI that are included in the overall differential diagnosis of bowing of the long bones, but attention will be given to the other OI types to allow differentiation of each type.

The mildest form of OI is Type I, and unlike the other types, the individual reaches normal height with minor skeletal deformities. Genetic transmission is autosomal dominant and parental mosaicism (differences in genotype) explains why a child may show symptoms, but not the parents (Hall and Spranger 2008). Fractures may occur at birth (Plotkin et al. 2003), and the risk for fractures will increase once the individual begins to walk, and throughout juvenile development, and then subsides when the individual reaches puberty (Rowe and Shapiro 1998; Glorieux and Rauch 2006; Byers and Steiner 1992).

As mentioned earlier, Type II OI is lethal in newborns. Genetic transmission is also autosomal dominant, and mosaicism explains any discordance with genotype expression between a child and parents. Clinical data suggests manifestations of the

Type II OI detectable as early as 16 weeks gestation and live-born individuals, who died shortly after, with a mean age of gestation of 36 to 40 weeks (Young 1987; Aerts et al. 2006). Skeletal malformations include a very low bone mineral density, intrauterine fractures of the skull, long bones and vertebrae, callus formations, beaded ribs, demineralization of the clavarium and facial bones, and bowed limbs (Glorieux and Rauch 2006; Plotkin et al. 2003). Type II OI is often differentiated into two subtypes, Type IIA (Figure 2-4) and Type IIC (Figure 2-5). Individuals suffering from Type IIA develop thick, short, squared long bones that are furrowed (Figure 2-4), while Type IIC (Figure 2-6)) results in very thin, twisted tubular bones (Spranger et al. 2002; Sillence et al. 1984; Young et al. 1987). Differentially, genetic transmission of Type IIC is autosomal recessive.

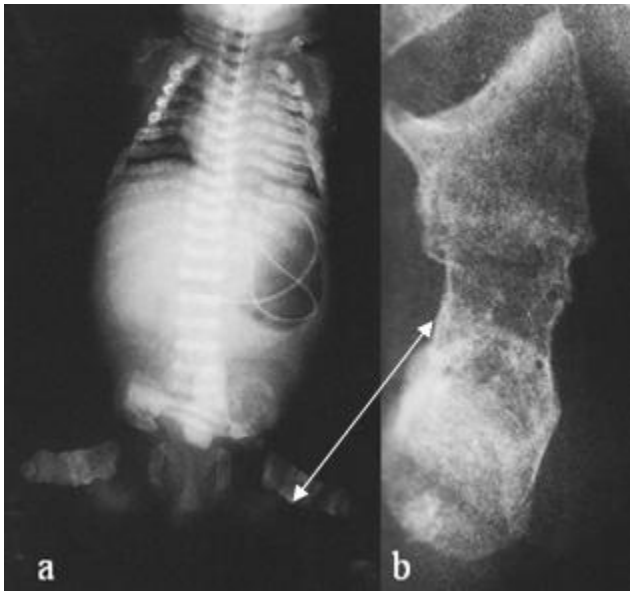

Figure 2-4: Type IIA osteogenesis imperfecta of a newborn. a) Decreased bone density evidenced by translucency of bones, broad ribs with continuous fractures, flat vertebral bodies, and b) wavy accordion-like contour of the femora (adapted from Spranger et al. 2002: 437).

Figure 2-5: Type IIC osteogenesis imperfecta of stillborn. Note the angulated, twisted long bones (adapted from Spranger et al. 2002: 439).

An individual affected with Type III (sometimes referred to as Type IIB) OI has similar skeletal deformities as those of Type II, but symptoms are not immediately lethal to the individual. The genetic transmission occurs through autosomal dominance in most cases and presents with heterogeneity (multiple origins of the disease in different people) (Spranger et al. 2002). The patient with Type III is usually wheelchair bound due to the debilitating malformations (Glorieux and Rauch 2006; Plotkin et al. 2003). Compared to Type II, individuals with Type III have compressed vertebral bodies, more ossification of the cranial bones, frontal and temporal bossing of the skull, and regular ribs and scapulae (Spranger et al. 2002). Radiographic features have identified the long bones as having broad metaphyses and thinner diaphyses (Figure 2-6) (Spranger et al. 2002). A possibly unique skeletal deformity of Type III is angulation at the posterior of ribs (Plotkin et al 2003).

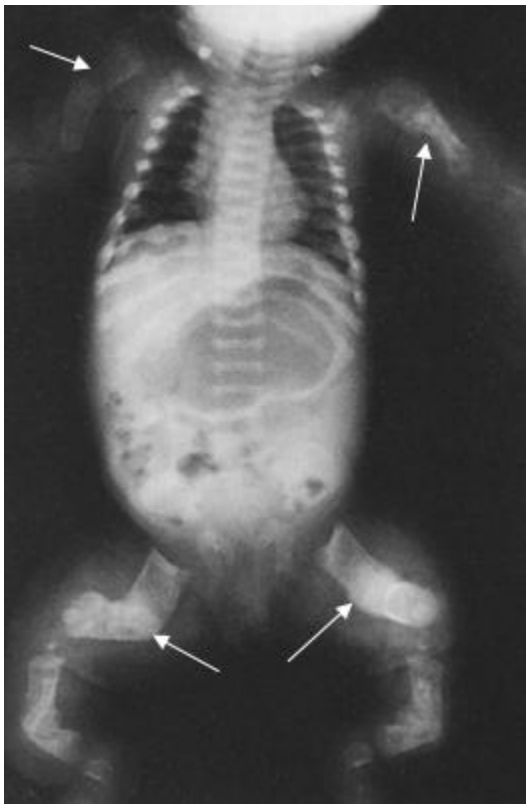

Figure 2-6: Type III osteogenesis imperfecta of newborn. Severe bowing of the long bones with shortening and thickening (adapted from Spranger et al. 2002: 442).

Skeletal deformities associated with Type IV osteogenesis imperfecta normally include short stature and bone fragility that is not identifiable at birth (Plotkin et al., 2003). Bowing of the long bones becomes progressively worse, dentinogenesis imperfecta is present, and hearing loss is common among older individuals (Spranger et al. 2002). The clinical manifestations of dentinogenesis imperfecta involve coloration of the teeth that ranges from grayish-blue to brown, exposure of dentin, short roots, bulbous crowns, and disorganization and irregularity of the dentin (Malmgren and Norgren 2002). Dentinogenesis imperfecta is more prevalent among individuals with Type IV OI and less common among Type I and Type III OI. Differentiation of Type V is possible due to

calcification of the interosseous membranes of the forearms, limiting pronation and supination, and hyperplastic (overgrowth) calluses on the long bones (Glorieux et al. 2000; Plotkin et al. 2003; Glorieux and Rauch 2006). Both Type IV and V are genetically transmitted by autosomal dominance (Spranger et al. 2002).

Type VI and VII rarely occur and are distinguished from other types in that affected individuals do not form blue sclera or dentinogenesis imperfecta. Inheritance of both is autosomal dominance and mosciasim has been suggested (Glorieux et al. 2002). Features of Type VI and Type VII include a "scale-like" structure of the bone lamellae, an increase in osteoid (uncalcified bone) thickness for Type VI, and a shortening of the femora and humeri characteristic of Type VII (Plotkin et al. 2003; Glorieux and Rauch 2006).

There is limited archaeological evidence of osteogenesis imperfecta. Only three cases have been reported in the literature. The first of these cases was reported by Wells (1965), who attributes the diagnosis of OI to the skeletal remains of an 18-year-old individual from an Anglo-Saxon cemetery at Suffolk, England (Figure 2-7). Wells (1965) describes angulation of the left femur, both distally and proximally, with the proximal end showing the greatest curvature and evidence of multiple fractures. From the morphological and radiographic analysis, Wells (1965) also notes an irregularity in the trabeculae structure. After excluding rickets and fibrous dysplasia, Wells (1965) determines osteogenesis imperfecta as the causative disorder of the individual's femur. Ortner (2003) assigns the OI described by Wells (1965) as Type I on the basis that the individual reached adulthood.

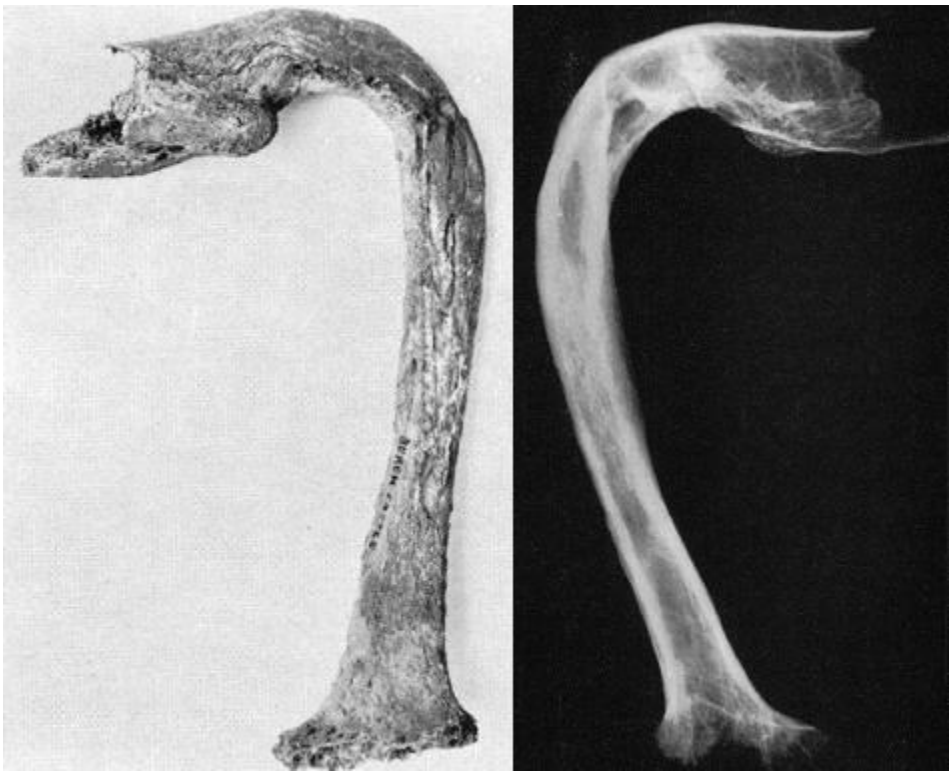

Figure 2-7: Paleopathological adult femur diagnosed with osteogenesis imperfecta. Severe bending is noted at the proximal end. Radiographs show reduced trabeculae that is also irregular and coarse, flaring at the distal metaphyses, and a narrow shaft (after Wells 1965:89-90).

A second diagnosed paleopathological case of osteogenesis imperfecta is of a child aged at 2 years old from the site of Speos Artemeidos in Egypt, dating to ca. 1000 BC (Gray 1969). The child's skeletal characteristics (Figure 2-8) were anterolateral bowing of the long bones with thickening, underdeveloped amber colored teeth (dentinogenesis imperfecta), overall lightness and fragility of the bones, and an expanded cranial vault with several wormian bones and elongated orbits (Gray1969). This specimen is currently housed at the Roxie Walker Galleries of Funerary Archaeology in the British Museum, London.

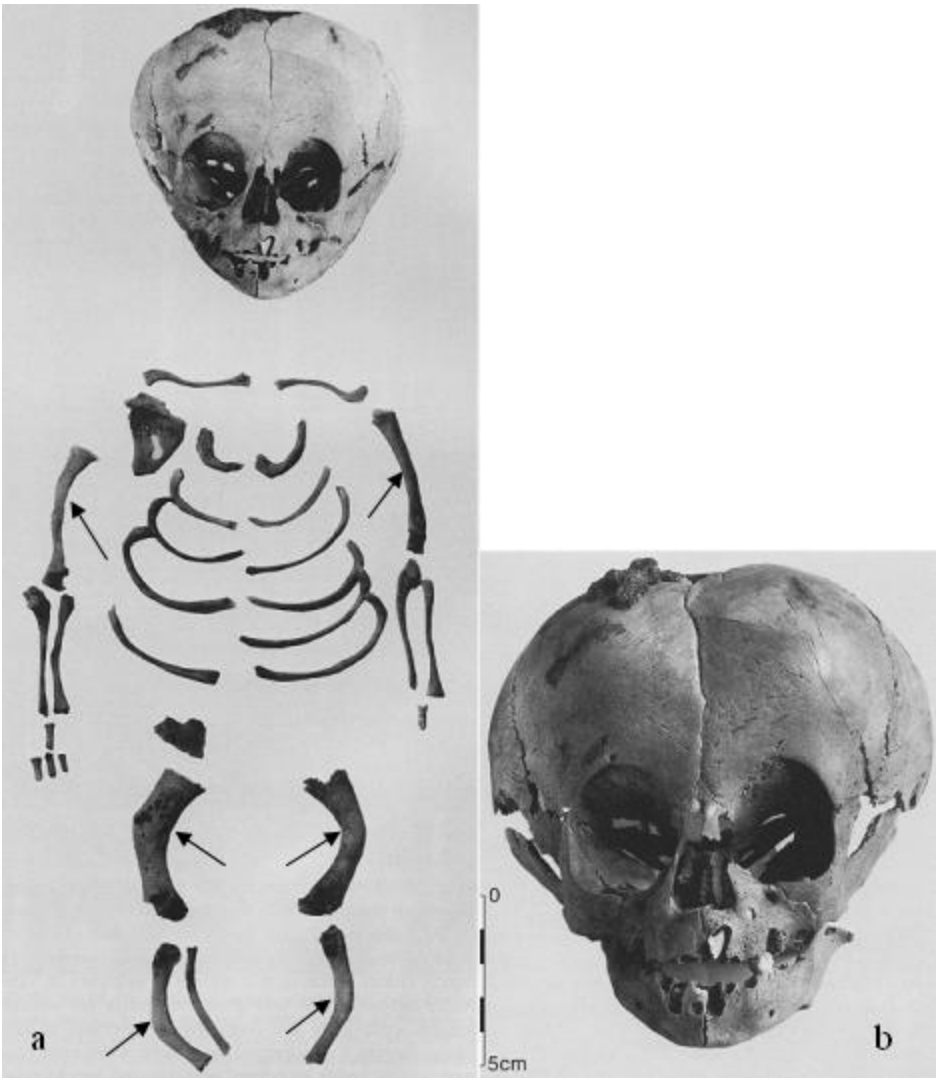

Figure 2-8: A paleopathological case of osteogenesis imperfecta occurring in a 2 year-old. a) Skull and postcranial bones with the long bones. Bone showing severe bowing and thin diaphyses; and b) anterior view of skull. Note the enlarged vault and elongated orbits (adapted from Ortner 2003: 493).

Osteogenesis imperfecta was also diagnosed at the Juhle site in Maryland (AD 1400 and 1500) in a late adolescent individual (Ortner 2003). Indicators of osteogenesis imperfecta were given by the narrow diameter of all the long bones in comparison to their length and the low osteon count that indicate a defect in intramembranous bone formation (Figure 2-9). Ortner (2003) could not identify fracture occurrences, callus formations or

angulations of the long bones, making this diagnosis very tentative. Even so, Ortner (2003) ascribes the remains as maybe Type IV or Type I OI due to the older age of the individual. A summary of clinical and paleopathological characteristics associated with osteogenesis imperfecta are found in Table 2-2.

Figure 2-9: Possible paleopathological case of osteogenesis imperfecta occurring in a late adolescent or adult skeleton. Arrows point to bones showing the thinnest diaphyses (adapted from Ortner 2003: 494).

Table 2-2: Skeletal and soft tissue abnormalities of the types of osteogenesis imperfecta.

OI Type	Skeletal abnormalities	Soft Tissue
Type I	**Limbs**: Slender shafts; decreased bone fragility; mild bowing. **Skull**: Rarely cranial deformities; abnormal ossification of cranial vault; mosaic pattern of wormian bones. **Spine**: Scoliosis; vertebral fractures. **Paleopathology**: Narrow diameter of long bones; bowing of femur; multiple fractures; low osteon count; chalky, fragile texture.	Skin hyperlaxity Blue sclera Short neck Round face
Type IIA (Lethal)	**Limbs**: Thick, short, crumpled shafts; femora have wavy accordion-like appearance; fractures; anterolateral bowing of all limbs. **Skull**: Large head; soft calvaria; wide fontanel's; wormian bones. **Thorax**: Short, thick ribs with beading. **Spine**: Flat and irregularly deformed vertebral bodies and vertebrae.	
Type IIC (Lethal)	**Limbs**: Thin and twisted; fractures; anterolateral bowing of all limbs. **Skull**: Large head; soft calvaria; demineralization of facial bones. **Thorax**: Varying thickness and discontinuous beading of ribs; distorted and irregularly ossified scapulae. **Spine**: Almost normal spine; spine is well ossified; vertebral bodies are normal height.	
Type III/IIB (Lethal)	**Limbs**: Short long tubular bones, thicker; broad metaphyses; thinner diaphyses. **Skull**: Frontal and temporal bossing; wide open fontanel's; wormian bones. **Thorax**: Thin ribs with discontinuous fractures. **Spine**: Compressed vertebral bodies; kyphoscoliosis (later in life).	
Type IV	**Limbs**: Bowing becomes progressively worse; short stature. **Skull**: Rarely cranial deformities; retarded ossification of cranial vault; sometimes mosaic pattern of wormian bones; dentinogenesis imperfecta.	
Type V	**Limbs**: Mild to moderate bowing of long bones; short stature; calcification of the interosseous membranes of the forearms; hyperplastic calluses. **Skull**: Rarely cranial deformities; retarded ossification of cranial vault; sometimes mosaic pattern of wormian bones.	
Type VI & VII	**Limbs**: Mild bowing; short stature; VII: Coxa vara; shortening of humeri and femora. **Skull**: No dentinogenesis imperfecta; **Other**: VI: Increase in osteoid thickness; fish-like pattern of bone of bone lamellation.	

2.6 Hypophosphatasia

Hypophosphatasia is a rare congenital disease of metabolic failure due to an insufficiency of liver-bone-kidney type alkalaine phosphatase. This failure leads to a disruption in the mineralization of the osteoid and subsequent undermineralization of the bone, due to a mutation on the tissue nonspecific alkaline phospatase TNLAP gene (Cole 2003; Ortner 2003; Herasse et al. 2002). Genetic transmission is autosomal recessive and dominant (Spranger et al. 2002). Hypophosphatasia ranges in severity and onset, and is classified according to age of onset as either perinatal (lethal), infantile, childhood, and adult (Cole 2003; Drezner 2006). Patients suffering with only dental abnormalities are classified as suffering from odontohypophosphatasia, while individuals who present with classical clinical features of hypophosphatasia but with normal alkaline phosphatase are classified as having pseudohypophosphatasia (Cole 2003; Drezner 2006). Of interest in developing the present differential diagnosis is the prenatal form of the disorder. The generalized clinical features due to abnormal alkaline phosphatase levels are undermineralization of the skeleton, fractures and tooth loss (Cole 2003).

Hypophosphatasia is described as a congenital form of rickets, as rickets also effects mineralization of the skeleton and produces similar skeletal defects (Cole 2003). Diagnostic evidence of prenatal hypophosphatasia has been revealed by ultrasound as young as 14 weeks gestation due to poor mineralization and shortened long bones (Tongsong and Pongsatha 2000). In a clinical review of 19 cases of individuals with a diagnosis of perinatal hypophosphatasia, ages ranged from 14 to 39 weeks gestation (Sohat 1991). Skeletal deformities resulting from the perinatal form of hypophosphatasia

often manifest as shortened and bowed extremities, short and thin ribs, poor ossification of the calvaria and skull, osteochondrol spurs that usually project from the fibula and ulna, and fractures (Figure 2-10) (Cole 2003; Spranger et al. 2002; Shohat 1991; Rudd et al. 1976). Infantile hypophosphatasia is similar to the perinatal form although ossification is more advanced with later craniostenosis (early closing of cranial sutures) and more congenital bowing is evidenced (Spranger et al. 2002). Childhood and adult hypophosphatasia present as milder forms of the disease with rachitic-like symptoms presented in the childhood form, such as bowing of the long bones, short stature, enlarged joints, and beading of the costochondral junction (articulation between ribs and cartilage). In addition, cranial sutures are uncalcified, craniostenosis is possible, while the adult form can present with fractures along with softening of the bones (Cole 2003; Spranger et al. 2002). There are no paleopathological cases of individuals affected by hypophosphatasia. Table 2-3 presents a summary of the clinical manifestations associated with hypophosphatasia.

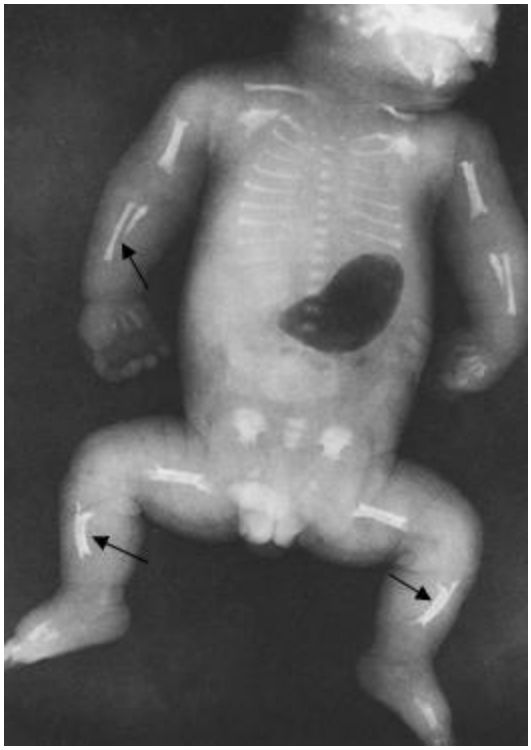

Figure 2-10: Perinatal hypophosphatasia at 37 weeks gestation. The long bones are shortened with bowing and the ulnae are only partially ossified. Ribs are thin and not ossified, absent ossification of cervical and lumbar vertebrae with poor ossification of the thoracic, ossification of pubic and ischial bones, calcanei, tali, lateral metacarpals and metatarsals and most of the phalanges is not visible (adapted from Spranger et al. 2002: 122).

Table 2-3: Skeletal and soft tissue abnormalities of hypophosphatasia.

Hypophosphatasia Type	Skeletal abnormalities	Soft tissue abnormalities
Perinatal	**Limbs**: Bowed; shortened; varying degree of demineralization; osteochondral spurs; metaphyseal cupping. **Skull**: Failure of ossification of calvaria, skull base and face. **Thorax**: Short and thin ribs; poor ossification; complete lack of ossification of rib; fractures of ribs. **Spine**: Poor ossification of vertebrae, usually the neural arches; some vertebrae not ossified; vertebral bodies rectangular/round, flattened, or sagitally clefted. **Pelvis**: Small pelvic bones with ossification defects; bending of pelvis.	Polyhydraminos Blue sclerae
Childhood	**Limbs**: Bowed; low bone density; abnormal ossification of long bones and metaphyseal. **Skull**: Wide cranial sutures; late ossification of cranial vault and base; craniostenosis; premature loss of deciduous teeth. **Thorax**: Abnormal ossification of ribs.	
Adult	**Limbs**: Bowed; thin cortex; diaphyseal spurs; frayed metaphyses; radiolucent defects on diaphyses that look like punched-out holes; fractures; enlarged joints. **Skull**: Craniostenosis; premature loss of deciduous teeth.	

2.7 Achondrogenesis

Achondrogenesis is a lethal type of osteochondrodysplasia, a disorder that affects both cartilage and bone development. Three types of achondrogenesis have been classified according to the effects of the individual and pathogenesis: achondrogenesis Type 1A (Houston-Harris type), achondrogenesis Type 1B (Fraccaro type) and achondrogenesis Type II (Langer-Saldino type). In all types the afflicted individual is either stillborn or dies within a few hours after birth (Spranger et al. 2002).

Skeletal manifestations of bowing of the long bones have been documented for only achondrogenesis Type 1A (Spranger et al. 2002; Borochowitz et al. 1988). Genetic inheritance is likely autosomal dominant (Spranger et al. 2002). Early diagnosis has been made in a fetus of 14 weeks gestation that showed changes in cartilage formation (Aigner et al. 2006). The tubular bones are described as being extremely short with slight concavity at the ends (Figure 2-11). Projecting spurs can develop at the periphery of the metaphyses. Bowing is mostly seen in the femora, radii and ulnae (Spranger et al. 2002).

Figure 2-11: Achondrogenesis of an infant after 30 weeks gestation. The long bones are severely shortened, with abnormal formation of a tubular shape and spurs projecting from diaphyses. The thorax is barrel-shaped, with thin and splayed ribs. The vertebral bodies are not ossified nor are the pubic bones (adapted from Spranger et al. 2002: 8).

Achondrogenesis Type 1A can also deform the pelvic bones. The iliac bone has a reduced vertical diameter, while the pubic and ischial bones are not ossified correctly. The thorax is barrel-shaped. The ribs are short with splayed ends and usually show multiple fractures. Ossification of the vertebral bodies and sacrum is retarded (Spranger et al. 2002). There have also been reported cases of encephalocele of the occipital (Chen et al. 1996). The archaeological record has not yet revealed any cases of achondrogenesis. Presented below is a summary table of the skeletal manifestations associated with achdonrogenesis (Table 2-4).

Table 2-4: Skeletal and soft tissue abnormalities of achondrogenesis.

Achondrogenesis type	Skeletal abnormalities	Soft tissue abnormalities
Type 1A	**Limbs**: Bowed, usually femora, radii and ulnae; short with concave ends; projecting spurs on periphery of metaphyses. **Skull**: Large head; encephalocele may occur. **Thorax**: Barrel-shaped; horizontally oriented; short ribs with splayed ends; fractured ribs. **Spine**: Absent or abnormal ossification of vertebral bodies and sacrum. **Pelvis**: Small iliac bones with reduced vertical diameter; abnormal ossification of pubic and ischial bones.	Short trunk; prominent abdomen; large head; chubby cheeks; small nose and mouth; flipper-like arms and legs
Type IB	**Limbs**: Very short; distal pointing of humeri. **Thorax**: Barrel-shaped; horizontally oriented; short ribs with splayed ends; small scapulae. **Pelvis**: Small iliac, irregular contours; failure of ossification of lower ilia, pubic and ischial bones.	Micromelia
Type II	**Limbs**: Very short; metaphyseal flare and cupping. **Skull**: Flat midface; micrognathia; cleft palate. **Thorax**: Barrel-shaped; short ribs **Spine**: Absence or abnormal ossification of vertebral bodies; lacking ossification of sacrum. **Pelvis**: Iliac bones have crescent-shaped inner and inferior margins; abnormal ossification of pubic and ischial bones.	Flat midface; micrognathia; prominent abdomen; short trunk

2.8 Thanatophoric Dysplasia

Thanatophoric dysplasia is categorized as either Type 1 or Type 2, according to the differential symptoms and pathogenesis. Both types of thanatrophoric dysplasias are caused by mutations in a gene that is responsible for growth factor receptors for fibroblast growth, which affects the structural integrity of connective tissues (Tavormina et al. 1995). Genetic transmission is autosomal dominant and individuals are either stillborn or die within the first hours or days due to respiratory failure (Spranger et al. 2002).

Only Type 1 thanatrophoric dysplasia, the more common of the two types, is known to cause bowing in the tubular bones (Spranger et al. 2002; Li et al. 2005).

Diagnosis of the disease has been made as early as 12 weeks gestation with diagnostic features of translucency of the skull and short limbs (Wong et al. 2008). The long bone shape is short and broad, with bowing and flaring at the metaphyseal end. The femora are described as being curved in the shape of telephone receiver, while in Type 2 the long bones are long and straight (Yang et al. 1976; Li et al. 2005). The literature mentions only the femora being affected by Type 1 and no other long bones. Other skeletal deformities involved with Type 1 are shortened ribs, small facial bones, deformity of the pubic bones, large calvaria, with a possibility for a cloverleaf shape skull deformity (Figure 2-12) (Spranger et al. 2002). A summary of the skeletal abnormalities associated with both Type 1 and Type 2 thanatrophoric dysplasia is presented on Table 2-5.

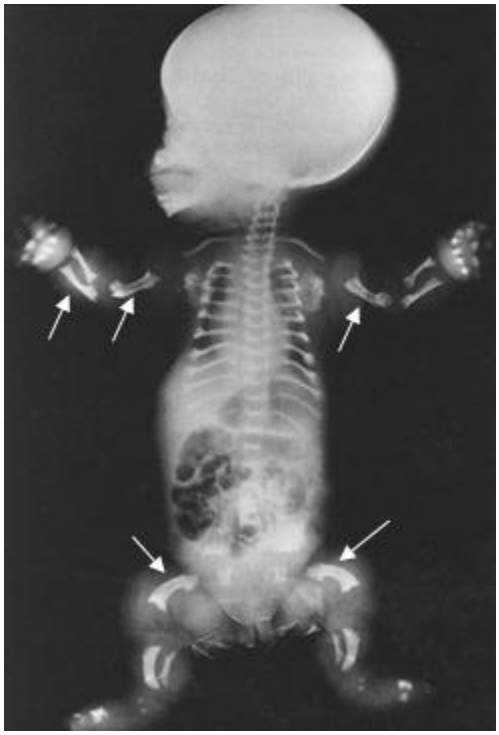

Figure 2-12: Thanatophoric dysplasia of a newborn that died after 36 hours. The long bones are short, bowed with flaring metaphyses. The thorax is extremely narrow due to short ribs. The vertebral bodies are flat. The pelvis is short and broad. Large calvarium with small facial bones is evidenced (adapted from Spranger et al. 2002: 5).

Table 2-5: Skeletal and soft tissue abnormalities of thanatophoric dysplasia.

Thanatophoric dysplasia type	Skeletal abnormalities	Soft tissue abnormalities
Type 1	**Limbs**: Bowed, usually femur; flaring at metaphyses. **Skull**: Large calvaria; small facial bones; cloverleaf skull, not always. **Thorax**: Narrow due to short ribs. **Spine**: Flattening of ossification centers of vertebral bodies. **Pelvis**: Decreased vertical diameter and horizontal inferior margins of iliac bones; small sacrosciatic notch; short and broad pubic and ischial bones.	Protruding eyes; large head
Type 2	**Limbs**: Straight; flaring at metaphyses. **Skull**: Large calvaria; small facial bones; cloverleaf skull, more often than type 2. **Thorax**: Narrow due to short ribs. **Spine**: Flattening of ossification centers of vertebral bodies. **Pelvis**: Decreased vertical diameter and horizontal inferior margins of iliac bones; small sacrosciatic notch; short and broad pubic and ischial bones.	

2.9 Infantile Cortical Hyperostosis (Caffey's Disease)

Infantile cortical hyperostosis (ICH) usually occurs in infants younger than 5 months, but the condition has also been reported in fetuses. This prenatal form has severe consequences and is lethal due to respiratory failure (Spranger et al. 2002; Pomerance et al. 2005; Wright et al. 2005). Both infantile and prenatal forms involve cortical thickening (hyperostosis) of the affected bone. Cases involving prenatal patients have reported hyperostosis occurring on the long bones, ribs, scapulae, pelvis and mandible (Kamoun-Goldrat et al. 2008; Wright et al. 2005). Genetic transmission has been reported as both autosomal recessive and dominant (Spranger et al. 2002). The molecular

etiology of Caffey's disease is unknown (Pomerance et al. 2005; Kamoun-Goldrat et al. 2008).

In a clinical case of a fetus at 28.5 weeks gestation, ultrasonic studies showed short and irregularly defined humeri and lower limbs, and angulation of the femora (Kamoun-Goldrat et al. 2008). The thorax, pelvis and spine did not appear to be affected and a diagnosis was given of osteogenesis imperfecta Type II. Radiographic analyses revealed additional skeletal deformities not evidenced with ultrasound. Both the femora and humeri had an angulated shape, the diaphyses of the long bones looked bloated (hyperostosis), and other irregularities in shape were found with the ribs, vertebral bodies, mandible, and scapulae (Kamoun-Goldrat et al. 2008). Differences in the severity of prenatal ICH have been identified. Individuals presenting with more severe symptoms of ICH died during pregnancy, at birth or shortly after. Fetuses with milder symptoms were born at term and did not present any symptoms before 35 weeks gestation (Schweiger et al. 2003). In a sample study of 26 severely affected infants with prenatal symptoms of cortical hyperostosis, bowing or shortness of the limbs was detected as early as the 14th week of gestation, with an average bone changes usually seen at the 27th week of gestation (Figure 2-13) (Schweiger et al. 2003). In 81% of these cases, nearly all the long bones showed deformities in bowing or shortness (Schweiger et al. 2003).

Figure 2-13: Infantile cortical hyperostosis of a newborn. Note thick extremities due to hyperostosis of the bone and bilateral bowing of the femora. There is also hyperostosis of the scapulae and mandible (adapted from Spranger et al. 2002: 497).

There exists a reported case of two individuals with infantile cortical hyperostosis in the paleopathological literature (Rogers and Waldron 1988). A Roman-British infant from England showed periostitis (inflammation of the periosteum) throughout the entire skeleton that affected the long bones, ribs, scapulae, and mandible. Thickening of the cortices was also evidenced, especially of the ribs. A second infant from a Saxon or medieval cemetery showed multiple hyperostosis lesions on the skeleton, including the mandible, clavicle, skull and long bone diaphyses. Hyperostosis of the skull was patchy with a honeycomb appearance, most severe on the parietals (Rogers and Waldron 1988). Unfortunately photographic documentation of the infants is of too poor of quality to be included in the present study. The table below list the clinical and pathological abnormalities associated with infantile cortical hyperostosis (Table 2-6).

Table 2-6: Skeletal and soft tissue abnormalities of prenatal infantile cortical hyperostosis.

Skeletal abnormalities	Soft tissue abnormalities
Limbs Bowing Resorption of cortex with widening of medullary canal Diaphyseal expansion Bone bridges between bones Shortened Cortical hyperostosis **Skull** Cortical hyperostosis, usually of mandible **Thorax** Cortical hyperostosis usually of ribs, scapulae and clavicles **Pelvis** Cortical hyperostosis **Paleopathological abnormalities**: Hyperostosis throughout skeleton; skull has honeycomb appearance	Firm soft-tissue swelling of cheeks, jaws, scapular region, arms and legs; modern micrognathia; protuberant abdomen; thickened periosteum

2.10 Stüve-Wiedemann Syndrome (Schwartz-Jampel Syndrome, Type 2)

The Stüve-Wiedemann syndrome (SWS) has similar clinical findings to Schwartz-Jampel syndrome (SJS) Type 2 (prenatal form) and both are referred by either name (Superti-Furga et al. 1998) and will be treated together in this section. Although very similar, there are some radiographic differences in the bone changes with each disease, with SJS having flat vertebrae, while SWS demonstrates normal vertebral bodies and more prominent osteopenia (low bone mineral density) (Spranger et al. 2002). In most cases SWS can lead to death unless the individual is has assisted ventilation and tube feeding. Death usually occurs during the first months (Spranger et al. 2002). Genetic transmission is autosomal recessive but the molecular etiology of the disease is

not specifically known, although a significant amount of mutations have been identified (Langer et al. 2007).

According to Spranger and colleagues (2002), SWJ is considered a skeletal dysplasia with prominent diaphyseal involvement. At birth an individual will demonstrate features of bowing of the tubular bones, most notably the femora and tibiae (Spranger et al. 2002). In a study of 11 individuals suffering from SWJ, bowing of the lower extremities, especially of the tibiae, was reported in all cases (Al-Gazali et al. 1996). Camptodactyly (bowing of the finger bones) was also evidenced in all cases. Other deformities of the long bones include cortical thickening at the medial aspects of the midshafts, shortening, and widening of the metaphyses with striation due to osteoporosis (Figure 2-14) (Spranger et al. 2002; Superti-Furga et al. 1998). The abnormalities most commonly associated with SWS are presented on Table 2-7.

Figure 2-14: Stüve-Wiedemann syndrome of a 3 day-old newborn. Note the severe bowing and broadening of the femora. Also note cortical thickening at medial aspect of diaphyses and demineralization at the metaphyses (adapted from Langer et al. 2007:205).

Table 2-7: Skeletal and soft tissue abnormalities of Stüve-Widemann syndrome.

Skeletal abnormalities	Soft tissue abnormalities
Limbs	Micrognathia
Bowed long bones, usually femora and tibiae	Small mouth
Shortening of long bones	Pursed lips when crying
Talipes equinovarus (club feet)	
Cortical thickening at medial aspect	
Osteopenia of metaphyses	
Camptodactyly	
Skull	
Micrognathia	
Spine	
Undermineralized vertebral bodies	
Pelvis	
Hypoplasia of lower portions of ilia; flared iliac wings	

2.11 Discussion

As Mays (1998) explains, a thorough knowledge of the range of diagnostic features presented on a skeletally diseased individual is needed in order to establish a starting point for reaching a possible diagnosis of the affliction. In the case of skeletal remains that show congenital bowing of the long bones, one is able to construct a lengthy differential diagnosis based only on the campomelic dysplasia. Differentiation of those selected disorders and probable diagnosis of what afflicted an individual is possible by comparing other skeletal deformities and variations of the campomelic affect on the long bones.

As presented, bowing of the long bones is a characteristic of the disorders of campomelic dysplasia, osteogenesis imperfecta, hypophosphatasia, achondrogenesis, thanatophoric dysplasia, infantile cortical hyperostosis, and Stüve-Wiedemann syndrome. Differentiation of each disorder is immediately possible, even if multiple skeletal parts are not available (Table 2-8). Several features set campomelic dysplasia apart from the other dysplasias. The mandible, tibiae, scapulae, and pelvis have all been reported as hypoplastic (underdeveloped) but still mineralized. Hypoplasia is not a symptom of the other listed disorders, but underdevelopment is evidenced in the form of undermineralization of bone structures which is a major feature of osteogenesis imperfecta and hypophosphatasia.

Table 2-8: Differential Diagnosis of Disorders Causing Congenital Bowing of the Long Bones Based on Clinical and Archaeological Findings

Disease/Condition	Limbs	Skull	Thorax	Spine	Pelvis
Campomelic Dysplasia (Mansour et al. 1995; Spranger et al. 2002)	Usually anterolateral bowing of femora and tibiae; hypoplastic fibula; dislocation of radial heads; delayed ossification of distal femoral and proximal tibial epiphyses; Short first metacarpals; Short middle phalanges of 2nd – 5th	Micrognathia (small jaw); Scaphocephaly (long and narrow); cleft palate; flat nasal bridge; hypoplastic mandible	Small bell-shaped thorax; eleven pairs of ribs; hypoplastic scapulae; delayed ossification of sternum	Scoliosis; kyphoscoliosis; hypoplastic cervical vertebrae; Hypoplastic thoracic vertebral pedicles	Dislocation of hip; narrow iliac bones; hypoplastic pubic bones
Osteogenesis Imperfecta (Sillence et al. 1984; Young et al. 1987; Spranger et al. 2002)	Anterorlateral bowing of all limbs; multiple fractures, callus Type IIA: Thick, short, crumpled shafts; femora has wavy accordion-like appearance Type IIB/III Short long tubular bones, thicker; broad metaphyses; thinner diaphyses Type IIC Thin and twisted	Type IIA Large head; soft calvaria; wide fontanels; wormian bones Type IIB/III Frontal and temporal bossing; wide open fontanels; wormian bones Type IIC Large head; soft calvaria; Demineralization of facial bones	Type IIA Short, thick ribs with beading Type IIB/III Thin ribs with discontinuous fractures Type IIC Varying thickness and discontinuous beading of ribs; Distorted and irregularly ossified scapulae	Type IIA Flat and irregularly deformed Type IIB/III Compressed vertebral bodies Kyphoscoliosis (later in life) Type IIC Almost normal spine Spine is well ossified Vertebral bodies are normal height	Type IIA None noted Type IIB/III None noted Type IIC Long, angulated ischial bones
Hypophospatasia (Shohat 1991; Spranger et al. 2002; Cole 2003)	Usually bowing of all limbs; short and thin tubular bones; irregular metaphyseal ossification; metaphyseal cupping; osseous spurs extending from midshafts	Failure of ossification of the calvaria, skull base and face	Short and thin ribs; poor ossification; complete lack of ossification of rib; fractures of ribs	Poor ossification of vertebrae; usually the neural arches; some vertebrae not ossified; vertebral bodies rectangular/round; flattened, or sagittally clefted	Small pelvic bones with ossification defects; bending of pelvis

Disease/Condition	Limbs	Skull	Thorax	Spine	Pelvis
Achondrogenesis, Type IA(Chen et al. 1996; Spranger et al. 2002)	Bowing of tubular bones, usually femur, radius and ulna; short with concave ends; projecting spurs on periphery of metaphyses	Large head; encephalocele may occur	Barrel-shaped thorax; horizontally oriented; short ribs with splayed ends; fractured ribs	Absent or abnormal ossification of vertebral bodies and sacrum	Small iliac bones; reduced vertical diameter; abnormal ossification of pubic and ischial bones
Thanatophoric Dysplasia (Spranger et al. 2002; Li et al. 2005)	Bowed long tubular bones, usually femora Short; flaring at metaphyses	Small facial bones; large calvaria; Cloverleaf skull, not always	Narrow thorax due to short ribs	Flattening of ossification centers of vertebral bodies	Decreased vertical diameter and horizontal inferior margins of iliac bones; small sacrosciatic notch; short and broad pubic and ischial bones
Infantile cortical hyperostosis (Spranger et al. 2002)	Bowing of the limbs, usually femora, humeri; shortening; thickened due to hyperostosis	Cortical hyperostosis of the mandible; macrocephaly in some cases	Cortical hyperostosis of ribs, scapulae and clavicles; Irregularly shaped ribs	Usually spared	Cortical hyperostosis of pelvic bones
Stuve-Wiedemann syndrome (Spranger et al. 2002; Al-Gazali et al. 1996)	Bowed long bones, usually femora and tibiae; shortening; talipes equinovarus (club feet); cortical thickening at medial aspect; osteopenia of metaphyses; camptodactyly	Micrognathia		Undermineralized vertebral bodies	Hypoplasia of lower portions of illia; flared iliac wings

Skeletal features of individuals affected by osteogenesis imperfecta are best distinguishable by the lack of mineralization, the presence of wormian bones, fractures, and callus formations. Differentiating OI from other disorders with similar bowing of the long bones can prove to be a difficult task, particularly in a differential diagnosis between campomelic dysplasia, hypophosphatasia and the varying types of OI, which are all remarkably similar (Sanders et al. 1994). The campomelic deformities characteristic of osteogenesis imperfecta occur differently for each type (Unger et al. 2003; Cheema et al. 2003; Bulas et al. 1994), although some report that Type I OI does not show bowing of the bones (Plotkin et al. 2003).

As listed on Table 2-8, the skeletal abnormities of osteogenesis imperfecta are also distinguishable between different OI types. With this information, one can review the skeletal abnormalities of the 2-year old child from the site of Speos Artemeidos in Egypt, which Gray (1969) reports as having anterolateral bowing of the long bones with thickening, underdeveloped amber colored teeth (dentinogenesis imperfecta), overall lightness and fragility of the bones, and an expanded cranial vault with several wormian bones. All the skeletal abnormalities match with Type IIB/III OI. Although Type I OI is a possibility due to the older age of the individual (Type IIB/III individuals have been able to live past infancy), the large cranial vault is not a symptom of Type I OI and neither are the thickened long bones. The case reported by Ortner (2003) involving a late adolescent individual that showed narrow long bones and the low osteon count, indicating a defective intramembranous bone formation, is most similar to the symptoms of OI Type I, as this type presents with a thin diameter of the bones that typically does not disrupt stature. In addition bowing and fractures are not normally seen at an

adolescent age, which is also consistent with a lack of these symptoms with Ortner's (2003) archaeological case (Spranger et al. 2002).

Hypophosphatasia can act very similar to osteogenesis imperfecta; if only bowing of the long bones and undermineralization is evident (fractures have also been reported for hypophosphatasia). But in the most severe cases of hypophosphatasia (prenatal form) the skeleton is grossly undermineralized, especially at the metaphyseal ends in which "punched-out" irregularities can occur (Spranger et al. 2002). A number of clinical sources have commented on a misdiagnosis of infantile cortical hyperostosis with osteogenesis imperfecta due to the severely angulated long bones that are evidenced by ultrasound (Pomerance et al. 2005; Wright et al. 2005; Kamoun-Goldrat et al. 2008). Radiographs of the individual eventually reveal the lack of fractures and sclerotic bone on the long bones that is typically seen with infantile cortical hyperostosis (Kamoun-Goldrat et al. 2008). In the case of a paleopathology, analysis is more than likely to involve skeletal remains, allowing for a more distinguishable analysis of the symptomatic features on the bony surface.

Achondrogenesis of the limb bones is quite similar to that of hypophosphatasia, due to the bowing and projecting spurs. These two disorders are distinguishable by their longer and thinner tubular bones of hypophosphatasia rather than the thicker and shorter bones of achondrogenesis. With additional skeletal parts, hypophosphatasia is clearly identifiable by the poor ossification affecting practically all bony parts, especially the calvaria. Additionally, thanatrophoric dysplasia is best discernible by the short, broader tubular bones without spurs, narrow thorax, and the overall mineralized skeleton.

2.12 Summary

Although most of the listed disorders on Table 2-8 are in reference to clinical cases with most skeletal observations deriving from radiographic sources, Ortner (2003) explains that the inclusion of radiographic studies in paleopathology allow for further documentation of abnormal diagnostic features by revealing evidence that is otherwise not apparent from gross analysis. In the same sense, features evidenced on the bone surface are dissimilar to what is documented in the clinical literature (Ortner 1991). As such, careful observation which is inclusive of exact recording of the skeletal abnormality on the bony surface is an imperative and a required process when conducting a paleopathological assessment (Ortner 2003).

When first developing a differential diagnosis, the observer must keep in mind any and all techniques in gathering sources of data and the feasibility of these methods (Pinhasi and Mays 2008). As discussed earlier, the inclusion of histological or DNA analysis is dependent on monetary and equipment resources, but also in the preservation of the skeletal remains as these methods often require destruction of the remains for analysis (Pinhasi and Mays 2008), thus their inclusion is not likely within a paleopathological study. The application of multiple sources of information is important in developing reasoned paleopathological interpretations (Ortner 2003; Pinhasi and Mays 2008) and some of these sources are available through the clinical literature. The differential diagnosis of long bone bowing discussed within this present study, although not inclusive of microscopic or chemical analysis, utilizes radiographic and soft tissue

analysis of medical cases and the gross morphology of paleopathological cases as a means differentiating between the selected disorders.

Overall, the criteria listed in Table 2-8 help create an exhaustive list of all possible symptoms associated with congenital bowing of the long bones and pinpointing the effects of a disease on specific bony elements. As evidenced from the differential diagnosis, the entire skeleton is not needed when assessing a diagnosis. A lack of major skeletal parts is an often common occurrence for archaeological specimens. Additionally, the inclusion of clinical data does not limit to the occurrence of a pathology to just paleopathological cases. The more exhaustive one is when developing a differential diagnosis, the less likelihood for hasty and narrow conclusions (Lewis and Flavel 2007). In the next chapter the differential diagnosis of congenital long bone bowing developed here will be used for the assessment of two archaeological fetal remains.

CHAPTER 3: PATHOLOGICAL LONG BONE BOWING IN THE ARCHAEOLOGICAL RECORD: ASSESSMENT OF TWO FETAL INDIVIDUALS FROM EGYPT

3.1 Introduction

The representation of fetal skeletons in the archaeological record is lacking and numbers are even lower for those presenting with a pathological condition (Malgosa et al. 1996; Lewis 2007). Fragility of the fetal skeleton, failure to recognize the fetal skeleton, funeral rites and burial customs of diseased fetuses (Tocheri et al. 2005), and a lack interest in the importance of fetuses and children in population studies (Malgosa et al. 1996; Lewis 2007; Halcrow and Tayles 2008) are all reasons which have led to an underrepresentation of subadults in the anthropological literature. Despite these exclusions, in recent years there has been growing attention paid to younger individuals, as their study has revealed new patterns in the health of a population and cultural attitudes attributed to fetal death (Lewis 2007; Halcrow and Tayles 2008).

Two fetal skeletons from the Kellis 2 cemetery (Roman period circa A.D. 50 — A.D. 450) in the Dakhleh Oasis, Egypt, present congenital skeletal anomalies that may explain their premature death. Congenital diseases are present at birth and may result from a genetic disorder, a developmental defect due to the intrauterine environment, or unknown factors (Mays 1998). Depending on the severity, a congenital disorder can be fatal at birth or a short time afterwards, while some individuals manage to survive the effects and live into adulthood, and still for others the expression of the disease occurs

later in life. In their study of the fetal and perinate (around the time of birth) remains from the Kellis 2 cemetery, Tocheri and colleagues (2005) attribute the majority of the fetuses as stillbirths and speculate that those who survived birth likely died within hours, days, or weeks. The authors do not discuss the specific etiology of the fetal deaths, as the purpose of the study was to develop an age distribution of the remains by metric analysis, so any skeletally deformed fetuses and perinates would have been excluded (Tocheri et al. 2005). The authors do speculate that incomplete lung development in the Kellis 2 stillborns, as evidenced in many modern cases of premature babies, would have led to respiratory failure or hyaline membrane disease.

Age at death assessments were conducted first for both specimens. Developing an age at death for the fetal individuals is important in not only relating their age cohort at Kellis 2, but also to assess their total development as this could be indicative of the severity of their abnormalities and pathologies that are a resultant of their age at death. Fetal specimens B532 and B625 exhibit bowing of the long bones in addition to other skeletal deformities. Measurements of long bone length constitute the primary methodology for estimating gestational age from fetal skeletal remains and rely on linear regression relationships (Ubelaker 1987; Lewis and Flavel 2007). Dental formation and eruption, although preferred for deriving an age estimate of subadult skeletons, is not a readily applicable method for fetal remains. Fetal teeth are easily lost during recovery due to their incompleteness, small size, fragmentation and open tooth crypts (Lewis 2007). Additionally, very few standards exist to correlate gestational age with development of the teeth in utero (Tocheri et al. 2005). Recently, though, several studies have revealed how reference samples (the sample of known age from with the linear

regression formulae originate from) enact their biases to a target sample (archaeological population of unknown age for which the age is being estimated), resulting in a mimicking of age distributions (Bocquet-Appel and Masset 1982; Gowland and Chamberlian 2002). This has led to alternative methods of age estimation from skeletal remains. One such approach by Gowland and Chamberlain (2002) uses Bayesian estimation methods and assumes realistic prior probabilities of fetal mortality to develop probabilities of age distributions of their target population from femoral length. The use of prior probabilities estimates a probability of an age rather than an exact age estimate, and eliminates the use of a reference sample enacting their age structure on the target sample. As previous studies at Kellis 2 (Tocheri et al. 2005) have effectively utilized posterior probabilities aging standards in determining age distributions, the same methodology is used for age estimations of both B532 and B625 fetal individuals.

The most severe long bone bowing is evident on B532, while B625 presents with less severe long bone bowing and more severe cranial malformations. The etiology of the cranial deformities of B625 is complicated by a lack of similar cases in the clinical and archaeological literature. In response, the differential diagnosis for both specimens is based on bowing of the long bones, with the expectation of finding a possible diagnosis that correlates with the accompanied skeletal deformities. The bowed long bones were used as the primary diagnostic pathological features for the differential diagnosis. Both macroscopic and radiographic analyses were used to determine the pathological abnormalities of each of these two individuals.

3.2 Materials and Methods

The fetal individuals investigated in this study are from the Dakhleh Oasis, one of five oases of Egypt (Figure 3-1) and one of the largest oases in Egypt's western desert. A multidisciplinary endeavor by the Dakhleh Oasis Project has been underway since 1977 in the Dakhleh Oasis, Egypt, where researchers are currently trying to understand the past life ways of the humans who inhabited the oasis and their relation to the changing environment of the harsh desert conditions (Mills 1999). Studies in bioarchaeology have focused on the human remains from the ancient village of Kellis (Ismant-el-Kharab), and the associated cemetery sites (Figure 3-1). Excavations have uncovered two cemetery sites, Kellis 1 (northwest) and Kellis 2 (northeast), together spanning a period of use from the late Ptolemaic to the Roman/Christian Period (Molto 2000; Molto 2002). Carbon-14 dating places the use of the Kellis 1 cemetery during the late Ptolemaic Period and the Kellis 2 cemetery in use during the Roman/Christian period, with calibrated radiocarbon dates from A.D. 50 to A.D. 450 (Tocheri et al. 2005). Stewart et al. (2003) has reported radiocarbon dates at Kellis 2 as late as A.D. 600. However, there is discordance with dates obtained for occupation of Kellis. Archaeological evidence from ceramics and Kellis 1 cemetery suggest the town of Kellis was initially occupied during the late Ptolemaic period and abandoned at the end of the fourth century (Hope 2001; Bowen 2003; Stewart et al. 2003; Dupras and Tocheri 2007). Based on the carbon-14 dates, the use of the Kellis 2 cemetery was in use later than the projected occupation dates of Kellis. Additionally, there is no archaeological evidence of individuals identifying as Christians before the mid-third century A.D. (Bowen 2003), yet Kellis 2 demonstrates Christian

burial traditions well before this time period. An earlier use of the cemetery is plausible if internment of the dead was by pagan individuals, although very little of pagan burial rituals have been found at Kellis 2 other than preparation of the body with resin (Dupras and Tocheri 2007). As the cemetery has not been fully excavated, additional representations of pagan burial rituals are possible. In reference to the later use of the cemetery, it has been suggested that people who were once occupants of Kellis, or those who lived nearby, may have migrated to the cemetery to bury their dead (Bowen 2003; Tocheri et al. 2005).

The combination of the arid environment of Egypt with the burial practices at Kellis 2 has resulted in the preservation of a large number of individuals, many of which are fetuses or neonates (Tocheri et al. 2005). The inclusion of fetal individuals, along with an east-west orientation of the body in a supine position with the head facing to the west, is similar to burial styles documented in other Egyptian Roman Period cemeteries (Parsche and Zimmerman 1991; Bowen 2003). Both fetal specimens of interest to this thesis were excavated from the Kellis 2 cemetery, from burial locations B532 and B625 (Figure 3-2). Both fetal specimens were found in the east portion of the excavated portion of the cemetery.

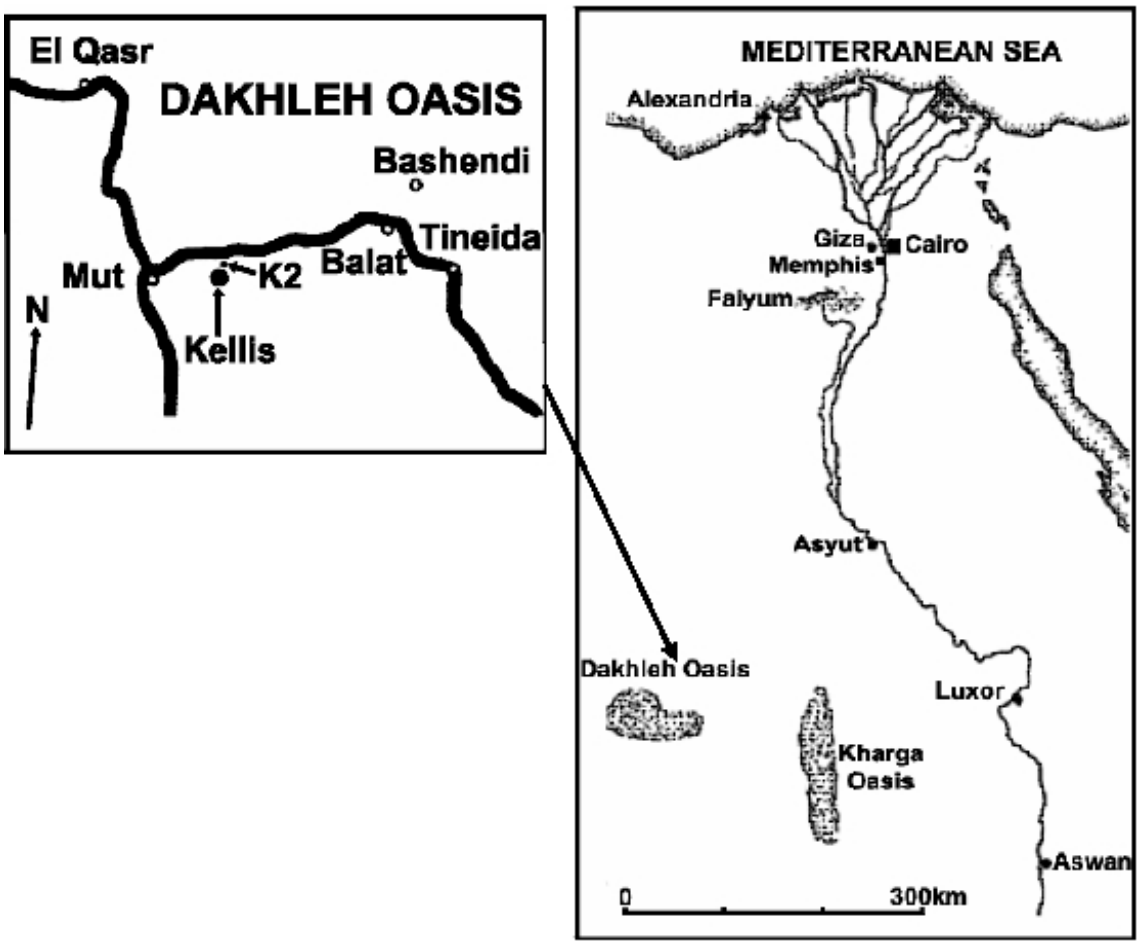

Figure 3-1: Location of the Dakhleh Oasis in Egypt, and Kellis 2 cemetery in Dakhleh (adapted from Tocheri et al. 2005: 328).

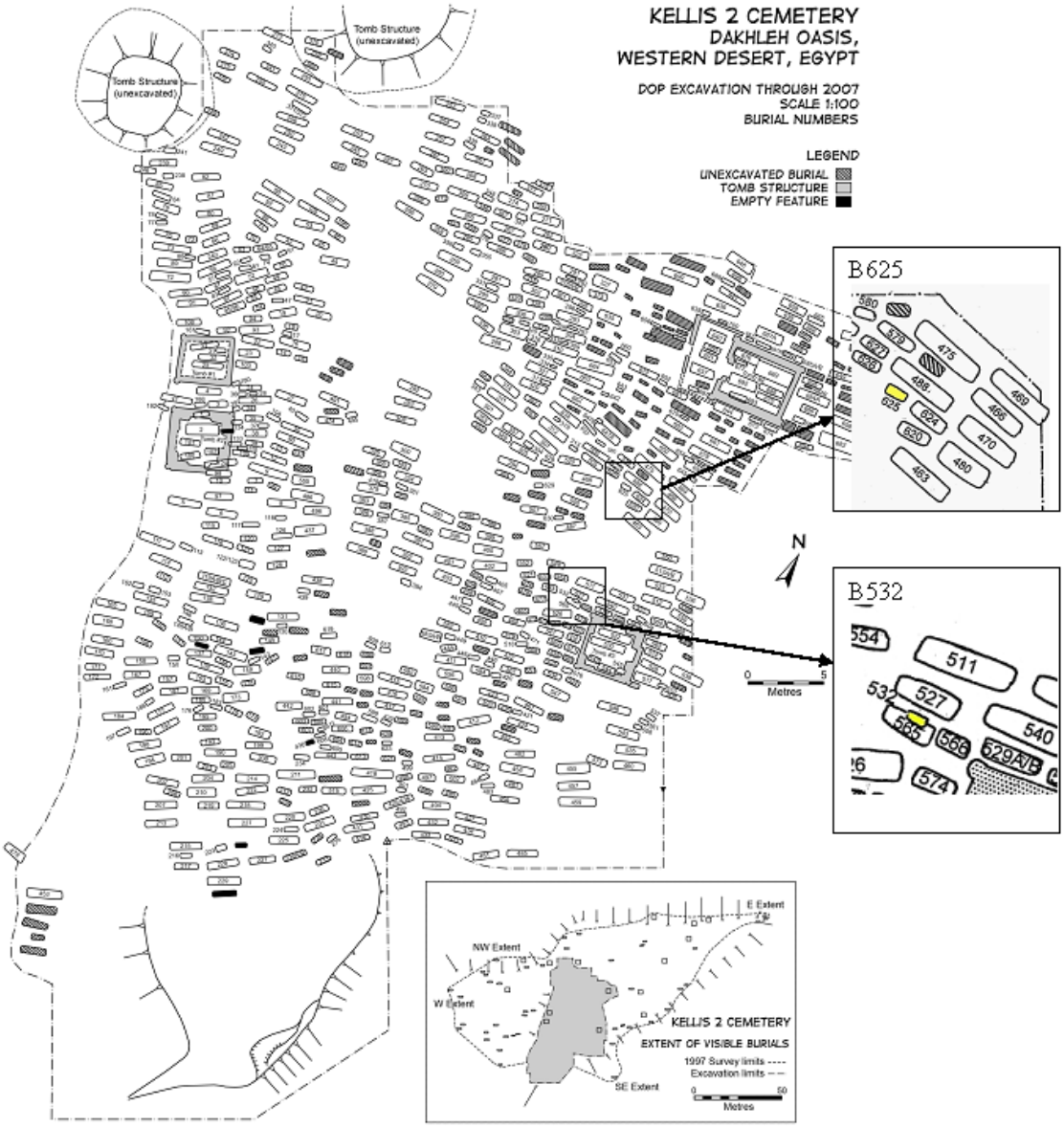

Figure 3-2: Kellis 2 cemetery. Insets show burial locations of B532 and B625 (map courtesy of Sandra Wheeler and Lana Williams).

Because of severe bowing of the long bones of B532 a correlation of actual long bone length and gestational age was not possible, thus alternative methods for aging had to be investigated. A cranial element that has shown promise in defining gestational age is that of the pars basilaris portion of the occipital. Growth of the pars basilaris bone, which is one of the four major bones that forms the foramen magnum, begins during the first trimester (0–14 weeks) and ossification typically begins in the 10th and 14th fetal weeks (Redfield 1970). The V-shape form is distinguishable at around 16 weeks (Scheuer and Black 2000) and fuses to the pars lateralis at about 6 years of age. Separate growth of the bone for a long period, from fetal age to childhood, and the tough resistant nature of the bone due to its robusticity, presents with a reliance on this bony element to provide for age at death estimates (Redfield 1970; Scheuer and MacLaughlin-Black 1994).

Several studies have revealed a positive correlation with age at death estimates and growth of the pars basilaris bone (Redfield 1970; Scheuer and MacLaughlin-Black 1994; Tocheri and Molto 2002). Studies by Tocheri and Molto (2002) at Kellis 2 revealed a correlation with age estimates when using osteometric measurements of the pars basilaris with age estimations from long bone length of fetal individuals and dental evidence for older individuals. There are three standardized measurements of the basilar bone (Figure 3-3): sagittal length (SL), maximum length (ML), and maximum width (MW). In examining the relationship of the three measurements of the pars basilaris bone, there is a consensus in the literature that when the sagittal length equals or exceeds the maximum width then the individual is younger than 32 weeks (Tocheri and Molto 2002). Alternatively, if the maximum width exceeds the sagittal length but not the maximum

length, the individual is probably older than 32 weeks. Finally, if the maximum width equals or exceeds the maximum length, the individual is likely 6 months or older of age (Tocheri and Molto 2002).

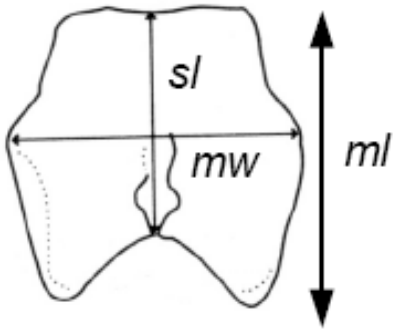

Figure 3-3: Measurements taken from the basilar bone: SL= sagittal length; ML= maximum length; MW=maximum length (illustration by Sandra Wheeler).

Determining that the fetal individuals are older or younger than 32 weeks leaves quite an unknown age at death and using death estimates from Fazekas and Kosa (1978) of the pars basilaris measurements imposes the pattern and rate of skeletal growth of their sample to the target sample (B532 and B625). Thus, it is better to use the pars basilaris measurements to predict long bone length and determine their posterior probability for age estimates. Because of the positive correlation of the pars basilaris with gestational age estimates from long bone length, there should also be a correlation with growth of long bones, as their lengths are the best determinates for the gestational age of fetal individuals.

In order to develop prediction formulae for the long bone lengths, the pars basilaris measurements are linearly related with long bone lengths of a sample population consisting of 37 fetal individuals from Kellis 2. Of these, 26 were measured by the

present author and 11 are based on previously published measurements (Tocheri and Molto 2002; Tocheri et al. 2005). Measurements of B532 and B625 as well as the sample population of fetal skeletons were taken with digital calipers calibrated to 1/10th of a millimeter and in accordance with the measurement standards provided by Fazekas and Kósa (1978). Measurements, consisting of cranial and postcranial elements (Appendix B) were limited by the preservation and abnormalities of each bone, and as such not all measurements were possible. For instance, B532's severe bowing of the femora did not allow for correct measurements. Long bone length measurements were possible for B625, although the right radius and both tibiae demonstrate bowing that could affect long bone length measurements. The actual and predicted femur lengths of B625 are both assessed for age at death estimation. Before estimating an age, the predicted femur lengths of each pars basilaris measurement are compared to the actual femur lengths of the Kellis 2 population sample. This comparison will determine which pars basilaris measurement is best linearly related to the growth of the femur, and thus provide for a more accurate age at death estimate.

As mentioned earlier, linear regression methods of long bone length for age at death estimation are dependent on the skeletal growth trends of the reference sample they originate from. When comparing three geographically dispersed archaeological sites with age distributions developed from linear regression formulae, Gowland and Chamberlain (2002) revealed a mimicking pattern of age distributions that correlated with the reference sample. This resulted in neonatal peaks of all three sites for individuals aged at 38 and 40 weeks gestation, an imitation of the peak ages from the reference sample (Gowland and Chamberlain 2002). To eliminate for the dependency of

reference samples, the predicted femur lengths of B625 and B532 were instead assessed for age by posterior probability analysis. Gowland and Chamberlain (2002) provide posterior probabilities of an age given the length of the femur. For example, a fetal individual with a femur length of 25 – 29.9 has a .84 posterior probability of 18 weeks and .16 for 20 weeks. Their posterior probabilities were developed from model prior probabilities which use prior knowledge of the mortality risk of each gestational age given a model life table that is based on natural patterns of mortality. Thus, posterior probabilities of age are concerned with attributing an age range of probabilities rather than an exact age for an individual, and eliminate a dependency on a reference sample's age structure on a target sample (Gowland and Chamberlain 2002: Tocheri et al. 2005).

A macroscopic assessment of the fetal skeletons was conducted to document all skeletal deformities. The more prevalent abnormalities were recorded and these data are presented in Figures 3-10 and 3-19. Digital photographs of the entire fetal skeletons (Figures 3-9 and 3-18) and specific bones presenting with pathological conditions are shown in Figures 3-11 to 3-16 for B532 and Figures 3-20 to 3-32 for B625. Radiographs for each specimen were assessed for bone deformities otherwise not observable on the bone surface. The radiographs were taken at the University of Western Ontario using a Faxitron X-ray Cabinet System with Kodak EC1 medical quality film. No screens were utilized as image quality was found to be superior without[1].

There are number of pathologies that can result in curvature of the long bones. For B532 and B625, the congenital occurrence of the bowing and possible lethality of the afflicting pathology can serve as a means of developing a list of possible diseases.

[1] Radiographs provided by Sandra Wheeler, a member of the Dakhleh Oasis Project who is also assessing the subadult remains from Kellis 2

The differential diagnosis developed in the previous chapter will serve as the differential diagnosis for the paleopathological specimens, which include the following diseases: campomelia dysplasia, osteogenesis imperfecta, hypophosphatasia, achondrogenesis type IA, thanatrophoric dysplasia, infantile cortical hyperostosis, and Stüve-Wiedemann syndrome. All the pathologies selected for the differential diagnosis are considered rare and their occurrences in the archaeological record even more of a rarity. The manifestations of these diseases, and many others found within the clinical literature, are not always represented in the archaeological record (Ortner 2003). Only two of the selected diseases have documented archaeological cases, osteogenesis imperfecta (Wells 1965; Gray 1969; Ortner 2003) and infantile cortical hyperostosis (Rogers and Waldron 1988). Despite the selection of these diseases in deriving a probable syndrome diagnosis, it is important to note that not all symptoms will match a disease presented in a differential diagnosis.

3.3 Estimation of Age at Death

The table presented in Appendix C shows the long bone lengths and pars basilaris measurements of the 37 fetal skeletons of the Kellis 2 sample population. Exact age estimates of each fetal individual are also documented from the mean of 11 linear regression formulae for age estimation from the long bones. These age estimates are not used in determining predicted long bone length, but are presented within the table to show an age distribution of the fetal individuals involved in the population sample. Age estimates range from 24 to 42 fetal weeks. Linear regression formulae and their

coefficient of determination, R^2, values for prediction of long bone length from each of the pars basilaris measurements of the Kellis 2 population sample are presented on Table 3-1. It is evident from Table 3-1 that the sagittal length presents with the lowest R^2 values (except in the instance of the humerus) and could be indicative of a lack of correlation with long bone length. This is clearly seen when B532 and B625 are estimated for long bone lengths (Table 3-2, 3-3, 3-4). In comparing the long bone estimates from the sagittal length to those of maximum length and width, estimates were off by as much as 13.7 mm and only 2.7 mm when comparing between maximum length and width.

Table 3-1: Formulas and R^2 values for prediction of long bone length by each of the pars basilaris measurements.

Long Bone	Sagittal Length		Maximum Length		Maximum Width	
	Formula	R^2 value	Formula	R^2 value	Formula	R^2 Value
Humerus	6.4482x - 13.922	0.7999	4.2463x - 1.8237	0.8314	3.1134x + 17.328	0.7947
Ulna	5.3528x - 6.0352	0.7303	3.5642x + 3.4468	0.7636	2.7528x + 17.714	0.7762
Radius	4.6545x - 4.3749	0.729	3.0899x + 4.024	0.7617	2.3916x + 16.333	0.7776
Femur	8.1022x - 25.042	0.7785	5.3337x - 9.6676	0.8019	4.0331x + 12.872	0.7816
Tibia	6.8327x - 19.128	0.7613	4.4767x - 6.0237	0.7818	3.4366x + 12.232	0.7822
Fibula	5.9205x - 10.746	0.6725	3.8761x + 0.8011	0.7216	2.911x + 17.251	0.6831

Table 3-2: Long bone estimations from sagittal length of the pars basilaris.

Burial #	Sagittal Length (mm)	Long bone estimate (mm)					
		Humerus	Ulna	Radius	Femur	Tibia	Fibula
B532	13.3	71.8	65.2	57.5	82.7	71.7	68.0
B625	10.8	55.7 (62.7)[1]	51.8 (57.5)	45.9 (50.7)	62.5 (76.6)	54.7 (65.3)	53.2 (61.8)

[1]Number in parenthesis indicates actual long bone length measurements for B625

Table 3-3: Long bone estimations from maximum length of the pars basilaris.

Burial #	Maximum length (mm)	Long bone estimates (mm)					
		Humerus	Ulna	Radius	Femur	Tibia	Fibula
B532	14.9	61.3	56.6	50.1	69.8	60.7	58.6
B625	15.9	65.5 (62.7)[1]	60.1 (57.5)	53.2 (50.7)	75.1 (76.6)	65.2 (65.3)	62.4 (61.8)

[1]Number in parenthesis indicates actual long bone length measurements for B625

Table 3-4: Long bone estimations from width of the pars basilaris.

Burial #	Maximum width (mm)	Long bone estimate (mm)					
		Humerus	Ulna	Radius	Femur	Tibia	Fibula
B532	14.8	63.2	58.5	51.7	72.7	63.1	60.3
B625	15.7	66.01 (62.7)[1]	60.9 (57.5)	53.9 (50.7)	76.2 (76.6)	66.2 (65.3)	62.9 (61.8)

[1]Number in parenthesis indicates actual long bone length measurements for B625

Because of the differences in measurement predictions of long bone lengths for the fetal individuals, it is necessary to establish which pars basilaris measurement is the best indicator for long bone length specifically that of femur length as this length will reveal posterior probabilities of age according to Gowland and Chamberlain (2002). The results of sagittal length are not surprising, as the sagittal length is a good age indicator

only when held in view as a ratio with width. This is due to the differential growth of the three measurements, with the sagittal and maximum lengths remaining relatively constant and somewhat static, and most evident with sagittal length (Scheuer and MacLaughlin-Black 1994). This indicates that the lengths reach a maximum growth despite the continued growth of other bones, in this case the femora. Alternatively, the width has been shown to retain a continued rate in its growth that is in response to the increased growth of the skull base (Scheuer and MacLaughlin-Black 1994). When applying predictions of femur lengths to the Kellis 2 population sample of 37 fetal individuals (Table 3-5), the differentiation between the three measurements is observable. Predictions of femur length from the sagittal length do not demonstrate a trend that is in correlation with the actual femur lengths, with some estimates as far off as 32.8 mm. When comparing the predictions of maximum length and width, noticeable trends reveal how each of these measurements is correlating with femur growth. The maximum length is overestimating on femur lengths in younger individuals and underestimating in older individuals. This suggests the maximum length is following its own trend, rather than that of growth of the femur length. When comparing the predicted femur lengths derived from the maximum width with the actual femur widths, there is differentiation in overestimation and underestimation across all femur lengths and is thus indicative of a trend that is more linearly related to the growth of femur length. As such, the maximum width is the best predictor for estimating the length of the femur, an outcome that is supported by its more dynamic and consistent growth (Scheuer and MacLaughlin-Black 1994).

Table 3-5: Comparison of predicted femur lengths to actual femur lengths of the Kellis 2 population sample.

		Femur predictions from pars basilaris measurements (mm)		
Burial #	Actual femur length (mm)	Sagittal length	Maximum length	Maximum width
334	35.3	68.1	43.1	41.9
298	41.8	45.4	47.4	56.0
316	42.9	54.8	51.7	48.2
332	49.5	54.0	53.3	49.4
180	50.9	43.4	46.3	46.1
319	54.8	60.8	57.5	53.4
318b	62	64.1	64.5	64.7
701	62.2	66.5	51.7	65.3
575b	62.8	64.9	65.5	61.3
436	65.1	67.3	59.7	68.9
297	67.3	70.6	69.8	66.5
154	68.7	67.3	68.7	72.6
601	69.6	69.8	69.8	71.8
209	70.0	67.3	69.3	73.0
462	70.2	72.2	76.2	65.7
387	70.3	74.6	80.5	74.6
333	71.2	68.1	69.5	71.2
568	71.4	69.8	69.3	64.9
572	71.7	69.8	67.7	70.5
338	72.1	64.1	72.2	71.6
419	72.3	74.6	81.0	83.5
608	72.6	55.2	70.9	67.3
449	72.9	75.4	71.4	68.5
513b	73.1	75.4	73.0	70.5
153	73.8	81.1	80.2	79.8
446	75.2	74.6	76.2	71.8
599	75.4	62.5	68.7	68.1
616	76.5	78.7	73.5	80.2
605	76.6	77.0	71.4	76.2
558	76.8	68.1	73.0	77.0
151	77.2	80.3	76.2	67.3
660	77.9	71.4	73.5	76.6
445	79.4	72.2	70.3	69.3
508	80.3	69.8	75.1	81.8
348	81.3	83.5	82.6	75.4

Shown on Table 3-6 are the results of the posterior probabilities of the predicted femur lengths from the maximum width of the pars basilaris of B532 and B625, in addition to the actual femur length of B625. These probabilities were assessed from the posterior probabilities of age given femur length based on model prior probabilities of age from Gowland and Chamberlian (2002: Table 5). The results indicate that predicted femur lengths of B532 has an age range between 36 and 44 weeks, with the highest probability of .47 for 38 weeks and B625 has an age range between 38 and 44 weeks, with the highest probability of .64 for 40 weeks.

Table 3-6: Posterior probabilities of age given femur length of B532 and B625.

Burial #	Predicted Femoral Length	Prior Probability of age category by femoral length				
		36 weeks	38 weeks	40 weeks	42 weeks	44 weeks
532	72.6	.19	.47	.25	.08	.01
625	76.2 (76.6)[1]		.15	.64	.19	.03

[1]Number in parenthesis indicates actual long bone length measurements for B625

Previous studies of Kellis 2 fetal individuals have reported on the proportion of fetal individuals and their age distributions in accordance with posterior probability of age (Tocheri et al. 2005). When comparing the posterior probabilities of B532 and B625 to the proportion of fetal individuals found at Kellis 2, their highest probabilities of 38 and 40 weeks, respectively, corresponds to the ages that have mostly represented at Kellis 2. This is indicative that B532 and B625 would most likely correspond to these age categories given the higher posterior probability of 38 and 40 weeks of gestation.

3.4 Pathological Analysis of Burial 532

Upon excavation, fetal individual B532 appeared to be a unique and unusual case in that its burial position is not typical as compared to that of other Kellis 2 fetal individuals. A typical fetal/infant burial at Kellis 2 is oriented east-west with the body lying on its back in an extended position (Figure 3-4). Burial 532 was found lying on its side with the femora bent anteriorly, towards the chest, and the lower leg bones bent posteriorly (Figure 3-5).

The individual displays pathological skeletal characteristics, particularly exaggerated curvature of the long bones and a barrel-shaped ribcage (Figure 3-6). All the long bones of B532 were recovered as were most of the remaining postcranial elements. Unfortunately, the cranial vault elements suffered intensive postmortem damage resulting in fragmentation. The occiput, in addition to the unfused basilaris and lateral parts of the occiput, are the cranial vault bones with the best preservation. The denser skull elements, such as the petrous portions, zygomatics, and mandible were also found intact. Bone composition is very brittle with a light beige coloration, which is not the "norm" for fetal skeletons excavated from Kellis 2. Burial notes at the time of excavation detail the location of the specimen close to the surface, directly underneath a layer of sand. Taphonomic processes such as wind and sun erosion may have altered the preservation of the individual. Distributions of the most obvious deformities are diagramed and include bowing, narrow medullary cavities, underdevelopment of cortical bone, and fractures (Figure 3-7).

Figure 3-4: Typical infant burial at Kellis 2 cemetery (courtesy of Dakhleh Oasis Project).

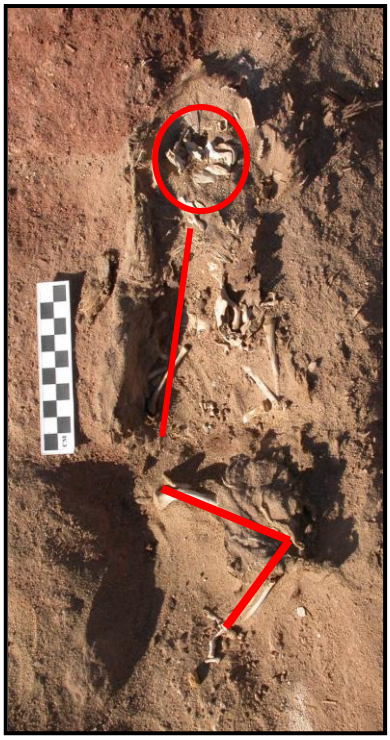

Figure 3-5: Abnormal burial position of B532 (courtesy of Dakhleh Oasis Project).

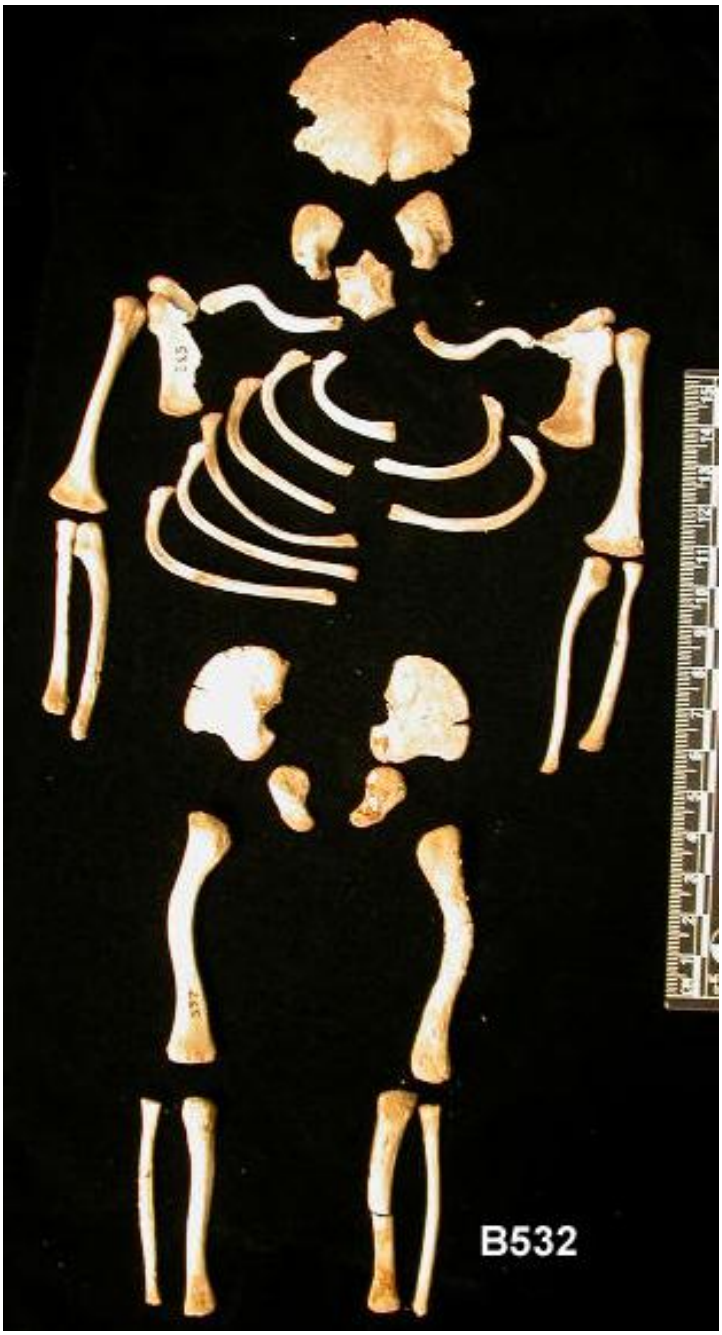

Figure 3-6: Anatomical view of B532. Note the curved long bones and barrel-shaped ribs.

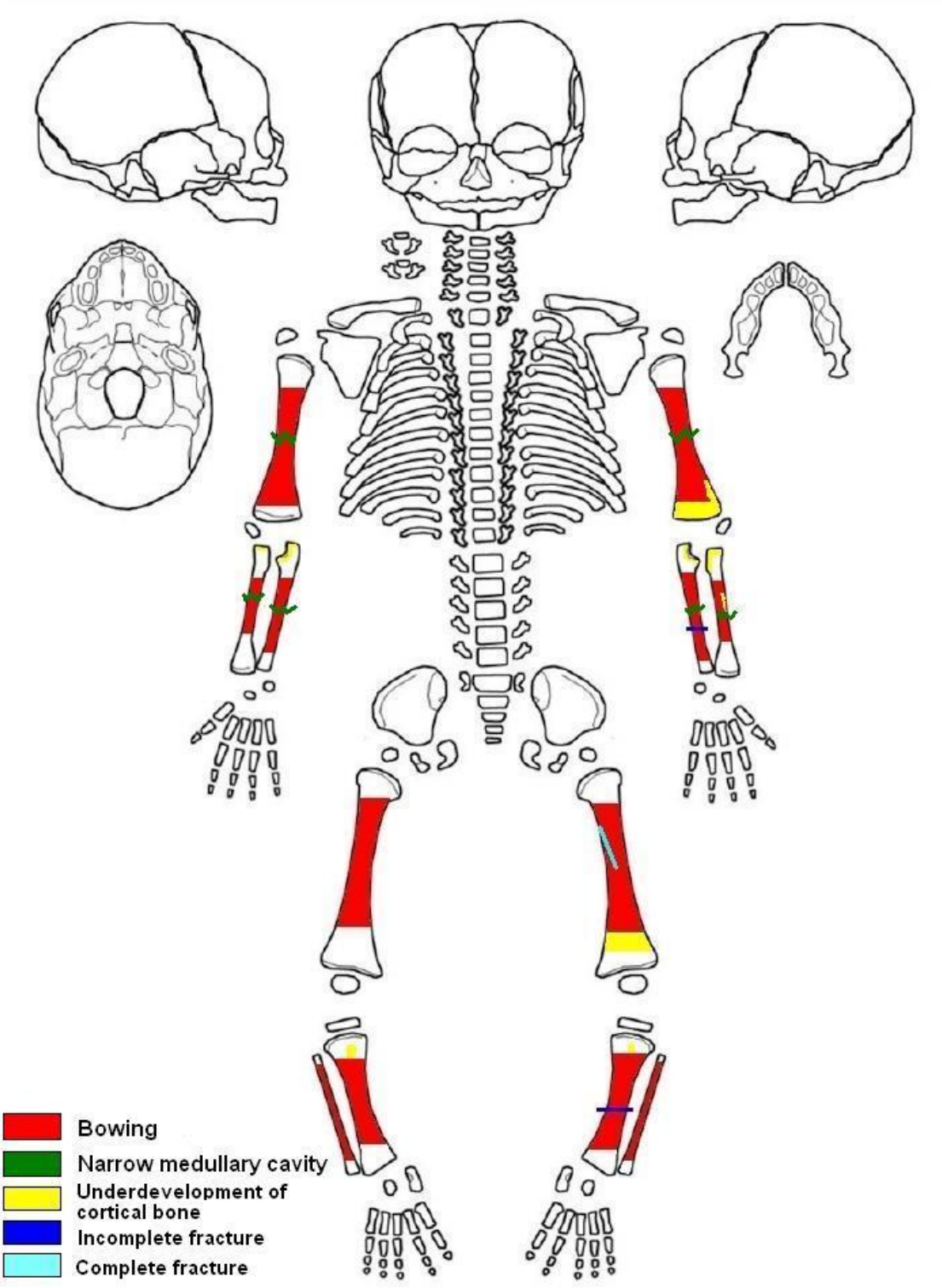

Figure 3-7: Diagram showing the distribution of pathological characteristics on B532.

All the long bones present with anterolateral bowing, expect the humeri which are bent posterolaterally (Figure 3-8). The most severe bending of the long bones occurs with the femora (Figures 3-6, 3-8) with extreme lateral bowing. The medial aspect of the left femur presents with an incomplete fracture and overall brittleness of the bone resulting in flaking of the bony surface (Figure 3-9). In addition to anterolateral bowing, complete perimortem fractures are evidenced on the left ulna and tibia (Fig. 3-10). It is possible that these fractures are a result of taphonomic processes as the individual was recovered from a very shallow grave. Several of the long bones, the right ulna and radius, left humerus, and left tibia, also show signs of what appears underdevelopment of the cortical bone (Figure 3-11). The cortical surface on these bones is coarse with a patchy appearance. At the distal and proximal ends there is observable differentiation of the cancellous, or spongy bone, and the cortical surface, and there is indication that cortical bone did not develop at these ends. Also affecting the long bones is a narrowing of the medullary cavities, occurring on the upper limbs (best observed on the humeri), as well as the right ulna and radius (Figure 3-12). Both clavicles also present with a distorted curvature of the medial and lateral ends that is extreme to what is customarily observed (Figure 3-13). All pathological conditions associated with B532 are summarized in Table 3-7.

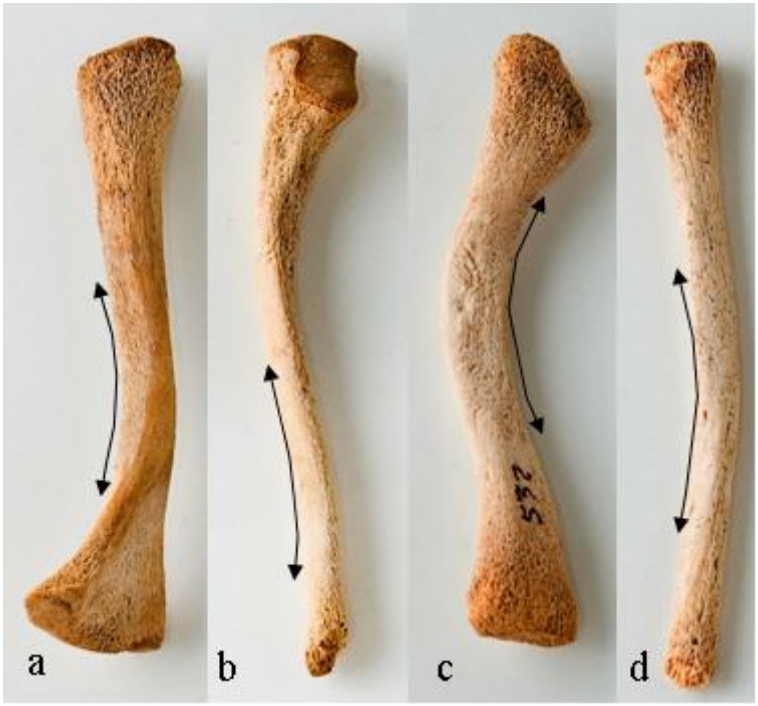

Figure 3-8: Arrows show bowing of the long bones of B532. a) right humerus, medial view; b) right ulna, anterior view; c) left femur, medial view; d) left fibula, anterior view.

Figure 3-9: Perimortem incomplete fracturing of left femur of B532.

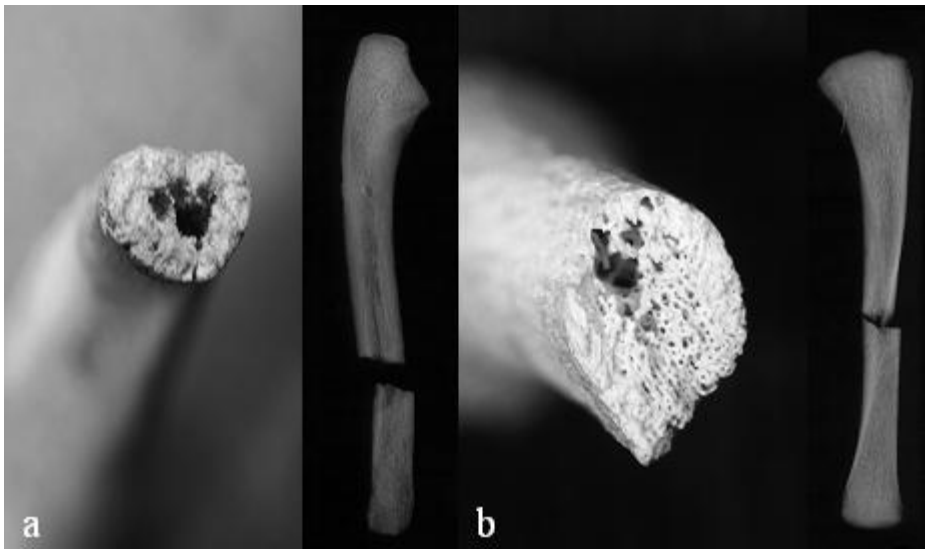

Figure 3-10: Possible complete perimortem fractures of the long bones of B532. a) left ulna, distal; b) left tibia, distal.

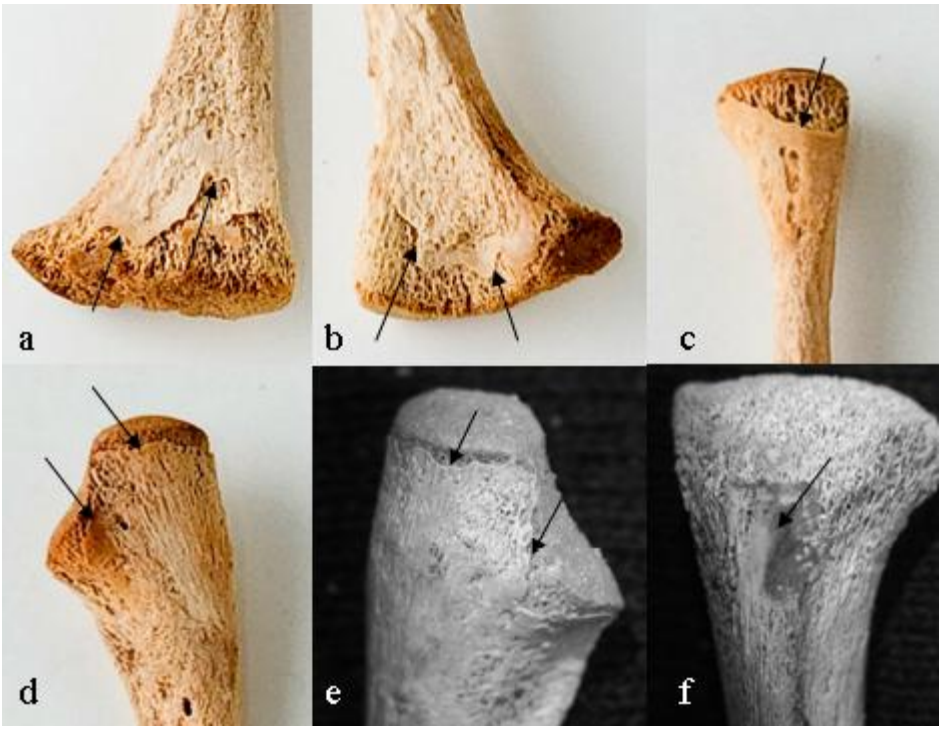

Figure 3-11: Underdevelopment of the cortical bone of B532. a) left humerus, anterior distal view; b) left humerus, posterior view distal view; c) right radius, proximal medial view; d) right ulna, proximal medial view; e) left ulna, proximal lateral view; f) left tibia, proximal anterior view.

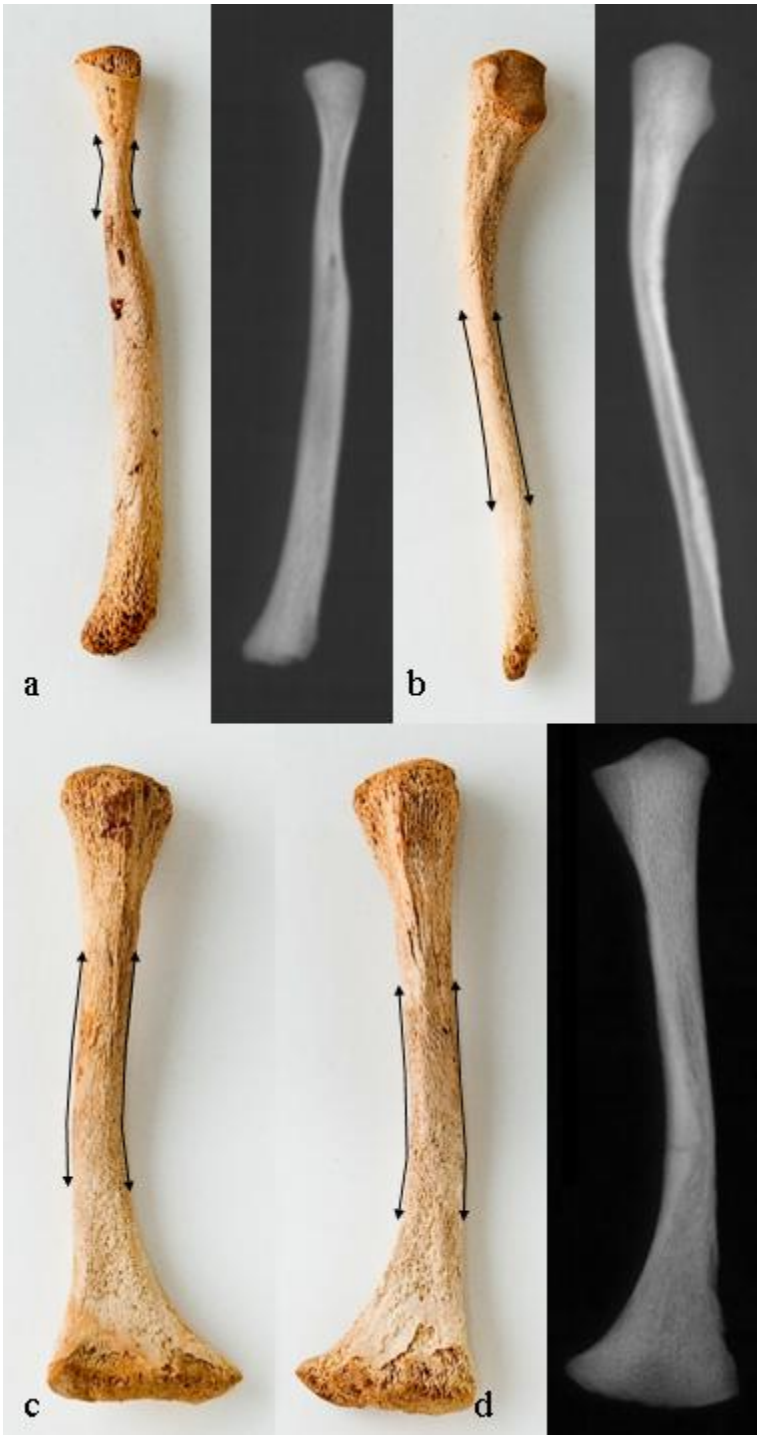

Figure 3-12: Long bones of B532 with narrowing of the diaphyses. Arrows indicate the narrow diaphyses, but this is more clearly evident on the radiographs. a) right radius, anterior view; b) right ulna, anterior view; c) right humerus, anterior view; d) left radius, anterior view.

Figure 3-13: Right clavicle of B532 showing severe curvature, posterior view

Table 3-7: Summary of pathological characteristics observable of B532

Abnormality	Limbs	Skull	Thorax	Spine	Pelvis
Bowing	Posterolateral bowing of humeri; anterolateral bowing of ulnae, radii, femora, tibiae, fibulae; femora most severely bowed	None	Barrel-shaped ribs; severely curved clavicles	None	None
Fractures	Incomplete fracture of left femur at proximal shaft; complete perimortem fractures of left tibia and left ulna at mid-shaft	None		None	Fracturing due to demineralization
Underdevelopment of cortical bone	Anterior, posterior, and lateral distal end of left humerus; proximal end of both ulnae at posterior edge of the olecranon process, the lateral and medial aspects of the trochlear notch, and distal to the coronoid process; proximal end of both radii, distally surrounding the head; anteriorly distal end of left femur; both tibiae at tibial tuberosity	None		None	None
Narrow medullary cavities	Right radius, at neck; both ulnae; both humeri	None		None	None

3.5 Pathological Analysis of Burial 625

Individual B625 has some pathological characteristics that are similarities to B532, but many of the malformations are unique to this individual. The orientation of B625 (Figure 3-14) was the same as that typically documented within the cemetery (e.g., Figure 3-4). The bones have a normal consistency, without any brittleness or coarse texture and a light brown coloration. An anatomical layout of B625 (Figure 3-15) shows the most obvious curvature of the long bones occurring at the distal end of the right radius and shafts of the tibiae as well as a barrel-shaped ribcage. A diagram of B625 illustrates the distribution of these abnormalities (Figure 3-16).

Figure 3-14: Burial conditions of B625 which show typical burial conditions (courtesy of the Dakhleh Oasis Project).

Figure 3-15: Anatomical layout of B625.

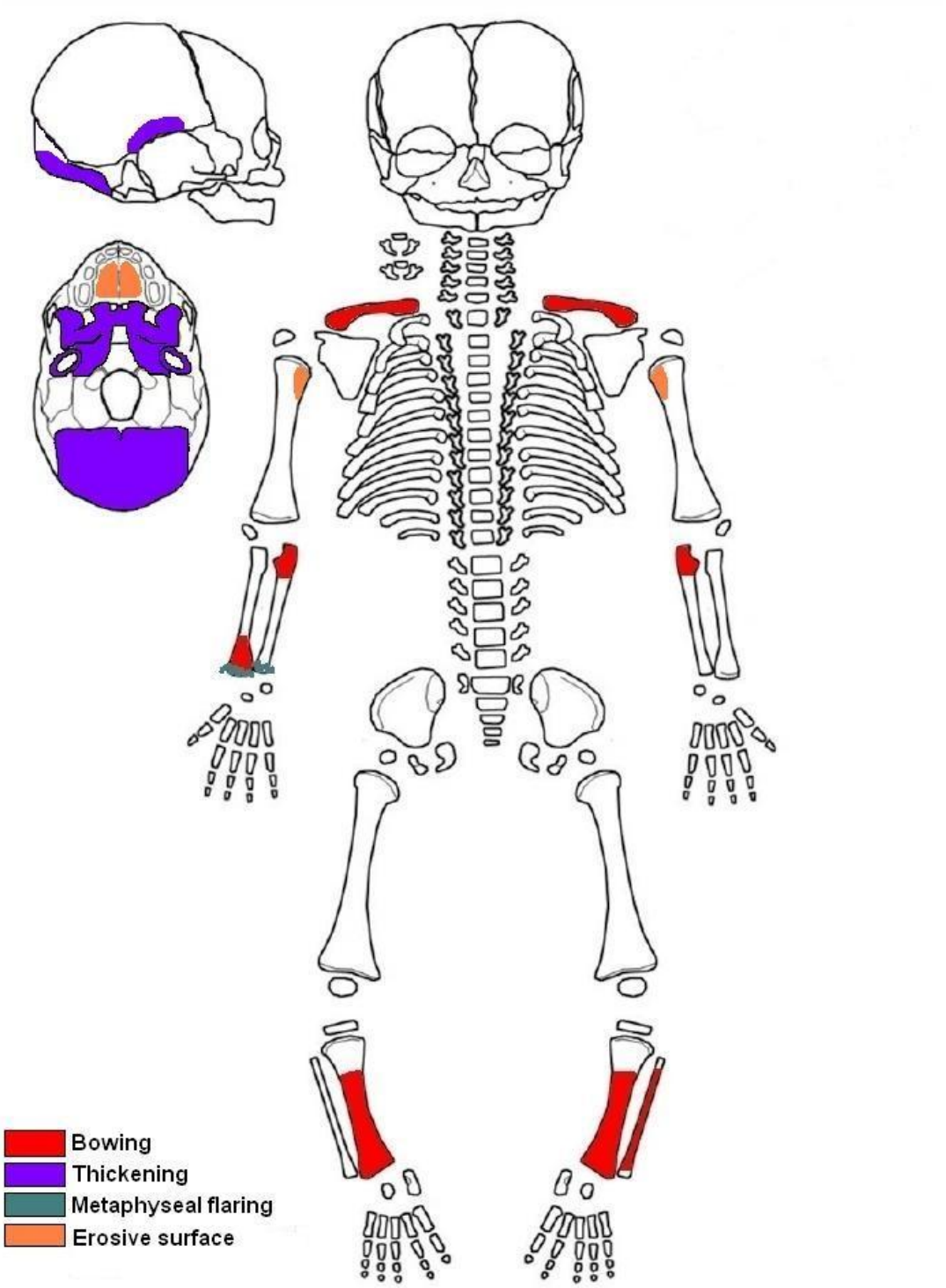

Figure 3-16: Diagram showing the distribution of pathological characteristics on B625.

There is bilateral medial curvature of the ulnae at the proximal ends, most evident on the left ulna, anterior curvature at the distal end of the right radius, bilateral anterior curvature of the tibiae, and lateral curvature of the left fibula (Figure 3-17). Both the right ulna and radius show metaphyseal widening (Figure 3-17). The clavicles also show extreme curvature, flattening that is observable at the lateral ends and bony protuberances at the anterior medial ends (Figure 3-18). This individual does not present with fractures or narrow medullary cavities, as is evidenced with B532. Instead, B625 shows severe deformation of the cranial bones. The occipital squama is thickened and shortened, creating an exaggerated protuberance of the external occipital surface (Figure 3-19). The shortening is in response to an absence of the superior portion of the squama, the portion of the lambdoidal suture that later fuses to the parietals. When the parietals and squama portion are placed in articulation, there is a noticeable gap between the posterior ends of the parietals and the superior portion of the squama (Figure 3-20). In addition to the malformations of the occipital, the pars basilaris bone has a distinctive lateral notch (Figure 3-21). The parietal bones present with a thickened squamosal suture and a curved appearance at the same border (Figure 3-22). Thickening of the sphenoid bone is noticeable as is shortening of the lesser wings (Figure 3-23). The greater wings of the sphenoid also present with thickening and shortening (Figure 3-24). Also unique to B625 are the petrous portions (Figure 3-25), which show bilateral curvature at their ends, a foramen at the junction of the petrous and squamous portions, as well as temporal rings that show significant thickening (Figure 3-26). Spinal abnormalities are evident at the anterior arches, where splaying of the bone is evident at the pedicle end (Figure 3-27).

The same abnormality is present on all the vertebral segments and is most severe on the neural arches of the axis (C2). The atlas (C1) also presents with an abnormal facet at the posterior neural arches (Figure 27). Additionally, what appears like enamel hypoplasia or severe effects from taphnomic processes is seen on the lateral incisors of the maxilla (Figure 3-28). Interestingly, this abnormality is not visible on any of the other teeth. Also distinct to B625 are the proximal medial aspects of the humeri, which show an underdevelopment of cortical bone (Figure 3-29). The palatine processes of the maxilla also show an erosive bone surface (Figure 3-329). Table 3-8 details the deformities observed on specimen B625.

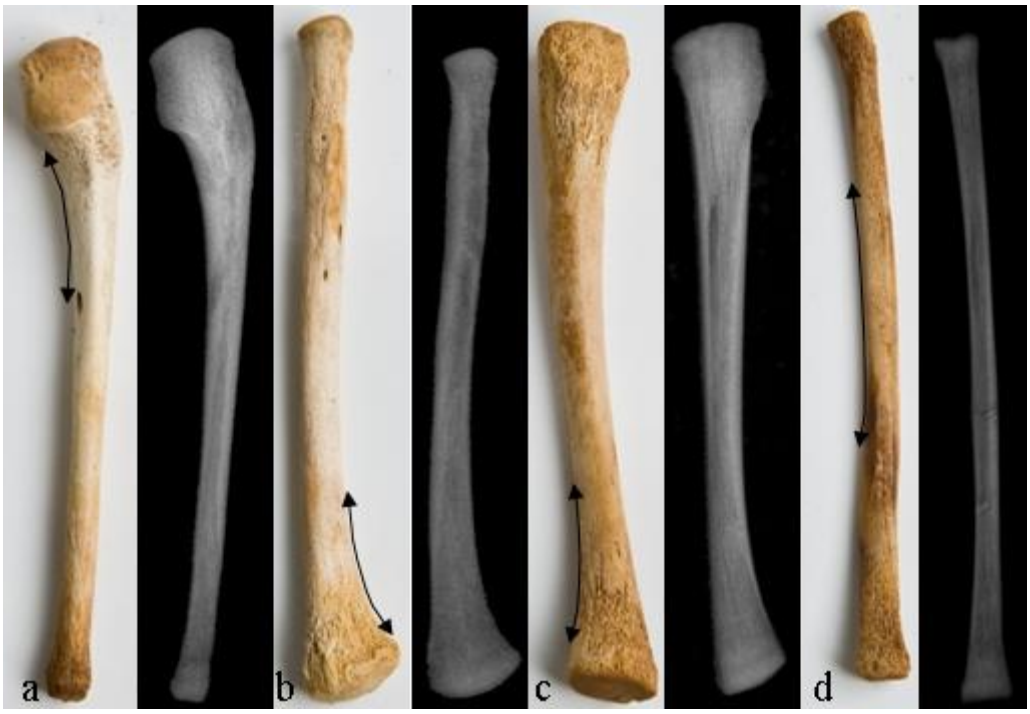

Figure 3-17: Long bone bowing of B625. Arrows show bowing of the long bones. a) left ulna, anterior view; b) right radius, anterior view; c) right tibia, anterior view; d) left fibula, anterior view.

Figure 3-18: Curvature of the clavicles of B625. Arrows point to bony protuberance on the anterior medial end.

Figure 3-19: Shortened and thickened occipital bone of B625.

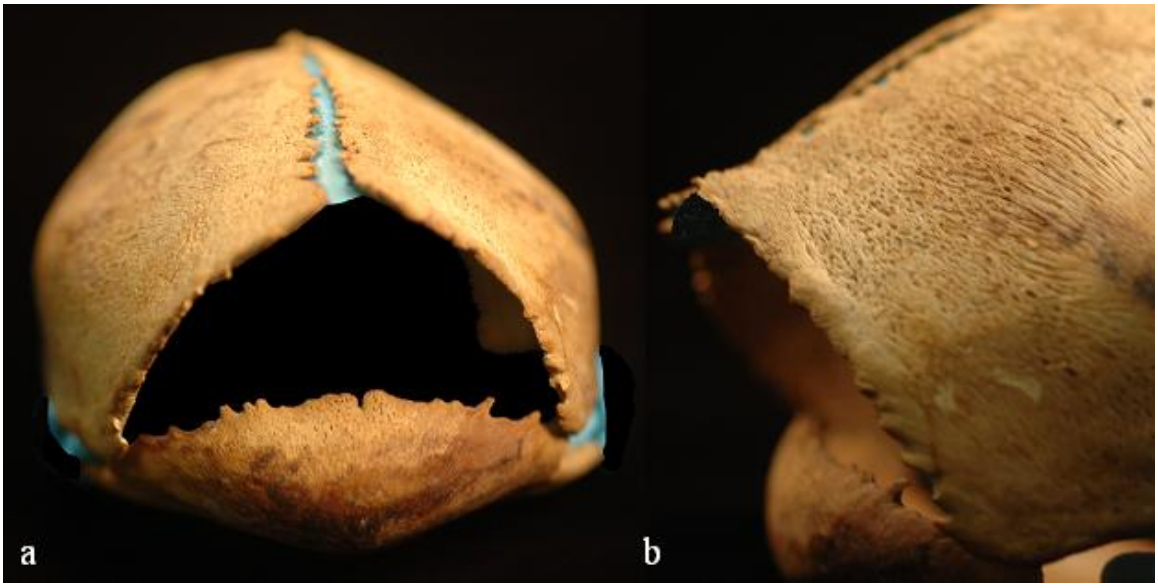

Figure 3-20: Articulation of parietals and deformed occipital of B625. a) Posterior view. Note the gap between the parietals and occipital due to in absence of the superior squama portion of the occipital bone; and b) lateral view.

Figure 3-21: Pars basilaris bone of B625. Arrow points to lateral notch.

Figure 3-22: Abnormal left parietal of B625. Arrow is pointing to thickened border of left parietal.

Figure 3-23: Sphenoid of B625 showing short, thick lesser wings, superior view.

Figure 3-24: Thick and short greater wings of B625, external view.

Figure 3-25: Malformed petrous portions of B625, internal view. Arrows point to curved ends and foramen at the junction of the petrous and squamous.

Figure 3-26: Extreme thickening of tympanic rings of B625.

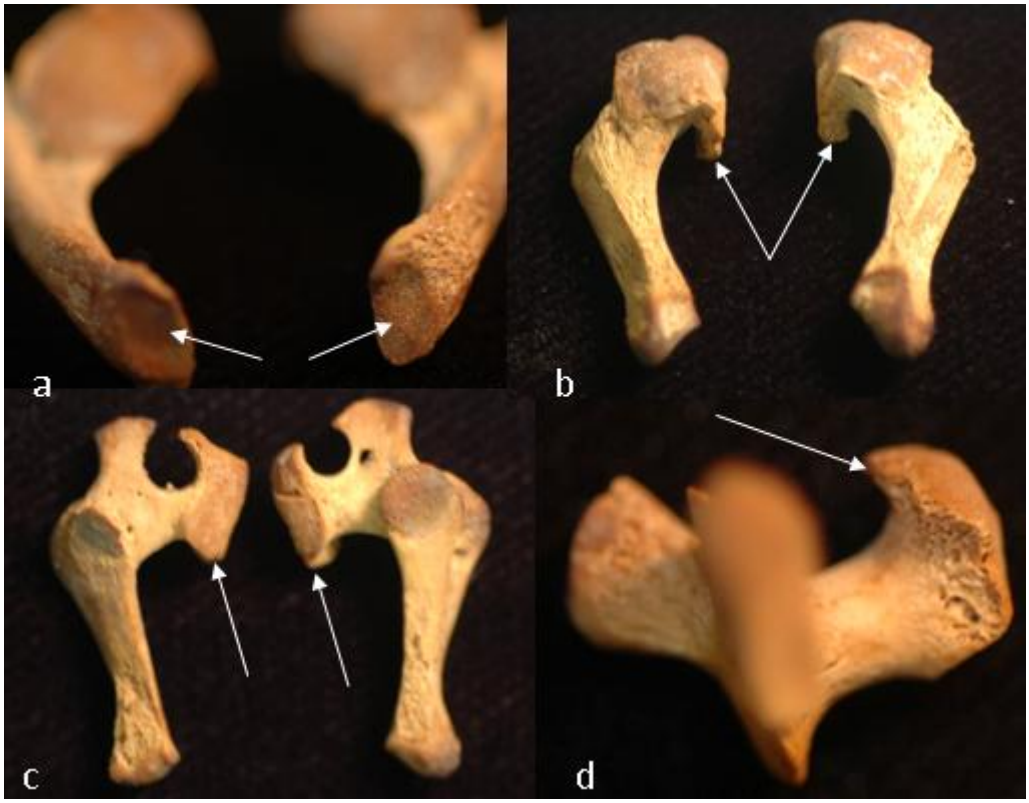

Figure 3-27: Abnormalities of the spine of B625. a) Atlas (C1), posterior-superior view. Arrows point to abnormal flattened facet at the vertebral arch ends; b) axis (C2), superior view. Arrows point to splayed anterior vertebral ends at the junction of the pedicle and body; c) typical cervical vertebrae, superior view. Arrows point to splayed bone at the anterior vertebral ends; and d) thoracic vertebra, posterior view. Arrow again points to splayed ends at the anterior vertebral ends.

Figure 3-28: Enamel defect of B625. Lateral maxillary incisors. The dark bands may represent enamel hypoplasia or taphnomic processes.

Figure 3-29: Erosive appearance of cortical bone of B625. a) Right and left humeri, anterior view. Arrows point to proximal and medial portion lacking cortical growth; and b) left maxilla, inferior view. Arrow points to the erosive surface of the palatine process.

Table 3-8: Summary of pathological characteristics observable of B625

Abnormality	Limbs	Skull	Thorax	Spine	Pelvis
Bowing	Bilateral medial curvature of the ulnae at the proximal end Anterior curvature at the distal end of the right radius Bilateral anterior curvature of the tibiae Lateral curvature of the left fibula	Bilateral curvature at the ends of the petrous portions	Curvature of clavicles Curvature of the ribs creating a barrel-shaped ribcage	None	None
Thickening of cortical bone	None	Short and thickened occipital bone Squamosal border of parietals Sphenoid, in particular the lesser wings Greater wings Tympanic rings	None	None	None
Erosive surface	Medial border of proximal humeri	Palatine processes	None	None	None
Other abnormalities	None	Enamel hypoplasia of lateral incisors of maxilla Foramen at petrous and squamous border of petrous portions	Bony protuberance at anterior medial ends of clavicles	Anterior neural arches show severe malformation at pedicle end Posterior neural arches of C1 show abnormal facet formation	None

3.6 Differential Diagnosis of B532 and B625

The differential diagnosis based on the bowing of the long bones, its congenital occurrence and lethality, are matched against the discernable pathological symptoms of B532 and B625 and results are presented in Table 3-9. As indicated by the differential diagnosis, symptoms of B532 are most similar to the symptoms of osteogenesis imperfecta. A diagnosis for B625 is difficult as the differential diagnosis did not result in a strong consistency with the pathological symptoms of B625. The symptoms of B625 are most consistent with achondrogenesis, type IA, but many symptoms of achondrogenesis are not present on B625, discounting the disease as the likely etiology of the skeletal deformations. A single disease as the causative factor of all the deformities of B625 is unlikely. As the bowing defect of the long bones is not helpful in diagnosing a possible disease, the pathological characteristics of the cranium should be further investigated. The malformations of the skull should provide an etiology but their lack of representation in the literature allows for only speculation in defining the deformities. The cranial deformities of the occipital, sphenoid, petrous, and temporal rings are unique in that both the clinical and paleopathological literature do not provide examples of these types of deformities. Such a severe malformation of the cranium is suggestive of a pathology that primarily involves a developmental defect of the brain, such as a neural tube defect (NTD).

Table 3-9: Differential Diagnosis of B532 and B625 Based on Clinical and Paleopathological Symptoms

Disease	Limbs		Skull	Thorax		Spine		Pelvis
Campomelic Dysplasia (Mansour 1995; Spranger et al. 2002)	Anterolateral bowing of femora and tibiae Hypoplastic fibula Dislocation of radial heads Delayed ossification of distal femoral and proximal tibial epiphyses Short first metacarpals Short middle phalanges	×	Micrognathia (small jaw) Scaphocephaly (long and narrow) Cleft palate Flat nasal bridge Hypoplastic mandible Dentinogenesis imperfecta	Small bell-shaped thorax Eleven pairs of ribs Hypoplastic scapulae Delayed ossification of sternum	×	Scoliosis Kyphoscoliosis Hypoplastic cervical vertebrae Hypoplastic thoracic vertebral pedicles		Dislocation of hip Narrow iliac bones Hypoplastic pubic bones
Osteogenesis Imperfecta (Sillence et al. 1984; Young et al. 1987; Spranger et al. 2002)	Anterorlateral bowing of all limbs Multiple fractures Callus Insufficient cancellous bone Fragile, chalky consistency Pale brown color Type IIA: Thick, short, crumpled shafts Femora has wavy accordion-like appearance Type IIB/III Short long tubular bones, thicker Broad metaphyses Thinner diaphyses Type IIC Thin and twisted	✓ ✓ ✓ ✓ ✓ ✓	Type IIA Large head Soft calvaria Wide fontanels Wormian bones Type IIB/III Frontal and temporal bossing Wide open fontanels Wormian bones Type IIC Large head Soft calvaria Demineralizatio n of facial bones	Type IIA Short, thick ribs with beading Type IIB/III Thin ribs Discontinuous fractures Type IIC Varying thickness and discontinuous beading of ribs Distorted and irregularly ossified scapulae	✓	Type IIA Flat and irregularly deformed Type IIB/III Compressed vertebral bodies Kyphoscoliosis (later in life) Type IIC Almost normal spine Spine is well ossified Vertebral bodies are normal height	✓ ✓ ✓	Type IIA None noted Type IIB/III None noted Type IIC Long, angulated ischial bones

Disease	Limbs		Skull		Thorax		Spine	Pelvis
Hypophospatasia (Shohat 1991; Spranger et al. 2002; Cole 2003)	Bowing of all limbs Short, thin tubular bones Irregular metaphyseal ossification Osseous spurs at midshafts	✓	Absence of ossification of major parts of the calvaria, bones of the skull base, and face		Short and thin ribs Poor ossification Complete lack of ossification of rib		Poor ossification of vertebrae, usually the neural arches Some vertebrae not ossified	Small pelvic bones with ossification defects Bending of pelvis
Achondrogenesis, Type IA(Chen et al. 1996; Spranger et al. 2002)	Bowing of tubular bones usually femur, radius and ulna Short with concave ends Projecting spurs on metaphyses	×	Large head Encephalocele may occur	○	Barrel-shaped thorax Horizontally oriented Short ribs with splayed ends Fractured ribs	× ×	Absent or abnormal ossification of vertebral bodies and sacrum	Small iliac bones reduced vertical diameter Abnormal ossification of pubic, ischial
Thanatophoric Dysplasia (Spranger et al. 2002; Li et al 2005)	Bowed long tubular bones, usually femora Short Flaring at metaphyses	×	Small facial bones Large calvaria Cloverleaf skull, not always		Narrow thorax due to short ribs		Flattening of ossification centers of vertebral bodies	Decreased vertical diameter and horizontal inferior margins of iliac bones Short and broad pubic and ischial
Infantile cortical hyperostosis (Spranger et al 2002)	Bowing of the limbs, usually femora, humeri Shortened Hyperostosis	×	Cortical hyperostosis of the mandible Macrocephaly		Cortical hyperostosis of ribs, scapulae and clavicles Rib shape irregular	 ×	Usually spared	Cortical hyperostosis of pelvic bones
Stuve-Wiedemann syndrome (Spranger et al. 2002; Al-Gazali et al. 1996)	Bowed, usually femora and tibiae Shortening of long bones Talipes equinovarus Cortical thickening Osteopenia Camptodactyly	×	Micrognathia				Undermineralized vertebral bodies	Hypoplasia of illia Flared iliac wings

Symbols denote presence of abnormality with fetal individuals. ×: Abnormality present with both B532 and B625; ✓: Abnormality present on B532 only; ○: Abnormality present on B625 only.

3.7 Discussion

Osteogenesis imperfecta (OI) involves a genetic mutation of the Type 1 collagen gene, resulting in retarded chemical composition of collagen that allows for easy fracturing of the bone. This disorder is often termed "brittle bone disease" in response to the individual's consistent fracturing throughout life (Plotkin 2003). Aging of the fetal individuals is important in not only documenting their age cohort within Kellis 2, but also in assessing how their growth progress is indicative of the health of the fetus and pathogenesis. An age range between 36 and 42 weeks for B532, with the highest probability of age at 38 weeks gestation, is indicative of a fetus that despite abnormal skeletal development was able to continue growing. Clinical cases report on an early detection of Type II osteogenesis imperfecta has been documented at 16 weeks of gestation (Young 1987). Development of OI abnormalities likely began before 16 weeks, as cartilage modeling and ossification of the long bones begins in the first trimester, at around seven to eight weeks (Scheuer and Black 2000; Baker et al 2005). Clinical cases have also reported a mean age of gestation between 36 and 40 weeks of live-born individuals with the Type II OI (Aerts et al. 2006). The age at death estimates for B532 also lie within this age range and are indicative of Type II OI as a diagnosis for the skeletal abnormalities.

The paleopathological literature presents with three possible OI cases (Wells 1965; Gray 1969; Ortner 2003), none of which are of fetal age, but Gray reports on the youngest victim, a child of about 2 years of age from Egypt. Both Wells (1965) and Gray (1969) report on angulation of the long bones and fractures. All three cases describe

narrowing of the medullary cavity. Their descriptions on the bone composition and color as being fragile, extremely light, chalky, and pale brown (Gray 1969; Ortner 2003) are consistent with the bones of B532. The bone deformities observed on B532 are consistent with the clinical data and paleopathological cases pertaining to OI and if the diagnosis is correct, B532 presents as the first documented archaeological case of a fetal individual afflicted with OI.

The lack of cortical development observed on the ends of the long bones and the coarse and uneven texturing of the bony surface is not mentioned in the paleopathological literature. Only a few clinical sources were helpful in deciphering the etiology of this symptom. Microscopic studies of OI, specifically type II, have reported on the often patchy bone mineralization that results from thinly disorganized osteoid, uncalcified bone matrix that represents the beginning stage of bone formation (Cohen-Solal et al. 1994; Traub et al. 1994; Sarathchandra et al. 2000). For B532, this patchiness may account for the uneven texturing of the bony surface. Additionally, light and electron microscopic studies of OI type II samples from Sarathchandra and colleagues (2000), revealed absence of mineralization at the distal ends of the growth plates, with mineralization instead starting further down the long bone. This defect could possibly explain the unmineralized zones that are observed at the ends of the long bones. This defect has not been associated with OI in the literature, but this is likely due to a lack of archaeological cases that have described this same abnormality, and also the clinical reliance on radiographic, ultrasound and soft tissue analyses for identifying indicators of the disorder. In the case of B532, the radiographs do not reveal the abnormality. Clinical cases,

however, are dependent on radiographic analysis for providing information on skeletal abnormalities, many of which are only discernable on the bony surface. Additionally, as there are only three archaeological cases of possible OI, not all bone abnormalities of OI are mirrored in such a small number of cases.

As mentioned earlier, a possible explanation for the skeletal abnormalities of B625 could be neural tube defects. Neural tube defects are congenital disorders in which the neural tube, a structure during embryonic life that involves development of the brain, spinal cord and its membrane coverings, or meninges, fails to correctly close resulting in major disabilities and often infant mortality (Botto 1999; Padmanabhan 2006). Closure occurs between 22 and 26 days after conception (Barnes 1994). Neural tube defects are one of the most common birth defects, preceded only by congenital cardiovascular deformities (Padmanabhan 2006). A NTD can either be open, resulting in direct exposure of the neural tube, or closed with the neural tube protrusions covered by skin. The etiology of NTDs is yet to be determined but it is generally agreed that the defects are multifactorial, ranging from genetic, environmental and nutritional factors (Botto 1999; Padmanabhan 2006).

The clinical and paleopathological literature frequently discuss three specific types of neural tube defects: anencephaly, spina bifida and encephalocele (Chen 2008a; Padmanabhan 2006; Ortner 2003). Anencephaly is considered the most common and most severe neural tube defect. Diagnostic features of anencephaly are unique in that there is an absence of the cranial vault and scalp, resulting in exposure of the brain and its subsequent destruction (Bianchi et al. 2000). Spina bifida is characterized by a bony

defect of the posterior vertebral arches, resulting in incomplete closure, and herniation of neural tissues. Spina bifida can either occur without skin tissue covering the defect, known as spina bifida cystica, or closed, with the presence of skin tissue, referred to as spina bifida occulta (Botto 1999). Encephalocele occurs when neural tissues, which include the brain and meninges, or just the meninges, herniate through a bony deformation of the skull (Mylannus et al. 1999; Afifi and Bregman 2005).

Encephaloceles can occur in various areas of the skull such as the frontal, occipital, parietal, nasal and nasopharyngeal, but the most common site is the occipital region (Afifi and Bregman 2005; Bui et al. 2007). An occipital encephalocele is one possible explanation for the cranial defect on B625, but the literature fails to explicitly describe the cranial abnormalities that can result from this disorder. This is primarily due to the clinical manifestations of the disease, which are limited to radiographic and soft tissue descriptions. There are no published paleopathological cases of the occurrence of occipital encephalocele, and presently only anterior encephaloceles have been documented (Ortner 2003). The clinical literature describes occipital encephaloceles as occurring in various areas of the occipital, either superiorly with the defect protruding above the foramen magnum or an inferior defect projecting through the foramen magnum and usually involving malformations of the posterior arches of C1 and C2 (Gorlin et al. 2001). Occipital encephaloceles can also occur at the occipital/parietal fontanelle and are considered as high occipital encephaloceles (Mahapatra et al. 2002). Figure 3-30 presents a clinical illustration of the various sites an occipital encephalocele can occur. Although the illustrations are helpful in indicating the site of protrusions, there is no

description of the exact cranial deformities associated with these protrusions. One of the only sources that clearly illustrate the occipital bone deformities associated with encephalocele is 3-D renderings from CT scans (Figure 3-31). The deformity of the occipital of B625 is suggestive of herniation occurring at the occipital/posterior fontanel, resulting in a disruption of growth of the superior squama of the occipital (Figure 3-20). However, occipital fontanelle encephalocele is rarely mentioned in the medical literature and a clear description of its exact locality has yet to be established (Brown and Sheridan-Pereira 1992; Patterson et al. 1998; Mahapatra et al. 2002). Most sources describe the herniation occurring at the junction of the parietals and occiput, as well as involving the occipital protuberance (Brown and Sheridan-Pereira 1992, Mahapatra et al. 2002; Moore and Persaud 2003). These descriptions, although limited, do match the bony absence of the superior squama of the occiput and are indicative of a herniation occurring at posterior/occipital fontanel region.

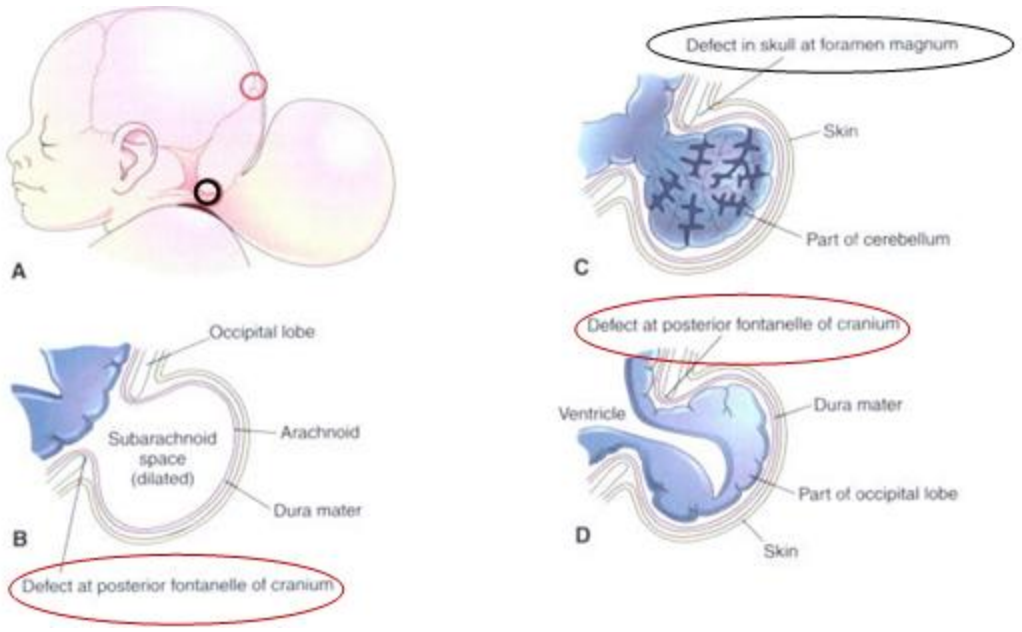

Figure 3-30: Illustrations demonstrate possible locations of herniations occurring at the cranial base. A) Top red circle indicates herniation at the posterior fontanelles. Lower black circle indicates herniation near the foramen magnum; B) herniation of only the meninges; C) meningoencephalocele, herniation of part of cerebellum, covered by meninges and skin; and D) meningoencephalocele, protrusion of the occipital lobe (adapted from Moore and Persaud 2003: 454).

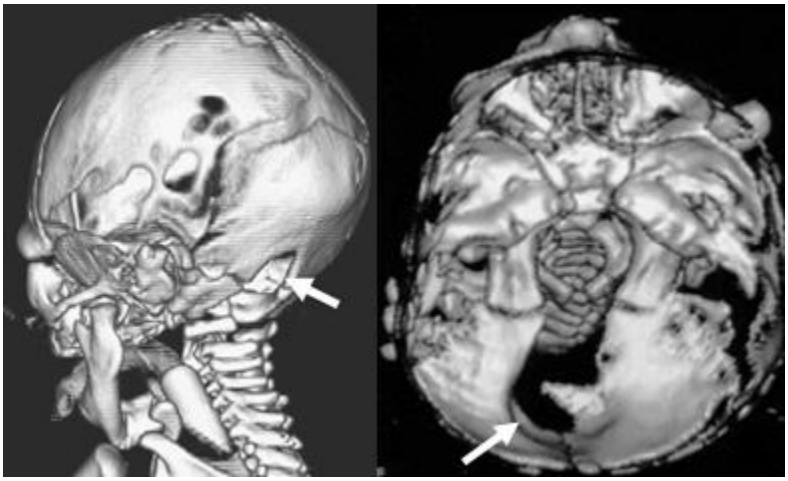

Figure 3-31: 3-D rendering of CT scan images. Left image shows occipital deformation due to an occipital encephalocele (adapted from Smith et al. 2007: 1037). Right image shows a cranial cleft extending from the occipital to the foramen magnum (adapted from Kita et al. 2002: 355).

The clinical literature does not provide a comprehensive review of cases involving occipital encephalocele as a means of providing the information on the age of deaths resulting from the neural tube defect. One study reviews 5 cases involving occipital encephalocele, with gestational weeks between 16 and 23 (Kjaer et al. 1999). These ages do not necessarily represent when the individuals died, as some cases report on the mother electing for induced termination of the fetus (Wen et al. 2007). In a review of 22 cases of occipital encephalocele, 45% of the individuals died (Brown and Sheridan-Pereira 1992). Cases reporting life births can best relate to the possible ages of individuals with occipital encephalocele. Unfortunately, cases are quite sporadic and not inclusive of a mean age of life births. Cases of live births are documented at 39 weeks and 42 weeks gestation, with some surviving thereafter with medical interference by removal of the encephalocele and reconstructive surgery of the skull base (Lin et al. 1996; Kita et al. 2002). In reference to the estimated age at death for B625 of between 38 and 42 weeks gestation, with the highest probability of 38 weeks, it can be said from the clinical literature that there is a possibility of an individual to survive to this age with an occurrence of encephalocele.

Associated deformities of the pars basilaris bone are also indicative of encephalocele. The lateral notch deformity of the basilar bone is documented in two fetal cases with occipital encephalocele that are diagnosed with Meckel-Gruber syndrome (Kjaer et al. 1999). The Meckel-Gruber syndrome is a lethal genetic condition that is characterized by occipital encephalocele, kidney abnormalities, and polydactyly (Ramachandran et al. 2006). Symptoms of Meckel-Gruber disease have also been

reported to include anterior bowing and shortening of the tubular bones, usually in the humerus, ulna, radius, tibia, and fibula (Majewski et al. 1983; Kjaer et al. 1999). Unilateral notching of the basilar bone is also a reported symptom of Trisomy-18 (Figure 3-32), a rare genetic disease that is also associated with occipital encephalocele (Kjaer et al. 1996).

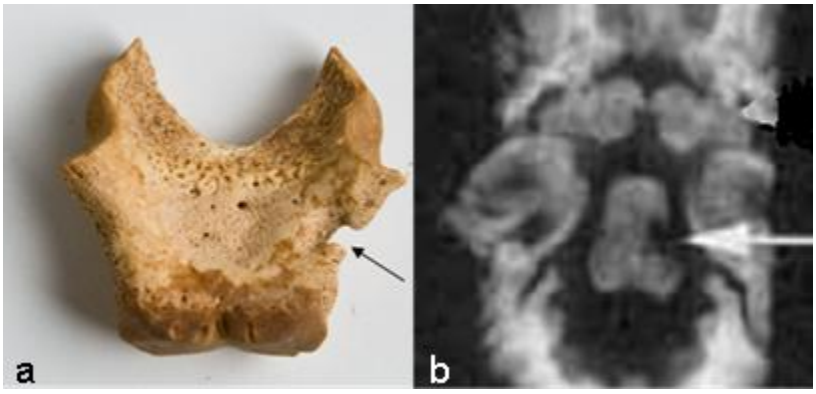

Figure 3-32: Unilateral notch of pars basilaris bone. a) notching of B625 pars basilaris; and b) notching of fetus individual with Trisomy 18 (after Kjaer et al. 1996).

The observed spinal deformities on B625 are symptomatic of rachischisis, a term that is associated with spina bifida, and both are characterized by the irregular fusion of the vertebral body and/or neural arches which can lead to neural tube protrusions through the spine (Bianchi et al. 2000; Ayter et al. 2007). The clinical literature describes rachischisis as occurring throughout the entirety of the spine, unlike spina bifida which occurs at isolated regions with involvement of a few vertebrae (Merz 2005). There is certainly a degree of severity with rachischisis, as some sources describe incomplete closure of the vertebral arch and/or bodies or irregular fusion (Bianchi et al. 2000; Dogan et al. 1996), total absence of the vertebrae, vertebral bodies or even lamina portions

(Dogan et al. 1996; Ayter et al. 2007), and also a shortening of the pedicles (Ayter et al. 2007). In the case of B625, there are definite irregularities in the formation of the pedicle end, where fusion occurs with the vertebral body, extending throughout the entire spine, although the severity lessens at the lumbar region. The posterior ends of the vertebral arches exhibit an irregular facet that is suggestive of a defect in normal fusion.

Rachischisis and occipital encephalocele are frequently described as symptoms of iniencephaly, a neural tube defect that also involves retroflexion of the head (Figure 3-33). This position sometimes results in a shortening of the spine or enlargement of the foramen magnum, in response to an occipital encephalocele protruding through the foramen magnum (Bianchi et al. 2000). Unfortunately, there are no archaeological cases pertaining to occurrence of iniencephaly reported in the literature. Evidence of rachischisis is not well documented in the paleopathological literature, with only the existence of craniorachischisis, a type of defect that involves anencephaly (a neural tube defect resulting in absence of the skull vault) and rachischisis (Johnson et al. 2004; Chen 2007), which is mentioned in the archaeological literature with little description of the spinal abnormality (Aufderheide and Rodriguez-Martin 1998; Charon 2005).

Figure 3-33: X-ray shows an iniencephalic fetus in the typical retroflexed position (arrow shows direction of head). The circle indicates an occipital encephalocele (adapted from Chen 2007: 201).

A comprehensive review of 63 iniencephalic individuals, with or without rachischisis, from published clinical cases is provided by Chen (2007). Prenatal diagnosis of the neural tube defect is reported at between 9 and 36 weeks gestation. A live birth study documents a gestational age as old as 36 weeks gestation (Kulaylat and Narchi 2000). These clinical cases are indicative that iniencephalic individuals are not likely to reach a gestational age as old as that estimated for B625, at least by 2 weeks.

The cranial deformities of the petrous portions, tympanic rings, and sphenoid are not mentioned as malformations that are associated with encephalocele or iniencephaly, and are not included within the clinical and archaeological literature. It is highly probable that the occurrence of these deformities is due to the structural skeletal changes

that are brought on by a neural tube defect, which create abnormal positioning of the skull and pressuring from the neural tube protrusions. Iniencephalic cases describe low-set ears as a symptom (Johnson et al. 1997; Loo et al. 2001; Tugrul et al. 2007). These cases do not include a description of the skeletal abnormalities accompanied by low-set ears, but one case, although not of an iniencephalic fetus, does describe an MRI study that shows downward alteration of the petrous portions in response to the low-set ears (Rustico et al. 2004). It is also hypothesized that malformations of the clavicles is a consequence of an iniencephalic positioning of the head. One clinical case pertaining to iniencephaly describes a high positioning of the clavicle and scapula that is at the same level as the mandible (Johnson et al. 1997). This positioning is expected due to the backwards flexion of the head. Additionally, the defect observed on the proximal medial humeri of B625 is likely a result of the repositioning of the clavicle. The soft tissue structures of the gleno-humeral ligaments, connecting the glenoid fossa of the scapula to the humerus, as well as attachments of the latissimus dorsi and teres major muscles, are located at the site of this defect (Mahasen and Sadek 2002). The clavicle and scapula are connected by ligaments at both the coracoid and acromion processes of the scapula, giving support in positioning to the humerus, scapula and clavicle (Figure 3-34). Malformation and erroneous positioning of the clavicle could result in major offsetting of these fibrous and muscular attachments, perhaps repositioning the scapula and creating a type of trauma-like effect on the bony surface of the humerus. Although cases are mostly of older children, some cases report that osteotomy (surgical operation of a bone) of the clavicle is performed as a means of correcting the positioning of the scapula due to the

erroneous formation of the clavicle (Cavendish 1972; Beals 2000; Nath et al. 2006). Additionally, the bone spur at the medial ends of the clavicles are likely a result of this same erroneous position. At the site of the bone spur is attachment of costoclavicular ligament, from the clavicle to the first rib (Figure 3-35). The ligament is responsible for resisting an upward pull of the clavicles from the sternocleidomastoid muscle and has been described as the most stabilizing ligament (Iannotti and Williams 2006; Marx et al. 2006). Bone spurs can develop from an adaptation of instability at a joint or ligament (Menkes and Lane 2004; van der Kraan and van den Berg 2007). Due to a distortion of positioning resulting from the iniencephaly, which involves a major constriction of the head in a backwards angle, it is quite possible that instability at these ligament joints would occur and could possibly morph the clavicle in reaction.

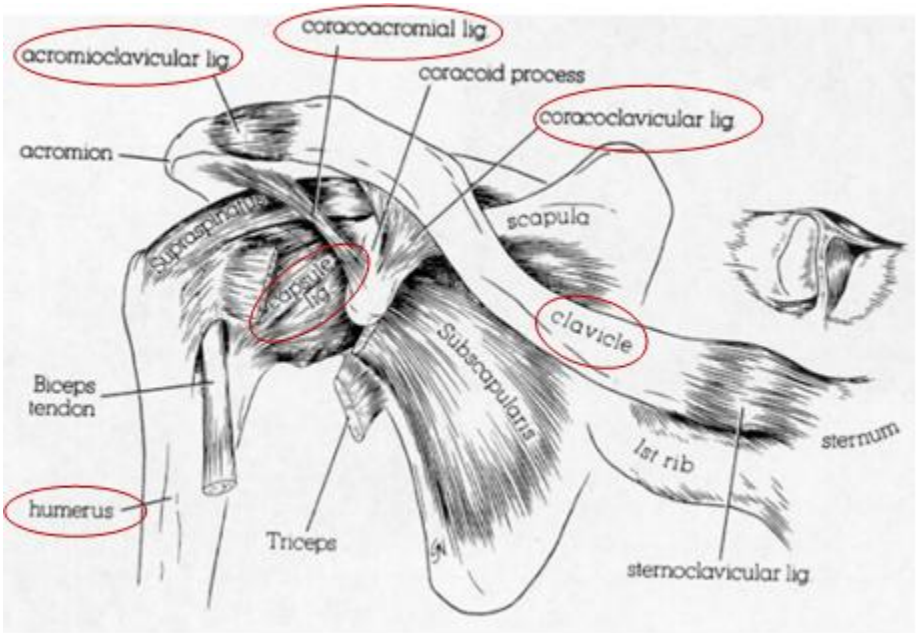

Figure 3-34: Glenohumeral, acromioclavicular, and sternoclavicular joints. Note the interplay of the ligaments with the clavicle, scapula and humerus (adapted from Bland 2001: 810).

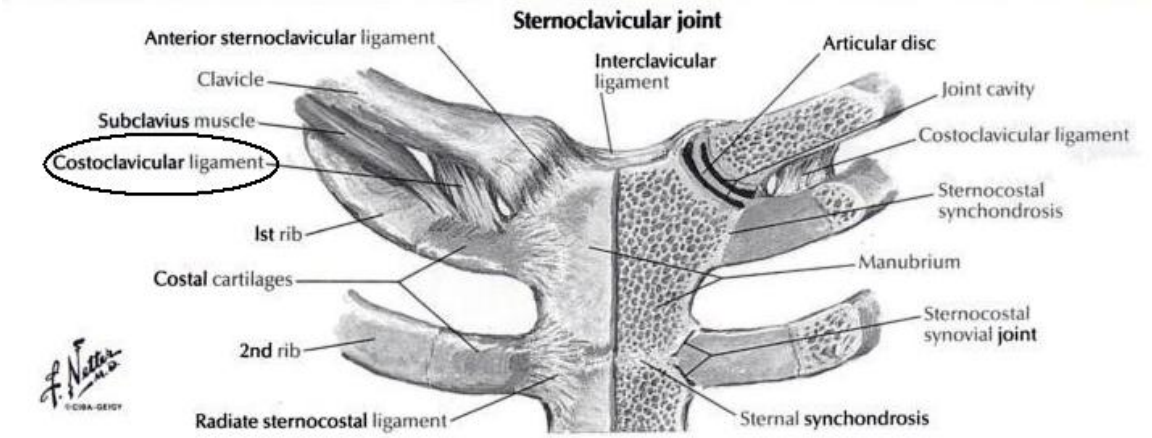

Figure 3-35: Sternoclavicular joint. The costoclavicular ligament that attaches to the medial end of the clavicle is circled. The abnormal head position of B625 could have resulted in the development of a bone spur at the site of the ligament (adapted from Dutton 2004: 414).

The clinical and archaeological literature provide very little pertaining to fetal individuals suffering from dental hypoplasia. The medical literature focuses on infants and children as this is when manifestations of enamel abnormalities are most noticeable due to dental eruption. Dental hypoplasia is one of the most common dental abnormalities in the archaeological record (Filer 1995), but archaeological cases pertaining to fetal enamel hypoplasia are deficient. This is likely due to a lack of fetal individuals in the archaeological record, especially those that show such unique features as B625. Abnormal development of dental tissues can begin as early as 4 months intrauterine when mineralization begins of the deciduous teeth (Bhat and Nelson 1989; Palmer 2001). The clinical literature suggests numerous causes for the occurrence of intrauterine enamel hypoplasia, such as maternal nutrition, viral infections such as rubella, ingestion of chemicals like fluorides and tetracycline (Bhat and Nelson 1989).

Of these causes, metabolic stress and infections are cited as the more common factors for dental hypoplasia of archaeological origin (Starling and Stock 2007; Ortner 2003). In the case of Kellis 2, studies have revealed the ingestion of tetracycline and its presence in fetal bones. The tetracycline is naturally occurring in grain products, thus consumption during pregnancy could have easily occurred and resulted its transmission through the placenta (Maggiano 2005). The presence of tetracycline within skeletal remains and nutritional levels that are significantly enriched are causative of a high number of fetal deaths at Kellis (Dupras et al. 2002). Additionally, tetracycline use has been associated with an occurrence of iniencephaly in one of five cases (Aleksic et al. 1983). The appearance of the dental defect of B625 as dental hypoplasia is quite questionable, as the presence of dental hypoplasia in the archaeological record is typically described as horizontal grooving and enamel pitting (distinct holes), neither of which matches the enamel defect of B625. A study of oral health from children of Kellis 2 has revealed that the youngest individuals in the study, 1 to 3.5 years, showed enamel defects of pitting (Shkrum 2008). One reference in the literature, specifically of archaeological type, describes a deciduous tooth as presenting a "horizontal band of brown discoloration" (Lovell and Whyte 1999: 73) that is similarity describes the dental defect of B625. Unfortunately, the authors do not go into further detail of the tooth abnormality. Interestingly, an abnormality also present with B625 is the erosive surface of the maxilla. For now it is possible to associate the abnormal development of the maxilla as the likely cause of the subsequent developmental stress of the maxillary incisors.

The bowing of the long bones of B625 could simply be a product of the abnormal positioning of the fetus due to the iniencephalic condition with the awkward retroflexion of the skull. This explanation relates to previous explanations regarding the abnormal intrauterine position as causative of bowed long bones (Caffey 1947, Angle 1954). Unfortunately, clinical cases do not list long bone bowing as a condition occurring with iniencephalic patients. As the long bone bowing was not as extensive with B625, a lack of mentioning of this defect is somewhat expected. But medical literature describes syndromes in which long bone bowing occurs in conjunction with occipital encephalocele. One study explores various degrees of long bone bowing as a symptom of Meckel syndrome, a lethal genetic disorder linked to abnormalities of chromosome 17 (Majewski et al. 1983). Dyssegmental dwarfism is also associated with long bone bowing, specifically of the femur, fibula, radius, and ulna (Handmaker et al. 1977); however, a prominent abnormality of the long bones is shortening, which is not an abnormality shared by B625. Both of these syndromes are rare and archaeological cases are nonexistent, but their mention within this present study is for purposes of initiating further inquiry into a diagnosis of fetal specimen B625.

3.8 Summary

As shown within this present study, using the pars basilaris measurements for predicting long bone lengths and subsequently using these predictions for age at death estimates is a plausible methodology. This is an especially valuable method when a skeletal abnormality prevents measurements of the long bones, as demonstrated with the severe bowing of the long bones of B532. In comparing actual and predicted femur lengths, the maximum width of the pars basilaris is proven as the best linear related measurement with growth of the femur length, which corresponds to consistent rate of growth of the pars basilaris width in response to growth of the skull base (Scheuer and MacLaughlin-Black 1994).

A differential diagnosis of congenital long bone bowing allowed for a possible disease diagnosis of fetal specimen B532. In total, the skeletal abnormalities of B532 match closely with the paleopathological and clinical features of osteogenesis imperfecta, specifically Type II OI. If a diagnosis of OI is correct, this could be the cause of death of the individual, but more importantly it is further revealed what type of abnormalities OI disease can cause on the skeleton. Additionally, the clinical literature reports on a mean age of live births of Type II OI occurring between 36 and 40 weeks of gestation, that correlates with the age at death estimate of B532. Differentially, the abnormalities of B625 are unique and neither the clinical nor the paleopathological literature provided precise examples of the malformations. A differential diagnosis based on the bowing of the legs did not resolve a possible etiology of the malformations. As such, this required further investigations into the abnormalities of the skull and vertebrae. Deformities of the

pedicle portions of the vertebrae were indicative of rachischisis and the abnormal structure of the occipital is best explained by an occurrence of encephalocele. Both rachischisis and encephalocele are major symptoms of iniencephaly. The backwards position of the head and trunk that results from iniencephaly, could further explain abnormalities of the proximal medial humeri and the clavicles due to disturbances in ligament attachments. Comparing clinical reports on the ages of fetuses with encephalocele and iniencephaly, suggests the possibility of B625 growing to its estimated age if beset with both disorders, although iniencephalic individuals are reported with a maximum age at death of 36 weeks.

In both fetal individuals, there are abnormalities that are not mentioned in the clinical and paleopathological literature. A lack of representation of the abnormalities within the paleopathological literature is expected, as not every syndrome or disease has an archaeological representation. Additionally, those with an archaeological representation may show different symptoms than what is presented in the present day. The use of clinical literature as a diagnostic tool proved to be quite difficult when identifying bony abnormalities, particularly when trying to differentiate the malformations of B625. This was an unexpected limitation during the present study although Ortner (1991) advises that radiographs do not account for the subtle features on the bone surface. In any case, these deficiencies in the clinical literature are advantageous to paleopathological studies, as archaeological representations of a syndrome can prove helpful for clinical studies. The skeletal representation of a disease can identify

abnormalities that perhaps have not been documented by the medical community and thus can contribute more diagnostic features for the diagnoses of diseases.

If the diagnoses of the fetal specimens are correct, which in the case of B532 OI Type 2 is positively favored and for B625 a neural tube defect is the most likely scenario, they both represent a "first" in paleopathology. Fetal individual B532 presents as the first documented archaeological case of fetal osteogenesis imperfecta. While B625 also presents as a distinctive addition to paleopathology, as the first archaeological documentation of iniencephaly and occipital encephalocele. Albeit the specificity of the type of neural tube defect of B625 is greatly speculated, there is no argument that abnormalities presented with B625 are not found in the paleopathological literature and present as an opportunity for further discussion within the paleopathological community.

CHAPTER 4: CONCLUSIONS, FUTHER STUDIES AND SUMMARY

4.1 What does it all mean?: Conclusions and further studies

During its time the ancient town of Kellis was a center of religious, economic and political importance from the Ptolemaic and throughout the Roman period (Hope 2001). Burial practices of nearby cemeteries are reflections of the cultural transitions between these two periods. Immediately north-west of Kellis is the cemetery site Kellis 1 and to the north is Kellis 2 cemetery. Burial practices of Kellis 1 are characteristic of rock-cut tombs, mummification and inclusion of burial goods. Multiple occupants are found within each tomb, but this is a disputable burial practice as looting is evidenced in the area (Aufderheide et al. 2003). Kellis 1 burials practices are a reflection of the pagan community of Kellis during the Ptolemaic period. No fetal remains have been found in Kellis 1 and very few subadults have been recovered, a phenomenon that is common among pagan communities as internment of the young is limited to the home rather than at communal graves (Bowen 2003). Excavations at Kellis 2, dating to the later Roman period, have revealed burial organization of individual mud-brick tombs, with an east-west orientation that is indicative of Christian practices.

From 1991 to 2007, a total of 701 burials have been excavated at the Kellis 2 cemetery. Molto (2002) has projected that Kellis 2 is composed of around 3,000 to 4,000 burials. Thus far, all the burials have shown Christian burial practices, although pagan practices have been identified with residues of resins for preparation of the body for burial (Dupras and Tocheri 2007). The graves are simple, rectangular and reach an

average depth of 1.3 m, with some adult burials at least 2 m (Bowen 2003). Mud-brick tomb enclosures have been identified and a number of graves have low mud-brick mastaba-like superstructures. All the burials are arranged on an east-west axis, with the head facing west and the body in a supine position and the hands resting on the sides or on the pelvis (Birrell 1999; Bowen 2003; Molto 2002). One individual is interred per grave, although there have been exceptions in the case of subadults (Bowen 2002). Linen wrappings typically cover the corpse and are believed to have been woven specifically for burial, although in the case of fetal remains, some linens are likely leftovers from adult burial linens (Bowen 2001; Bowen 2002; Tocheri et al. 2005). Subadult burials are intermixed with adult burials, meaning burials were positioned next to each other without organization by age category. This is easily observed on the cemetery diagram (Figure 4-1), in which the smaller burial drawings represent fetal or juvenile remains and the larger burials are that of adults. Additionally, subadults and adults are buried in the same fashion, although fetal and juvenile burials tend to be shallower, possibly due to their short height that could correspond to the length and width of the burial (Tocheri et al. 2005). The spatial distribution of the burials is indicative of a pattern that involves organization of the burials by familial lines, as groupings do occur around and radiate from the tomb structures (Figure 4-1). This is a working hypothesis of the Dakhleh Oasis Project (Molto 2002; Tocheri et al. 2005). Studies in paleogenetics have already revealed a semblance of metric and non-metric traits at these specific groupings, indicating an inheritance of these traits and thus relatedness of those individuals (Molto 2002). Analyses on mtDNA also indicate that the Kellis population was heterogeneous and

included multiple maternal lineages, allowing for the occurrence of multiple traits and differentiation of familial lines (Graver et al. 2001; Molto 2002; Parr 2002).

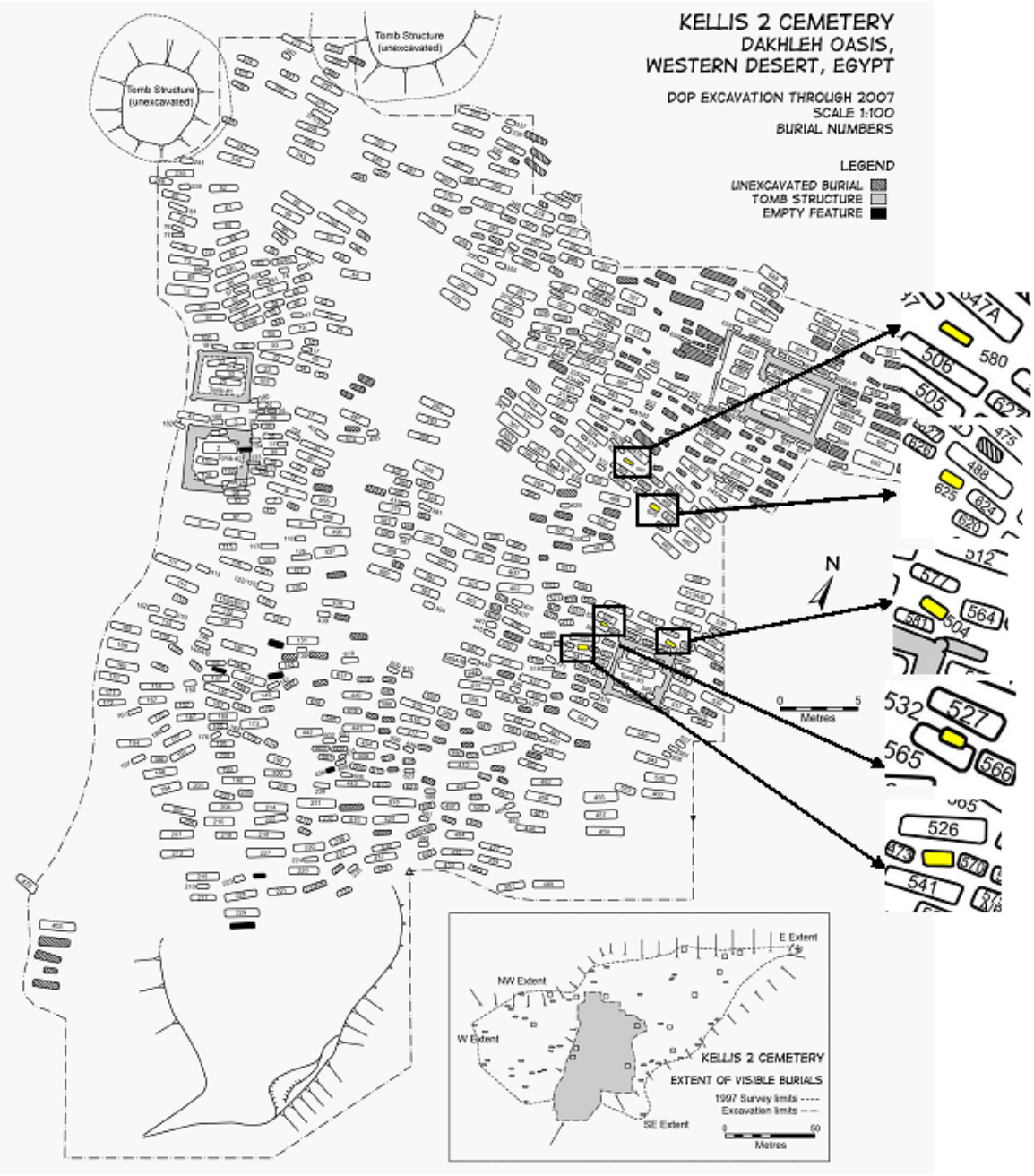

Figure 4-1: Kellis 2 cemetery showing the location of fetal individuals with congenital pathologies. Fetal individuals 504, 625, 580, and 563 are suspected of dying from neural tube defects (courtesy of Sandra Wheeler and Lana Williams).

The locations of fetal specimens B532 and B625 within the Kellis 2 cemetery can reveals a pattern to their pathologies that is indicative of the cultural practice of burying the dead in accordance to family lines. A number of additional fetal individuals show skeletal abnormalities suggestive of lethal neural tube defects. These individuals and the specimens discussed within this study are indicated on the Kellis 2 cemetery map (Figure 4-1). Aside from B532 who has been diagnosed with osteogenesis imperfecta, all other fetal specimens have characteristics that are suggestive of neural tube defects. Burial 653 has been studied and determined as afflicted with anencephaly (Matthews 2008). Preliminary assessment of B504 and B580 describe similar abnormalities as those presented with B625. A full assessment of their pathologies has yet to be conducted, but it has been documented that B580 has a similar malformation of the occiput and clavicles as that of B625, in addition there are malformations of the temporal and petrous portions (per communication with Sandra Wheeler). There is conflicting documentation of the abnormalities present with 580, as documented an occipital abnormality similar to B625, but this was not reported by Sandra Wheeler, who documented pathologies of the temporal and petrous portions. Interestingly, there is a close proximity of the occurrence of the neural tube defects to one another, resulting in clustering at the eastern end of what has been excavated of the cemetery. The larger density of the neural tube cases is found at the northeast corner of the cemetery. The locality of these individuals is suggestive of an inheritance of neural tube defects. If the hypothesis that the cemetery was organized by familial lines is supported, the occurrence of these neural tube defects within these groupings is expected as the defect would be passed on through a family line.

Unfortunately, one major setback of the familial line hypotheses for Kellis 2 is a lack of temporal assurance of the burials (Molto 2002).

The Kellis population also suffered from the infectious diseases of leprosy and tuberculosis, which have been identified from a number of burials at Kellis 2 (Molto 2002). The placement of the diseased individuals at the cemetery also presents with clustering at the potential familial groupings (Figure 4-2). This is most evident with tuberculosis (studies of the leprosy cases indicate the individuals as outsiders of the Kellis population) in which three cases are closely grouped at the east portion of the cemetery (Figure 4-2) and are suggested as occurring contemporaneously (Molto 2002), and they could quite possibly be related to one another. The neural tube defect spina bifida has also been identified on skeletal remains from Kellis 2 and at a high frequency (22%) (Molto 1998). It was suggested by Parr (2002) that homogeneity of the Kellis population could explain the occurrence of spina bifida, as a high prevalence of the disorder has been linked to inbred populations in India and Egypt. Results from mtDNA analysis by Parr (2002) are not consistent with his hypothesis. Instead Parr (2002) concludes from a subset of individuals (not those presenting with spina bifida), that there is significant heterogeneity at Kellis. But again, temporal definitions have yet been determined for many of the burials of Kellis 2 which could indicate if the Kellis population was homogenous at some point. Nonetheless, continued genetic studies specifically that of diseased individuals could result in a support of the familial line hypothesis at Kellis 2.

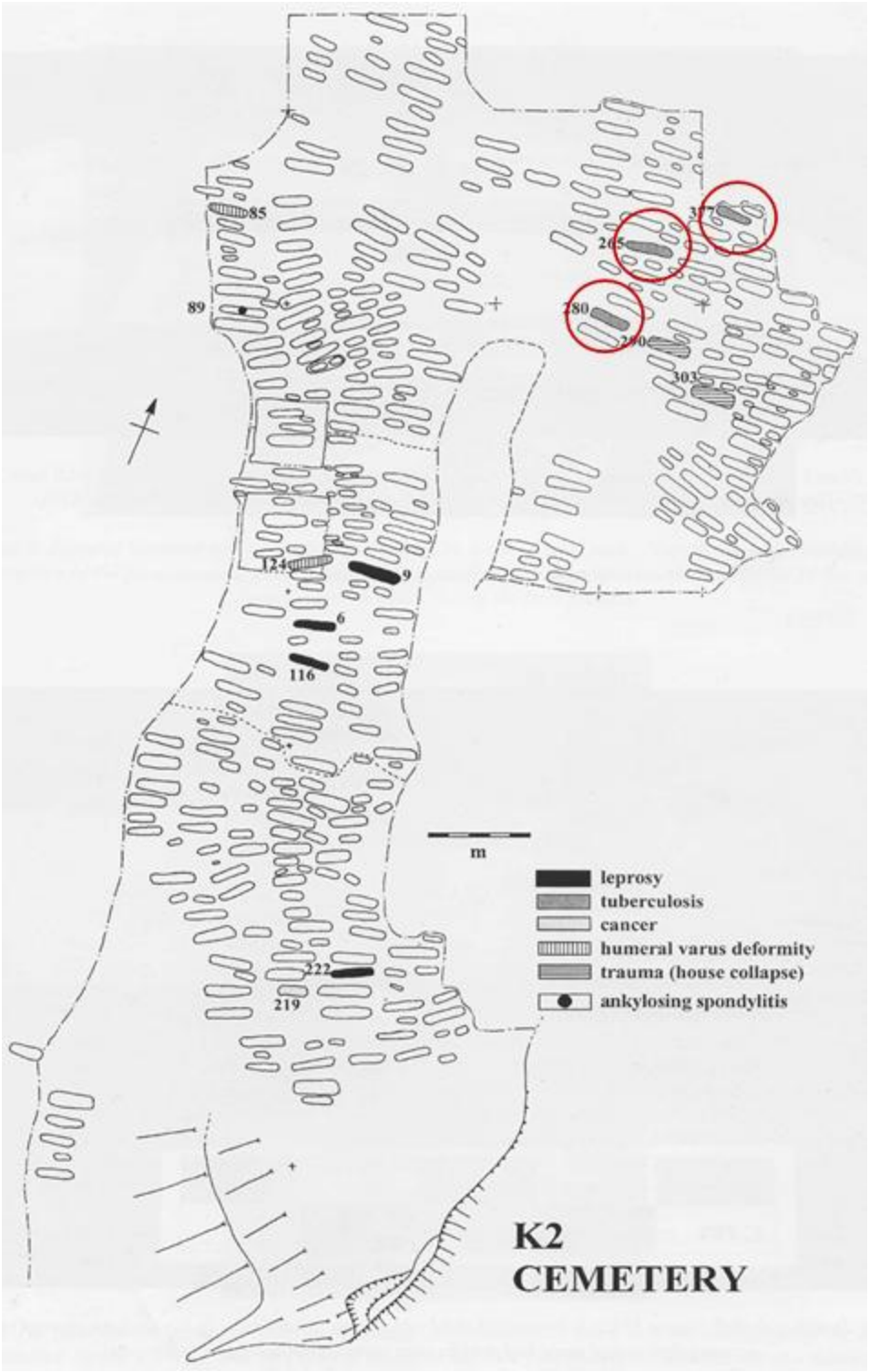

Figure 4-2: Distribution of pathologies at Kellis 2. Note the clustering of tuberculosis. (adapted from Molto 2002:245).

The etiology of the neural tube defects witnessed at Kellis 2 and the case of osteogenesis imperfecta and the expression of congenital disorders at Kellis 2 requires further study. One potential avenue of research is the presence of tetracycline in fetal individuals affected with neural tube defects and distinguishing the levels of folic acid intake of the Kellis population, specifically that of females. As mentioned in the previous chapter, tetracycline ingestion from grain sources at Kellis could serve as possible cause of neural tube defects, particularly that of iniencephaly (Maggiano 2005; Aleksic et al. 1983) . Additionally, it is well known that a deficiency in the vitamin folic acid (folate) can cause neural tube defects and that supplementation of the vitamin in food sources has led to decrease of neural tube defects cases (Chen 2008b). Low levels of folic acid disrupt the synthesis of amino acid bases, particularly thymine, resulting in abnormalities of DNA replication and cell division, but it is yet unknown how higher levels of folic acid contribute to a decreased incidence of neural tube defects (Geisel 2003; Blom et al. 2006). Natural sources of folic acid are found in leafy vegetables, especially spinach and broccoli, liver, nuts, egg, cereals, cheese, fruits, yeast, and beans (Gupta and Gupta 2004). Dietary studies of Kellis report the availability of a wide variety of foods during the Roman period, including a variety of nuts, fruits, animals, and vegetables (Dupras 1999). This brings up the question, could folic acid levels have been low at Kellis? Isotope studies that compare dietary consumption of females and males of Kellis 2 reveal that males consumed more C_4 plants, which include maize, sorghum, millet, tropical grasses, and sugar cane. It is inferred that lower levels of C_4 plants in females indicates their diet typically involved lower consumption of millet, cow or goat

meat, but more C_3 plants, which include wheat, barley, rice, grasses, trees and most fruits and vegetables (Dupras 1999), which also have higher folic acid concentrations. Interestingly, some clinical studies have reported that ingestion of tetracycline deplete levels of folic acid (Klipstein et al. 1966; Holt 1998). Future studies at Kellis 2 could concentrate on comparing tetracycline levels of diseased individuals with projected levels of folic acid of females.

In reference to the case of osteogenesis imperfecta of B532, clinical studies have expressed difficulties in pinpointing a genetic source of its occurrence in many affected individuals. Determining a familial source is likely due to the wide variations in the expression of the disease (parents are asymptomatic) (Sarathchandra 2000; Kuurila et al. 2000). Additionally, cases of osteogenesis imperfecta have revealed that many times parents that are mildly affected by the disorder can have children that are severely affected and explanations for this are unknown (Cheung and Glorieux 2008). The presence of osteogenesis imperfecta at other archaeology sites has not been accompanied with any other individuals expressing the same disorder. But, "absence of evidence is not evidence of absence" (Sagan 1977) and thus the existence of a donor of the disorder at Kellis 2 cannot be discounted. For now it can only be suspected that the individual represents a sporadic case of osteogenesis imperfecta. Future studies could concentrate on establishing heterogeneity with the individual from those in close proximity to its location. Perhaps this could reveal a possible contributor of the disorder.

4.2 Summary

The burial customs at Kellis 2 have allowed for an incredible preservation of subadult remains, permitting a unique opportunity to examine the cause of death of the smallest individuals of the cemetery, the remains of fetal individuals. The present study of skeletal individuals B532 and B625 has revealed how disease diagnosis of pathologically affected skeletal remains, from an archaeological context, is sometimes compounded by limitations in the clinical and the paleopathological literature. The paleopathological literature is not inclusive of the type of abnormalities that are seen with B625. Without paleopathological cases to compare to, clinical cases became the primary source to extrapolate a diagnoses for B625. Neural tube defects of occipital encephalocele and iniencephaly proved as the best explanation for the skeletal abnormalities. Soft tissue and radiographic descriptions from clinical cases are tentatively congruent with the abnormalities but bony defects are not well defined in the medical literature. This is problematic for defining a more confident diagnosis of the B625. Alternatively, fetal specimen B532 presented with similarities of both the clinical and paleopathological cases and proved for a more certain diagnosis of its pathologies. Although it should be noted that some defects of B532, such as the cortical underdevelopment at the ends of the long bones, are better explained in the clinical literature than the paleopathological cases.

The incongruence evidenced in the present study has only been of value for the medical and paleopathological community. As skeletal remains do present with a more exact and observable view of pathologies affecting the skeleton, those abnormalities not

mentioned with clinical cases can now be evaluated more closely and hopefully provide more diagnostic evidence for diagnoses of pathologies. This could eventually be of aid in assessing more paleopathological cases that yet have an archaeological counterpart to compare to. In this same regard, both B532 and B625 are literally one of a kind in their addition to the paleopathological studies. Fetal specimen B532 presents as the first archaeological case of osteogenesis imperfecta and B625 as a first in representing occipital encephalocele and iniencephaly. Additionally the site of Kellis 2, with its high occurrence of fetal deaths and ideal preservation, have allowed for differential treatment of age estimates by using measurements of the pars basilaris. Future studies could focus on the congruency of the linear regression formulae of the pars basilaris with other populations.

Finally, the disease diagnosis, at least for B625, has revealed some interesting patterns in the cemetery of Kellis 2. Clustering of individuals presenting with neural tube defects within familial groupings could bolster the working hypothesis of familial organization within the cemetery. It is hoped that more genetic studies, as well as comparisons of tetracycline and folic acid intake could uncover further trends of congenital disorders of the Kellis population. These present as exciting possibilities addressing the biological and cultural aspects that existed within the population that occupied Roman period Kellis.

APPENDIX A: AGE CATEOGIRES USED IN THIS THESIS

General age term[1]	Chronological age range
Fetal	8 weeks intra-uterine to birth
Perinate	Around the time of birth
Infant	Birth to the end of the 3rd year
Child	3 – 12 years
Adolescent	10 – 14 for Girls; 12 – 16 or 17 for Boys
Adult	>17 years
Juvenile	used in a general sense, includes any stage previous to adult

[1] Age terms after Scheuer and Black 2000; Lewis 2007

APPENDIX B: DATASHEET FOR RECORDING CRANIAL AND POSTCRANIAL SKELETAL REMAINS

Fetal/Infant Recording Sheet

Recorded by:_____ Date:_____ Burial #:_____

Cranial Measurements

(record to nearest tenth of mm; mark 0 if bone is not present, or X if cannot be measured due to breakage)

Bone	Measurement	L	M	R
LW Sphenoid	length			
	width			
GW Sphenoid	length			
	width			
Sphenoid Body	length			
	width			
Petrous & mastoid	length			
	width			
Pars basilaris	sagittal length			
	max length			
	width			
Zygomatic	length			
	width			
Maxilla	alveolar length			
	alveolar width			
	height			
Mandible	length of ½ mandible			
	arc width			
	body length			
Frontal	length			
	width			
Pars squama (occipital)	height			
	width			
Parietal	length			
	width			
Nasals	length			
	width			

Infracranial Measurements

(record to nearest tenth of mm; mark 0 if bone is not present, or X if cannot be measured due to breakage)

Bone	Measurement	L	R
Clavicle	length		
	diameter		
Scapula	length		
	width		
	length of spine		
Humerus	length		
	distal width		
	diameter		
Ulna	length		
	diameter		
Radius	length		
	diameter		
Femur	length		
	distal width		
	diameter		
Tibia	length		
	diameter		
Fibula	length		
	diameter		
Ilium	length		
	width		
Ischium	length		
	width		
Pubis	length		

Datasheet format adapted after Sandra Wheeler

Burial #:_____

APPENDIX C: AGE ESTIMATES, LONG BONE LENGTH AND PARS BASILARIS MEASUREMENTS OF THE KELLIS 2 SAMPLE OF FETAL INDIVIDUALS

Burial #	Mean Age[1]	Mean Diaphyseal Length (mm)						Pars Basilaris Measurements (mm)		
		Humerus	Ulna	Radius	Femur	Tibia	Fibula	Sagittal Length	Maximum Length	Maximum Width
334	24.0	35.7	32.8	29.9	35.3	30.9	.	8.05	9.90	7.20
298	26.3	40.8	36.3	32.4	41.8	36.2	35.7	8.70	10.70	10.70
316	26.9	42.9	38.2	34.6	42.9	37	35.9	9.85	11.50	8.75
332	29.3	45.3	44.2	39.2	49.5	42.5	42.1	9.75	11.80	9.05
180	29.5	43.3	42.5	38.0	50.9	45.9	44.5	8.45	10.50	8.25
319	31.3	48.4	46.9	41.9	54.8	48.3	47.1	10.60	12.60	10.05
318b	34.1	54.7	50.9	44.8	62	55.2	52.9	11.00	13.90	12.85
701	34.3	54.9	52.2	45.7	62.2	54.8	52.5	11.3	11.5	13.0
575b	34.4	55.6	52.5	45.4	62.8	54.1	52.6	11.1	14.1	12.0
436	35.8	59.1	54.6	48.3	65.1	57.8	54.8	11.4	13.0	13.9
297	36.6	59.3	55.2	50.3	67.3	59.9	57.1	11.8	14.9	13.3
154	36.9	59.9	56.3	50.2	68.7	60.1	56.8	11.4	14.7	14.8
313	37.0	.	55.7	.	.	.	.	11.1	14.4	13.6
209	37.3	59.1	57.1	51.5	70.0	61.5	58.5	11.4	14.8	14.9
333	37.4	61.6	56.2	49.0	71.2	60.9	57.9	11.5	14.85	14.45
462	37.5	63.3	55.9	49.8	70.2	61.9	.	12.0	16.1	13.1
387	37.7	63.9	57.2	50.8	70.3	60.4	57.1	12.3	16.9	15.3
572	37.8	61.0	55.5	49.6	71.7	63.6	60.2	11.7	14.5	14.3
601	37.8	62.9	57.7	50.8	69.6	62.0	59.9	11.7	14.9	14.6
518	38.3	60.4	59.6	51.5	.	62.0	59.6	11.2	15.3	14.6
568	38.3	63.1	57.8	50.7	71.4	62.0	63.9	11.7	14.8	12.9
513b	38.7	65.1	58.3	51.6	73.1	62.7	60.7	12.4	15.5	14.3
153	38.8	63.5	58.9	51.9	73.8	54.1	60.5	13.1	16.85	16.6
449	39.0	64.7	59.5	53.0	72.9	63.5	62.1	12.4	15.2	13.8
558	39.2	63.7	58.3	52.0	76.8	63.7	62.2	11.5	15.5	15.9
608	39.2	66.6	60.8	53.2	72.6	63.5	61.2	9.9	15.1	13.5
419	39.6	65.9	61.4	53.6	72.3	67.0	62.8	12.3	17.0	17.5
599	39.6	65.5	60.8	52.9	75.4	65.0	62.1	10.8	14.7	13.7
446	39.7	65.8	61.3	54.7	75.2	64.2	61.2	12.3	16.1	14.6
151	40.0	65.2	60.0	52.7	77.2	66.3	64.2	13.0	16.1	13.5
605	40.1	66.2	60.8	53.1	76.6	66.7	63.7	12.6	15.2	15.7
616	40.1	66.6	61.3	55.1	76.5	66.2	62.4	12.8	15.6	16.7
348	40.6	.	58.3	51.3	81.3	66.5	63.8	13.4	17.3	15.5
495	40.6	65.4	.	.	.	65.9	63.8	11.9	15.5	14.5
660	40.6	68.9	61.9	55.5	77.9	66.0	61.9	11.9	15.6	15.8
508	42.0	69.5	65.1	58.0	80.3	68.7	67.7	11.7	15.9	17.1
445	42.1	67.4	64.6	57.6	79.4	70.9	67.3	12.0	15.0	14.0

[1]Mean gestational age estimates based on linear regression formulae provided in Scheuer et al. (1980); Scheuer & Black (2000) and Sherwood et al (2000)

"." Indicates missing data due to lack of measurable bone

REFERENCES

Aerts M, Van Holsbeke C, de Ravel T, Devlieger R. 2006. Prenatal diagnosis of type II osteogenesis imperfecta, describing a new mutation in the COL1A1 gene. Prenatal Diagnosis 26:393-394.

Afifi AK, Bregman RA. 2005. Functional neuroanatomy: text and atlas. 2nd edition. New York: McGraw-Hill.

Aigner T, Rau T, Niederhagen M, Zaucke F, Schmitz M, Pohls U, Stöss H, Rauch A, Thiel CT. 2007. Achondrogenesis type IA (Housten-Harris): a still-unresolved molecular phenotype. Pediatric and Developmental Pathology 10:328-334.

Alanay Y, Krakow D, Rimoin DL, Lachman RS. 2007. Angulated femurs and the skeletal dysplasias: experience of the International Skeletal Dysplasia Registry (1988-2006). American Journal of Medical Genetics Part A 143A:1159-1168.

Aleksic S, Budzilovich G, Greco MA, Feigin I, Epstein F, Pearson J. 1983. Iniencephaly: a neuropathologic study. Clinical Neuropathology 2: 55-61.

Al-Gazali LI, Varghese M, Varady E, Talabani JA, Scorer J, Bakalinova D. 1996. Neonatal Schwartz-Jampel syndrome: a common autosomal recessive syndrome in the United Ara Emirates. Journal of Medical Genetics 33:203-211.

Angle CR. 1954. Congenital bowing and angulation of long bones. Pediatrics 13: 257—268.

Aufderheide AC, Rodriguez-Martin C. 1998. The Cambridge encyclopedia of human paleopathology. New York: Cambridge University Press.

Aufderheide AC, Cartmell L, Zlonis M. 2003. Bio-anthropological features of human mummies from the Kellis 1 cemetery: the database for mummification methods. In: Bowen GE, Hope CA, editors. The oasis papers. III. The Proceedings of the Third International Conference of the Dakhleh Oasis Project. Oxford: Oxbow Books. p. 137-151.

Ayter MH, Dogulu F, Cemil B, Ergun E, Kurt G, Baykaner K. 2007. Iniencephaly and long-term survival: a rare case report. Child's Nervous System 23:719-721.

Bain AD, Barrett HS. 1959. Congenital bowing of the long bones: report of a case Archives of Disease in Childhood 34: 516–524.

Baker BJ, Dupras TL, Tocheri M. 2005. The osteology of infants and children. College station: Texas A&M University Press.

Barnes E. 1994. Developmental Defects of the Axial Skeleton in Paleopathology. Niwot: University Press of Colorado.

Beals RK. 2000. The short clavicle syndrome. Journal of Pediatric Orthopedics 20:389-91.

Bhat M, Nelson KB. 1989. Developmental enamel defects in primary teeth in children with cerebral palsy, mental retardation, or hearing defects: a review. Advances in Dental Research 3:132-142.

Bianchi DW, Crombleholme TM, D'Alton ME. 2000. Fetology: Diagnosis and Management of the Fetal Patient. McGraw-Hill Professional.

Birrell M. 1999. Excavations in the cemeteries at Ismant el-Kharab. In: Hope CA, Mills AJ. Dakhleh Oasis Project: Preliminary Reports on the 1992–1993 and 1993–1994 Field Seasons. Oxbow: Oxford. p 29–41.

Bland JH. 2001. Disorders of the shoulder. In: Noble J, editor. Textbook of primary care medicine. St. Louis, Missouri: Mosby, Inc. p 810-814.

Blom HJ, Shaw GM, Heijer MD, Finnell RH. 2006. Neural tube defects and folate: case far from closed. Nature Publishing Group 7:724-731.

Bleyer A. 1940. The antiquity of achondroplasia. Annals of Medical History 2:306-307.

Borochowitz Z, Lachman R, Adomian GE, Spear G, Jones K, Rimoin DL. 1988. Achondrogenesis type 1: delineation of further heterogeneity and identification of two distinct subgroups. Journal of Pediatrics 112:23-31.

Botto LD, Moore CA, Khoury MJ, Erickson JD. 1999. Neural-tube defects. The New England Journal of Medicine 341:1509-1519.

Bowen GE. 2001. Text and textiles: a study of the textile industry at ancient Kellis. Artefact 24:18–27.

Bowen GE. 2002. Textiles, basketry and leather goods from Ismant el-Kharab. In: Hope CA, Bowen GE, editors. The Dakhleh Oasis Project: preliminary reports on the 1994-1995 to 1998-1999 field season. Oxford: Oxbow Books. p 87-104.

Bowen GE. 2003. Some observations on Christian burial practices at Kellis. In: Bowen GE, Hope CA, editors. The oasis papers. III: the proceedings of the Third International Conference of the Dakhleh Oasis Project. Oxford: Oxbow Books. p 166–182.

Brothwell D. 1967. Major congenital anomalies of the skeleton: evidence from earlier populations. In: Browth D, Sandison A, editors. Diseases in antiquity: a survey of the diseases, injuries and surgery of early populations. Springfield: Thomas. p 320-345.

Brown MS, Sheridan-Pereira M. 1992. Outlook for the child with a cephalocele. Pediatrics 90: 914-919.

Bui CJ, Tubbs RS, Shannon CN, Acakpo-Satchivi L, Wellons JC, Blount JP, Oakes WJ. 2007. Institutional experience with cranial vault encephaloceles. Journal of Neurosurgery 107:22-25.

Bulas DI, Stern HJ, Rosenbaum KN, Fonda JA, Glass RB, Tifft C. 1994. Variable prenatal appearance of osteogenesis imperfecta. Journal of Ultrasound in Medicine 13(6):419-427.

Buikstra JE, Cook DC. 1980. Paleopathology: an American account. Annual Review of Anthropology 9:433-470.

Byers PH, Steiner RD. 1992. Osteogenesis imperfecta. Annual Review of Medicine 43:269-282.

Byers SN, Roberts CA. 2003. Baye's theorem in paleopathological diagnosis. American Journal of Physical Anthropology 121:1-9.

Caffey J. 1947. Prenatal bowing and thickening of tubular bones with multiple cutaneous dimples in arms and legs: a congenital syndrome of mechanical origin. Am J Dis Child 74:543-562.

Cavendish ME. 1972. Congenital elevation of the scapula. Journal of Bone and Joint Surgery 54-B: 395-408.

Charon P. 2005. Tératologie du tube neural: histoire et paléopathologie. Antropo 10 83-101.

Cheema, JI, Grissom LE, Theodore H. 2003. Radiographic characteristics of lower extremity bowing in children. Radiographics 23:871-880.

Chen CP. 2007. Prenatal diagnosis of iniencephaly. Taiwan Journal of Obstetrics and Gynecology 46:199-208.

Chen CP. 2008a. Syndromes, disorders and maternal risk factors associated with neural tube defects (I). Taiwan Journal of Obstetrics and Gynecology 47:1-9.

Chen CP. 2008b. Syndromes, disorders and maternal risk factors associated with neural tube defects (iv). Taiwan Journal of Obstetrics and Gynecology 47:141-150.

Chen CP, Liu FF, Jan SW, Lin YN, Lan CC. 1996. A case of achondrogenesis type IA with an occipital encephalocele. Genetic Counseling 7:193-9.

Cheung MS, Glorieux FH. 2008. Osteogenenesis imperfecta: update on presentation and management. Reviews in Endocrine and Metabolic Disorders 9: 153-160.

Cohen-Solal L, Zylberberg L, Sangalli A, Gomez LM, Mottes M. 1994. Substitution of an aspartic acid for glycine 700 in the alpha 2I chain of type I collagen in a recurrent lethal type II osteogenesis imperfecta dramatically affects the mineralization of bone. Journal of Biological Chemistry. 269: 14751-14758.

Cole DEC. 2003. Hypophosphatasia. In: Glorieux FH, Pettifor JM, Juppner H, editors. Pediatric bone: biology and disease. Amsterdam: Academic Press. p. 651-678.

Dogan MM, Ekicl E, Yapar EG, Soysal ME, Soysal SK, Gokmen O. 1996. Iniencephaly: sonographic-pathologic correlation of 19 cases. Journal of Perinatal Medicine. 24: 501-511.

Drezner MK. 2006. Osteomalacia and rickets. In: Glorieux FH, Pettifor JM, Juppner H, editors. Pediatric bone: biology and disease. Amsterdam: Academic Press. p. 739-754.

Dupras TL. 1999. Dining in the Dakhleh Oasis, Egypt: Determination of Diet using Documents and Stable Isotope Analysis [dissertation]. Hamilton (Ontario): McMaster University, 319 p.

Dupras T, Tocheri M, Maggiano C, Molto E. 2002. The fetal skeletons of Kellis: the isotopic, fluores-cent microscopic, and osteometric evidence. American Journal of Physical Anthropology 117 (suppl.34): 65–66.

Dupras T, Tocheri M. 2007. Reconstructing infant weaning histories at Roman period Kellis, Egypt using stable isotope analysis of dentition. American Journal of Physical Anthropology 134:63–74.

Dutton M. 2004. Orthopaedic examination, evaluation, and intervention. New York: McGraw-Hill Professional. p 414.

Fazekas IG, Kósa F. 1978. Forensic fetal osteology. Akademiai Kiado: Budapest.

Filer J. 1995. Egyptian bookshelf: disease. Austin: University of Texas Press.

Frayer D, Macchiareli R, Mussi M. 1988. A case of chondrodystrophic dwarfism in the Italian Late Upper Paleolithic. American Journal of Physical Anthropology 75:549-565.

Geisel J. 2003. Folic acid and neural tube defects in pregnancy: a review. Journal of Perinatal and Neonatal Nursing. 17: 268-279.

Glorieux FH, Rauch F, Plotkin H, Ward L, Travers R, Roughley P, Lalic L, Glorieux DF, Fassier F, Bishop NJ. 2000. Type V osteogenesis imperfecta: a new form of brittle bone disease. Journal of Bone Mineral Research 15:1650-1658.

Glorieux FH, Ward LM, Rauch F, Lalic L, Roughley PJ, Travers R. 2002. Osteogenesis imperfecta type VI: a form of brittle bone disease with a mineralization defect. Journal of Bone Mineral Research 17:30-38.

Glorieux FH, Rauch F. 2006. Osteogenesis imperfecta. In: Siebal MJ, Robins SP, Bilezikian JP, editors. Dynamics of bone and cartilage metabolism: principles and clinical applications. 2nd ed. San Diego: Academic Press. p 831-842.

Gorlin RJ, Cohen MM, Hennekam RCM. 2001. Syndromes of the head of neck. Oxford University Press: Oxford.

Graver AM, Molto JE, Parr RL, Walters S, Praymak RC, Maki JM. 2001. Mitochondrial DNA research in the Dakhleh Oasis, Egypt: a preliminary report. Ancient Biomolecules 3:239–253.

Gray PHK. 1969. A case of osteogenesis imperfecta, associated with dentinogenesis imperfecta, dating from antiquity. Clinical Radiology 20:106-108.

Gupta H, Gupta P. 2004. Neural tube defects and folic acid. Indian Pediatrics 41:577-586.

Halcrow S, Tayles N. 2008. The bioarchaeological investigation of children and social age: problems and prospects. Journal of Archaeological Method and Theory 15: 190-215.

Hall BD, Spranger J. 1980. Congenital bowing of the long bones: a review and phenotype analysis of 13 undiagnosed cases. European Journal of Pediatrics 133: 131-138.

Handmaker SD, Campbell JA, Robinson LD, Chinwah O, Gorlin RJ. 1977. Dyssegmental dwarfism: a new syndrome of lethal dwarfism. Birth Defects Original Article Series 13: 79-90.

Herasse M, Spentchian M, Taillandier A, Mornet E. 2002. Evidence of a founder effect for the tissue-nonspecific alkaline phosphate (TNSALP) gene E174k mutation in hypophosphatasia patients. European Journal of Human Genetics 10:666-668.

Hoffman J. 1976. An achondroplastic dwarf from the Augustine Site (Ca-Sac-127). Contribution of the University of California Archaeological Research Facility 30:65-119.

Holt GA. 1998. Food and drug interactions Chicago: Percept Press.

Hope CA. 2001. Observations on the dating of the occupation at Ismant el-Kharab. In: Marlow CA, Mills AJ, editors. The oasis papers. I. The Proceedings of the First Conference of the Dakhleh Oasis Project. Oxford: Oxbow Books. p 43–59.

Houston CS, Opitz, JM, Spranger JW, Macpherson RI, Reed MH, Gilbert EF, Herrmann J, Schinzel A. 1983. The campomelic syndrome: review, report of 17 cases, and follow-up on the currently 17-year-old boy first reported by Maroteaux et al in 1971. American Journal of Medical Genetics 15: 3-28.

Hovmöller ML, Osuna A, Eklöf O, Fredga K, Hjerpe A, Linsten J, Ritzen M, Stanescu V, Svenningsen N. 1977. Camptomelic dwarfism. A genetically determined mesenchymal disorder combined with sex reversal. Hereditas. 86:51-62.

Iannotti JP, Williams GR. 2006. Disorders of the shoulder: diagnosis and management. California: Lippincott Williams & Wilkins.

Johnson KMK, Suarez L, Felkner MM, Hendricks K. 2004. Prevalence of craniorachischisis in a Texas-Mexico border population. Birth Defects Research Part A 70:92-94.

Johnson VP, Keppen LD, Carpenter MS, Randall BR, Newby PE. 1997. New syndrome of spondylospinal thoracic dysostosis with multiple pterygia and arthrogryposis. American Journal of Medical Genetics 69:73-78.

Kamoun-Goldrat A, Martinovic J, Saada J, Sonigo-Cohen P, Razavi F, Munnich A, Merrer ML. 2008. Clinical report: prenatal cortical hyperostosis with COL1A1 gene mutation. American Journal of Medical Genetic Part A 146A:1820-1824.

Kita D, Munemoto S, Ueno Y , Fukunda A. 2002. Goldenhar's syndrome associated with occipital meningoencephalocele: case report. Neurologia Medico-Chirugica 42: 354-355.

Kjaer KW, Hansen BF, Keeling JW, Kjaer I. 1999. Skeletal malformations in fetuses with Meckel Syndrome. American Journal of Medical Genetics 84:469-475.

Kjaer I, Keeling JW, Hansen BF. 1996. Pattern of malformations in the axial skeleton in human trisomy 18 fetuses. American Journal of Medical Genetics 66: 332-336.

Klipstein FA, Schenk EA, Samloff IM. 1966. Folate repletion associated with oral tetracycline therapy in tropical sprue. Gastroenterology 51:317-332.

Kuurila K, Grenman R, Johansson R, Kaitila I. 2000. Hearing loss in children with osteogenesis imperfecta. European Journal of Pediatrics 159:515-519.

Kulaylat NA, Narchi H. 2000. Iniencephaly: an uncommon neural tube defect. Journal of Pediatrics 136:414.

Kwok C, Weller PA, Guioli S, Foster JW, Mansour S, Zuffardi O, Punnett HH, Dominguez-Steglich MA, Brook JD, Young ID, Goodfellow PN, Schafer AJ. 1995. Mutations in SOX9, the gene responsible for campomelic dysplasia and autosomal sex reversal. American Journal of Human Genetics 57:1028-1036.

Langer R, Al-Gazali L, Raupp P, Verady E. 2007. Radiological manifestations of the skeleton, lungs and brain in Stüve-Wiedemann syndrome. Australasian Radiology 51: 203-210.

Lee FA, Isaacs H, Strauss J. 1972. The "campomelic" syndrome. American Journal O of Diseases of Children 124:485-496.

Lewis ME. 2007. The bioarchaeology of children: perspectives from biological and forensic anthropology (Cambridge studies in biological and evolutionary anthropology). Cambridge: Cambridge University Press.

Lewis ME, Flavel A. 2007. Age assessment of child skeletal remains in forensic contexts. In: Schmitt A, Cunha E, Pinheiro J, editors. Forensic anthropology and medicine: complementary sciences from recovery to cause of death. New Jersey: Human Press.

Li D, Liao C, Ma X. 2005. Prenatal diagnosis and molecular analysis of type 1 thanatophoric dysplasia. International Journal of Gynecology and Obstetrics 91:268—270.

Lin HJ, Cornford ME, Hu B, Rutgers JKL, Beall MH, Lachman RS. 1996. Occipital encephalocele and MURCS Association: case report and review of central nervous system anomalies in MURCS patients. American Journal of Medical Genetics 61:59-62.

Loo CKC, Freeman B, Stanford D. 2001. CNS findings in iniencephaly: case report and literature review. Pathology 33: 112-115.

Lovell NC, Whyte I. Patterns of dental enamel defects at ancient Mendes, Egypt. American Journal of Physical Anthropology 110: 69-80.

Maggiano C. 2005. Confocal laser scanning microscopy as a tool for the investigation of tetracycline fluorescence in archaeological human bone [thesis]. Orlando (FL): University of Central Florida. 65 p.

Majewski F, Stob H, Goecke T, Kemperdick H. 1983. Are bowing of the long tubular bones and preaxial polydactyly signs of the Meckel syndrome. Human Genetics 65: 125-133.

Malgosa A, Aluja MP, Isidro A. 1996. Pathological evidence in newborn children from the sixteenth century in Huelva (Spain). International Journal of Osteoarchaeology 4:388-396.

Malmgren B, Norgren S. 2002. Dental aberrations in children and adolescents with osteogenesis imperfecta. Acta Odontologica Scandinavica 60:65-71.

Mahapatra AK, Gupta PK, Dev EJ. 2002. Posterior fontanelle giant encephalocele. Pediatric Neurosurgery 26: 40-43.

Mahasen LMA, Sadek SA. 2002. Developmental morphological and histological studies on structures of the human fetal shoulder joint. Cells Tissues Organs 170: 1-20.

Mansour S, Hall CM, Pembrey ME, Young ID. 1995. A clinical and genetic study of campomelic dysplasia. Journal of Medical Genetics 32:415-420.

Mansour S, Offiah AC, McDowall S, Sim P, Tolmie J, Hall C. 2002. The phenotype of survivors of campomelic dysplasia. Journal of Medical Genetics 39:597-602.

Maroteaux P, Spranger J, Opitz JM, Kucera J, Lowry RB, Schimke RN, Kagan SM. 1971. The campomelic syndrome. La Presse Médicale 79:1157–1162.

Marx JA, Hockberger RS, Walls RM, Adams J, Rosen P. 2006. Rosen's emergency medicine: concepts and clinical practice. St. Louis: Mosby.

Mathews S. 2008. Diagnosing Anencephaly in Archaeology: A Comparative Analysis of Nine Clinical Specimens from the Smithsonian Institution National Museum of Natural History, and One from the Archaeological Site of Kellis 2 Cemetery in Dakhleh Oasis, Egypt [thesis]. Orlando (Florida): University of Central Florida 90 p.

Mays S. 1998. The archaeology of human bones. London: Routledge.

Menkes CJ, Lane NE. 2004. Are osteophytes good or bad? OsteoArthritis and Cartilage 12:553-554.

Merz E. 2005. Ultrasound in obstetrics and gynecology. New York : Thieme.

McDowall S, Argentaro A, Ranganathan S, Welleri P, Mertin S, Mansour S, Tolmie J, Harley V. 1999. Functional and structural studies of wild type SOX9 and mutations

causing campomelic dysplasia. The Journal of Biological Chemistry 274(34):24023-24030.

Mills AJ. 1999. Introduction. In: Chrucher CS and Mills AJ, editors. Reports from the survey of the Dakhleh Oasis western desert of Egypt 1977-1987. Oxbow Books: Oxford. p ix – xii.

Molto JE. 1998. Disease history from the Dakhleh oasis Egypt. Paper presented at the annual meeting of the Society for the Study of Egyptian Antiquities, Toronto.

Molto JE. 2000. Humerus varus deformity in Roman period burials from Kellis 2, Dahkleh, Egypt. American Journal of Physical Anthropology 118:108-109.

Molto JE. 2002. Bio-archaeological research of Kellis 2: An overview. In: The Dakhleh Oasis Project: preliminary reports on the 1994-1995 to 1998-1999 field season. Oxbow Books: Oxford p. 239-255.

Moore KL and Persaud VN. 2003. The developing human: clinically oriented embryology. Philadelphia: Saunders.

Nath RK, Melcher SE, Paizi M. 2006. Surgical correction of unsuccessful derotational humeral osteotomy in obstetric brachial plexus palsy: evidence of the significance of scapular deformity in the pathophysiology of the medial rotation contracture. Journal of Brachial Plexus and Peripheral Nerve Injury 1: 1 – 7.

Mylannus EAM, Marres HAM, Vlietman J, Kollee LAA, Freihofer HPM, Thijssen HOM, Vries JD, Wesseling P. 1999. Translar sphenoidal encephalocele and respiratory distress in a neonate: a case report. Pediatrics 103: 1-4.

Olney PN, Kean LS, Graham D, Elsas LJ, May KM. 1999. Campomelic syndrome and deletion of SOX9. American Journal of Medical Genetics 84:20-24.

Ortner DJ. 1991. Theoretical and methodological issues in paleopathology. In: Ortner DJ, Aufderheide AC, editors. Human paleopathology: current syntheses and future options. Washington, D.C.: Smithsonian Institution Press.

Ortner, DJ. 2003. Identification of pathological conditions in human skeletal remains. San Diego (CA): Academic Press page 494.

Padmanabhan R. 2006. Etiology, pathogenesis and prevention of neural tube defects. Congenital Anomalies 46:55-67.

Palmer CA. 2001. Important relationships between diet, nutrition, and oral health. Nutrition in Clinical Care 4:4-14.

Parr RL. 2002. Mitochondrial DNA sequence analysis of skeletal remains from the Kellis 2 cemetery. In: Hope CA, Bowen GE, editors. Dakhleh Oasis Project: preliminary reports on the 1994–1995 to 1998–1999 field seasons. Oxford: Oxbow Books. p 257–261.

Parsche F, Zimmerman P. 1991. Results of computer assisted studies of population structure and burial practices of adults of the late Roman burial ground in the Minshat Abu Omar (east Nile delta). Anthropologischer Anzeiger (Stuttgart) 49: 65–83.

Patterson RJ, Eglehoff JC, Crone KR, Ball WS. 1998. Atretic parietal cephaloceles revisited: an enlarging clinical and imaging spectrum?

Pinhasi R, Mays S. 2008. Advances in human paleopathology. England: Wiley.

Plotkin H, Primorac D. Rowe D. 2003. Osteogenesis imperfecta. In: Glorieux FH, Pettifor JM, Juppner H, editors. Pediatric bone: biology and disease. Amsterdam: Academic Press.

Pomerance HH, Wallis-Crespo C, Barnes EB. 2005. Lethal infantile cortical hyperostosis. Fetal and Pediatric Pathology 24:89-94.

Promsonthi P, Wattanasirichaigoon D. 2006. Prenatal diagnosis of campomelic dysplasia with three-dimensional ultrasound. Ultrasound in Obstetrics and Gynecology 27:583-585.

Ramachandran U, Malla T, Joshi KS. 2006. Meckel-Gruber syndrome. Kathmandu University Medical Journal 4:334-336.

Rauch F, Glorieux FH. 2004. Osteogenesis imperfecta. Lancet 363:1377-1385.

Redfield A. 1970. A new aid to aging immature skeletons: development of the occipital bone. American Journal of Physical Anthropology 33: 207–220.

Richardson WS, Glasziou P, Polashenski WA, Wilson MC. 2000. A new arrival: evidence about differential diagnosis. Evidence-Based Medicine 5:164-165.

Ries L, Frydman M, Barkai G, Goldman B, Friedman E. 2000. Prenatal diagnosis of a novel COL1A1 mutation in osteogenesis imperfecta type I carried through full term pregnancy. Prenatal Diagnosis: 20:876-880.

Rimoin DL, Cohn D, Krakow D, Wilcox W, Lachman RS, Alanay Y. 2007. The skeletal dysplasias: clinical-molecular correlations. Annals of the New York Academy of Sciences 1117:302-309.

Roberts CA, Lewis ME, Manchester K (eds.). 2002. The past and present of leprosy. British Archaeological Reports International Series S1054. Oxford: Archaeopress.

Roberts C, Manchester K. 2005. The archaeology of disease, 3rd edition. Ithaca, New York: Cornell University Press.

Robinson S, Nicolson R, Pollard A, O'Connor T. 2003. An evaluation of nitrogen porosimetry as a technique for predicting taphonomic durability in animal bone. Journal of Archaeological Science 30. 391-403.

Rogers J, Waldron T. 1988. Two possible cases of infantile cortical hyperostosis. Paleopathology Newsletter 35:7-10.

Rogers JG, Cranley RE, Dorst JP, Levin LS, Williams BR. 1975. A variant of campomelia. Birth Defects Original Article Series 11:119–125.

Romero R, Pilu G, Jeanty P, G Alessandro, Hobbins J. 1988. Prenatal diagnosis of congenital anomalies. Norwalk: Appleton and Lange.

Rudd NL, Miskin M, Hoar DI, Benzie R, Dora TA. 1976. Prenatal diagnosis of hypophosphatasia. The New England Journal of Medicine 295:146-148.

Rustico MA, Lalatta F, Righini A, Spaccini L, Fabietti I, Nicolini U. 2004. The role of integrate imaging techniques for prenatal prediction of phenotype in two cases of facial anomalies. Prenatal Diagnosis 24:508-512.

Rowe DW, Shapiro JR. 1998. Osteogenesis imperfecta. In: Aviolie LV, Krane SM, editors. Metabolic bone disease and clinically related disorders. San Diego: Academic Press. p. 651-695.

Sagan C. (1977) The Dragons of den: speculations on the evolution of human intelligence. New York: Radom House.

Sanders RC, Greyson-Fleg RT, Hogge WA, Blakemore KJ, McGowan KD, Isbister S. 1994. Osteogenesis imperfecta and campomelic dysplasia: difficulties in prenatal diagnosis. Journal of Ultrasound in Medicine 13:691-700.

Sandler TW. 2006. Langman's Medical Embryology. 10th edition. Philadelphia: Lippincott Willams & Wilkins.

Sarathchandra P, Pope FM, Kayser MV, Ali SY. 2000. A light and electron microscopic study of osteogenesis imperfecta bone samples, with reference to collagen chemistry and clinical phenotype. Journal of Pathology 192:385-395.

Scheuer JL, Black S. 2000. Developmental Juvenile Osteology. Academic Press: London.

Scheuer L, MacLaughlin-Black S. 1994. Age estimation from the pars basilaris of the fetal and juvenile occipital bone. International Journal of Osteoarchaeology 4: 377–380.

Scheuer JL, Musgrave JH, Evans SP. 1980. The estimation of late fetal and perinatal age from limb bone length by linear and logarithmic regression. Annals of Human Biology 7: 257–265.

Schweiger S, Chaoui R, Tennstedt C, Lehmann K, Mundlos S, Tinschert S. 2003. Antenatal onset of cortical hyperostosis (Caffey's disease): case report and review. American Journal of Medical Genetics 120A: 547-552.

Sherwood RJ, Meindl RS, Robinson HB, May RL. 2000. Fetal age: methods of estimation and effects of pathology. American Journal of Physical Anthropology 113: 305–315.

Shkrum SA. 2008. The paleoepidemiology of oral health in the children from Kellis 2, Dakhleh, Egypt [thesis]. London (Ontario): The University of Western Ontario. 180 p.

Spranger JW, Brill PW, Poznanski A. 2002. Bone dysplasias: an atlas of genetic disorders of skeletal development. Oxford: Urban and Fischer Verlag.

Sillence DO, Barlow KK, Garber AP, Hall JG, Rimoin DL. 1984. Osteogenesis imperfecta type II delineation of the phenotype with reference to genetic heterogeneity. American Journal of Medical Genetics 17:407-23.

Sillence DO, Senn A, Danks DM. 1979. Genetic heterogeneity in osteogenesis imperfecta. Journal of Medical Genetics 16:101-16.

Smith AB, Gupta N, Otto C, Glenn OA. 2007. Diagnosis of Chiari III malformations by second trimester fetal MRI with postnatal MRI and CT correlation. Pediatric Radiology 37: 1035-1038.

Shohat M. 1991. Perinatal lethal hypophosphatasia: clinical, radiological, and morphologic findings. Pediatric Radiology 21:421-427.

Starling AP, Stock JT. 2007. Dental indicators of health and stress in early Egyptian and Nubian agriculturalists: a difficult transition and gradual recovery. American Journal of Physical Anthropology 134:520-8.

Stewart JD, Molto JE, Reimer P. 2003. The chronology of Kellis 2: the interpretive significance of radiocarbon dating of human remains. In: Bowen GE, Hope CA, editors.

The oasis papers. III. The Proceedings of the Third International Conference of the Dakhleh Oasis Project. Oxford: Oxbow Books. p 345–364.

Storer J, Grossman H. 1974. The campomelic syndrome: congenital bowing of limbs and other skeletal and extraskeletal anomalies. Radiology 111:673–681.

Stüve A, Wiedemann HR.1971. Congenital bowing of the long bones in two sisters. Lancet. 2(7722):495.

Superti-Furga A, Tenconi R, Clementi M, Eich G, Steinmann B, Boltshauser E, Giedon A. 1998. Schwartz-Jampel syndrome type 2 and Stüve-Wiedemann syndrome: a case for "lumping". American Journal of Medical Genetics 78:150-154.

Tavormina PL, Shijan R, Thompson LM, Ya-Zhen Z, Wilkin DJ, Lachman RS, Wilcox WR, Rimoin DL, Cohn DH, Wasmuth JJ. 1995. Thanatophoric dysplasia (types I and II) caused by distinct mutation in fibroblast growth factor receptor 3. Nature Genetics 9:321-328.

Tocheri MW, Dupras TL, Sheldrick P, Molto JE. 2005. Roman period fetal skeletons from the East Cemetery (Kellis 2) of Kellis, Egypt. International Journal of Osteoarchaeology 15: 326-34.

Tocheri MW, Molto JE. 2002. Aging fetal and juvenile skeletons from roman period Egypt using basiocciput osteometrics. International Journal of Osteoarchaeology 12:356-363.

Tongsong T, Pongsatha P. 2000. Early prenatal sonographic diagnosis of congenital hypophosphatasia. Ultrasound Obstetrics and Gynecology 15:252-255.

Traub W, Arad T, Vetter U, Weiner S. 1994. Ultrastructural studies of bones from patients with osteogenesis imperfecta. Matrix Biology 14: 337-345.

Tugrul S, Uludogan M, Pekin O, Uslu H, Celikc C, Ersan F. 2007. Iniencephaly: prenatal diagnosis wit postmortem findings. Journal of Obstetrics and Gynaecology Research 33:566-569.

Ubelaker DH. 1987. Estimating age at death from immature human skeletons: an overview. Journal of Forensic Sciences 32:1254-1263.

Unger S, Superti-Furga A, Rimoin DL. 2003. A diagnostic approach to skeletal dysplasias. In: Glorieux FH, Pettifor JM, Juppner H, editors. Pediatric bone: biology and disease. Amsterdam: Academic Press.

van der Kraan PM, van den Berg WB. 2007. Osteophytes: relevance and biology. OsteoArthritis and Cartilage 15: 237-244.

Ward LM, Rauch F, Travers R, Chabot G, Azouz EM, Lalic L , Roughley PJ, Glorieux FH. 2002. Osteogenesis imperfecta type VII: an autosomal recessive form of brittle bone disease. Bone 31:12-18.

Wells C. 1965. Osteogenesis imperfecta from an Anglo-Saxon burial ground at Burgh Castle, Suffolk. Medical History 9:88-89.

Wen S, Ethen M, Langlois PH, Mitchell LE. 2007. Prevalence of encephalocele in Texas, 1999-2002. American Journal of Medical Genetics Part A 143A: 2150-2155.

Winter R, Rosenkranz W, Hofmann H, Zierler H, Becker H, Borkenstein M. 1985. Prenatal diagnosis of campomelic dysplasia by ultrasonography. Prenatal Diagnosis 5:1-8.

Wong HS, Kidd A, Zuccollo J, Tuohy J, Strand L, Trait J, Pringle KC. A case of thanatophoric dysplasia: the early prenatal 2D and 3D sonographic findings and molecular confirmation of diagnosis. Fetal Diagnosis and Therapy. 24: 71-73.

Wright JR, Van den Hof MC, Macken MB. 2005. Prenatal infantile cortical hyperostosis (Caffey's disease): a 'hepatic myeloid hyperplasia-pulmonary hypoplasia sequence' can explain the lethality of early onset cases. Prenatal Diagnosis 25:939-944.

Yang SS, Heidelberger KP, Brough AJ, Corbett DP, Bernstein J. 1976. Lethal short-limbed chondrodysplasia in early infancy. Perspectives in Pediatric Pathology 3:1-40.

Young ID, Thompson EM, Hall CM, Pembrey ME. 1987. Osteogenesis imperfecta type IIA: evidence for dominant inheritance. Journal of Medical Genetics 24:386-389.